A Model of the Olfactory Bulb and Beyond

Thesis by

Zhaoping Li

In Partial Fulfillment of the Requirements

for the Degree of

Doctor of Philosophy

California Institute of Technology

Pasadena, CA 91125

1990

(Submitted September 18, 1989)

Acknowledgements

The work in this thesis was supported by ONR contract N00014-87-K-0377.

I have been looking forward to writing this acknowledgement. It is a great pleasure to thank all the people who have helped to make this thesis possible.

I take great pleasure in thanking my advisor, John J. Hopfield. It was his suggestion of the olfactory bulb as a research project that led to this fruitful thesis. His scientific insight, experience, and enthusiasm have been a great help and inspiration. I am also grateful for having had the opportunity to learn from him how to communicate with others effectively.

It has been fun working with a nice research group which includes (past and present) Professor John Hopfield, Eric Baum, Jose Onuchic, John Platt, Brooke Anderson, Dawei Dong, Joe Bryngelson, Doug Kerns, Fernando Fontanari, Ronny Meir, David Mackey, Ron Benson and secretary Debbie Chester. The communication within the group has been very pleasant and the encouragement from them has been very helpful. Special thanks to to Eric, Dawei, Brooke, and Joe for their patience in listening to me and giving me suggestions.

Thanks go to many others at Caltech who gave me different kinds of help. Among them are Professor Bower and Matt Wilson, who helped me with references, Professor Fraustchi, who always gave his time and advice, my former roommates and friends Lois, Ann, and Debbie and other friends: Cole Miller, Shouleh Nikzad, Boris Hasselblatt, Mike Hoenk, and Robert Walker, who helped me to adapt to the new environment, my friends Zhe Zhang, Keyue Ma, Yang Tse Cheng, Boning Gao, Dan Ashlock, Xiaolan Hsu, Chong Chen, Christoph, Ojvind, and Thomas, who offered me friendship and shared joy with me. Thanks go to Caltech, which provided a nice atmosphere with supportive professors and staff, with friendly and stimulating students (including those in cns185 and the Freshman lab that I TAed), and with the friendly community.

Special thanks go to Mike Newton, who has given me invaluable and persistent support, and has stayed by my side.

Thanks go to my brother Zhaofeng and high school teacher Zhang Jin-Fu, who sparked my enthusiasm in science or physics, my parents for their belief in me, my brothers and sister and my friend Sun Jin-lan for their love and friendship.

Abstract:

The olfactory bulb of mammals aids in the discrimination of odors. A mathematical model based on the bulbar anatomy and electrophysiology is described. Simulations of the highly non-linear model produce a 35-60 Hz modulated activity, which is coherent across the bulb. The decision states (for the odor information) in this system can be thought of as stable cycles, rather than as point stable states typical of simpler neuro-computing models. Analysis shows that a group of coupled non-linear oscillators are responsible for the oscillatory activities. The output oscillation pattern of the bulb is determined by the odor input. The model provides a framework in which to understand the transformation between odor input and bulbar output to the olfactory cortex. This model can also be extended to other brain areas such as the hippocampus, thalamus, and neocortex, which show oscillatory neural activities. There is significant correspondence between the model behavior and observed electrophysiology.

It has also been suggested that the olfactory bulb, the first processing center after the sensory cells in the olfactory pathway, plays a role in olfactory adaptation, odor sensitivity enhancement by motivation, and other olfactory psychophysical phenomena. The input from the higher olfactory centers to the inhibitory cells in the bulb are shown to be able to modulate the response, and thus the sensitivity, of the bulb to odor input. It follows that the bulb can decrease its sensitivity to a pre-existing and detected odor (adaptation) while remaining sensitive to new odors, or can increase its sensitivity to discover interesting new odors. Other olfactory psychophysical phenomena such as cross-adaptation are also discussed.

Table of contents

List of Figures and Tables

solid curve and its slope G' with the dotted curve. For the X_o or Y_o value on or outside dashed lines, the cell internal states can be considered either before firing threshold or at saturation regions, the gain G' is too small for the possibility of non-damping oscillation modes, while for X_o and Y_o values inside the dashed lines, the gain is larger and non-damping oscillation modes are possible in some circumstances. The circle indicated with "0" is the possible X_o and Y_o locations with no odor input $I_{odor} = 0$, and the circle "1" for possible X_o and Y_o locations during the inhale with odor inputs. The arrow indicates the direction in which the X_o and Y_o are raised by input odors.

Figure 6.1 p.57 — Internal states of mitral and granule cells and the outputs of the mitral cells in one sniff cycle with odor input I_{odor_1}. The cells are arranged in the normal reading sequence, i.e., from left to right and from top to bottom.

Figure 6.2 p.60 — **A:** A segment of a simulated surface EEG wave pattern during the oscillatory bursts with the odor input I_{odor_1}. **B:** Multi-channel recorded bulbar surface EEG wave pattern during 100 msec of bursts, taken from Freeman 1978. Both signals in A and B are band-passed filtered.

Figure 6.3 p.61 — Mitral output response patterns for different inputs I_{odor} of one sniff cycle lasting 370 msec. **A,B:** oscillatory responses for two different inputs. **C:** non-oscillatory response for an input. **D:** response for no odor inputs.

Table 6.1 p.63 — Differences between responses to different odor inputs and between responses to the same odor inputs with different noises and between the input patterns.

Figure 7.1 p.73 — This figure illustrates the possible positions of Y_o indicated by circles on the input-output curve G_y under different circumstances. The circle numbered "0" is the Y_o with no odor input $I_{odor} = 0$, "2" with inhaled odor without enhancing, "1" with the same odor input with enhancing, "3" with a stronger odor input, "-1" without odor input while with enhancing. The region inside the dashed lines is the linear region of G_y where the oscillation output is insensitive to the exact position of Y_o.

Table 7.1 p.78 — Differences between adapted and non-adapted responses.

1. Introduction

1.1 Motivations of the Study

1.1.1 Complex systems

It is already known how bodies or point particles interact with each other, using the basic laws of most interactions that are relevant: electromagnetic, weak, strong, and gravitational interactions. Physicists can continue their efforts and study the details of interactions to find out how everything is made and of which elementary particles and what governs the evolution of the universe. In principle, almost everything in the world we live in, such as the chemical reactions , and blood flows in the body can be explained.

But it is only in principle in most of the cases. Although the detailed equations of motion are usually available, they can rarely be carried out to the extent that phenomena such as turbulence in fluid flow, and consciousness of living bodies can be explained. The difficulties are that, for example, the equations are non-linear such that no analytical solution can be found, or the number of degrees of freedom is too large to handle. Special systems (e.g., systems near equilibrium, without dissipation, and with some symmetries) have usually been selected to avoid these difficulties. But systems not in equilibrium and/or with dissipation display some interesting behaviors and intriguing complexities. A living biological body is a good example of such complex systems, which open new opportunities to understand how the interplay of basic physics laws produce complex, interesting, and useful phenomena.

An equilibrium system, whose future is is equal to its present, cannot tell us any new information other than that of its present. A non-equilibrium system has a time direction; its present tells possible past states and predicts possible future states. The dynamics and the changes of the system in certain directions can be used in many fruitful ways. A waterfall can produce energy; different shapes of snowflakes can imply different paths that the snowflakes went through in the sky, etc.

The nervous system is one of those biological systems displaying interesting complex behaviors. Different parts of the nervous system, each make of many cells called neurons, interacting in various ways, give different possible dynamics. These allow the system to

perform different tasks, such as seeing, motion coordination, and language performance. Biological information processing is complex, and it is not surprising that a nervous system with complex dynamics is used for it.

1.1.2 Olfactory system as a complex system

The sensory system is a good candidate for the study of the functions of the brain because its input is easily accessible and its information processing goal, pattern recognition, is not as vague as that of higher perceptual areas in the brain. Vision, audition, olfaction, and somatic sensation (touch), the four senses of human beings, can be assumed independent by crude approximations. Other than the possibility of the somatosense, olfaction may be the simplest and the most fundamental of all the senses because of the (presumed) simplicity of its signal-processing task, its cortical structure, and its primordial status phylogenetically.

In its simplest tasks, the olfactory system need only identify the odor type and concentration. The possible odor types and, because of the low resolution of the olfactory system, the possible answers to input odor concentration are both limited. In the visual system, the problems need to be solved are: 1) what, which object, or who, is in which part of the visual scene and 2) how it is changing with time. The mamallian auditory system needs to locate the informative sound source from the background and to recognize the sound content. The possible numbers of visual and auditory scenes are huge because of the higher information content, making vision and audition difficult problems to solve. For mammals, the olfactory input is sampled by slow and discontinuous sniffs, whereas the visual and auditory inputs change rapidly and continuously, and make adding to the heavy processing load. Evolutionarily, the olfaction is phylogenetically primitive (Shepherd 1979). The olfactory cortex was first differentiated and become recognizable in the brains of primitive aquatic species. It is often stated that the olfactory cortex is the precursor from which the other types have been differentiated. It is also the principal cortical region of most lower vertebrate species, the simplest of the cortical regions in terms of its intrinsic structure. Other parts of the brain such as hippocampus, thalamus, and neocortex have similar or modified neural circuitry organizations related to that of the olfactory system

(Shepherd 1979). They also generate rhythmic activities just as the olfactory system does. Olfaction may therefore give insights into the functions of other brain areas.

The olfactory system is composed of several different structures in the information pathway. Most of the present thesis is devoted to studying the information processing of the structure termed the olfactory bulb. It is the first processing center immediately following the olfactory sensory cells. Receptors in the sensory cells bind to the odor molecules in the respiratory airway, resulting in electrical signals which are sent to the olfactory bulb (Fig. [2.1]). The bulb then sends the processed information to the higher olfactory centers, which also return feedback to the bulb. It makes sense to study the olfactory bulb in isolation first (before going on to the higher olfactory centers), and, then to study the consequences to the bulb of the feedback inputs. The function of this feedback input is largely unknown. One major accomplishment of this thesis research is to describe in detail the operation of a plausible computational function of these inputs.

1.2 Neural Networks and Formulations

The nervous system is composed chiefly of a special kind of cell called neurons (Fig [1.1], Kandel and Schwarz 1985). The morphological and functional diversity of a neuron is very large. A "typical" neuron has a cell body on a length scale of $\sim 10\ \mu m$, branches of arbor called dendrites (input fibers), and axons (output fibers) stretching out to a distance $\sim 10\ \mu m$ to $1\ m$. A small electrode inserted into the cell body can measure the potential difference across the cell membrane, which changes with time. Such a potential difference signal will typically consist of spikes of $\sim 100\ mv$ with width $\sim 1\ ms$ superimposed on a $\sim -90\ mv$ baseline. These spikes are called action potentials and are propagated without attenuation down the cell branches, termed axons, by an active regenerative process. The axon terminal is normally $\sim 200\ \mathring{A}$ away from a dendritic branch (or the cell body) of another neuron. When the action potential arrives at the terminal, a chemical transmitter is released into the gap between the axon and the dendrite, and this opens certain ion

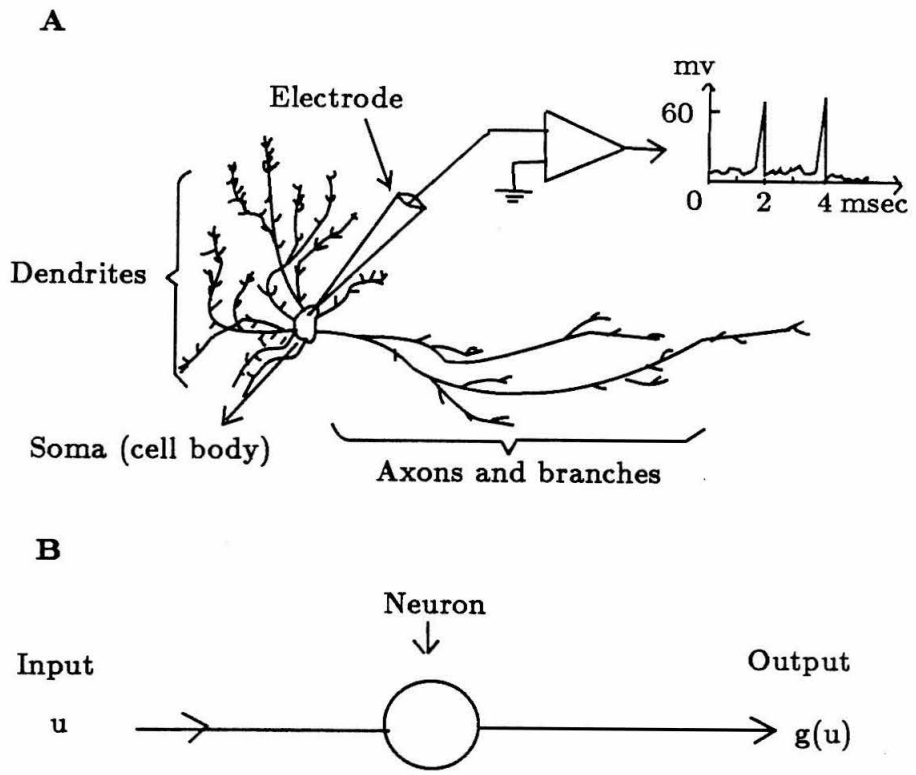

Figure 1.1, A: a typical neuron with its cell body (soma), input receiving dendrites, output axons and the illustrative recording setup. **B:** a neuron seen as a device.

channels in the dendrite and causes a current flow across the dendritic membrane. The junction where axons and dendrites meet is called a synapse. Thus the action potentials passing down the axons of the presynaptic cell, cause a current flow across the postsynaptic cell membrane. According to the direction of this current flow, hyperpolarization or depolarization happens at the post-synaptic membrane and is passed to the cell body. The cell membrane time constant for integrating the (leaky) current is $\sim 10\ ms$. When enough depolarization exists at the cell body, an action potential is generated. Each neuron can typically only either depolarize or hyperpolarize the post-synaptic cells, and is termed accordingly as an excitatory or inhibitory cell. Neurons interact with each other through the synapses. Neurons called receptors receive external inputs from photons (the eyes), odor molecules inhaled (olfactory sensory cells) or heat sources (thermoreceptors in the skin). Others give outputs to other tissues, such as a muscle fiber, which contracts because of the "firings" of the action potentials in a particular neuron that synapses on it. Since the nervous system has as many as $\sim 10^{11}$ neurons (for humans, for instance), even if each neuron only connects to about 100 other neurons, there are numerous dynamical patterns made possible myriad of possible neural interactions. Through these dynamics, a light pattern on the retina receptors can cause the activities of another neuron group deep in the brain to signal the recognition of a visual object; a particular activation of olfactory receptors in the nasal airway can induce another neural group to signal the presence of a predator, etc. The network dynamics transforms selected inputs into sensible outputs.

The neural network computation has the following special properties (Hopfield 1984):

1) resistance to failures of a small number of neurons or synapses;

2) insensitivity to the input noise and tolerance to input errors, e.g., the noise in a visual input image or a grammatical error in a sentence;

3) fast computations (compared with normal computers), using dynamics in both time and space (of the neurons) efficiently;

4) emergence of collective phenomena from the collection of " simple-minded" neurons irrespective of (some of) their detailed properties (Hopfield 1984).

To study the network dynamics and functions, a model should discard the trivial or irrelevant details and preserve only enough necessary features of the network to keep the significant functional dynamics and emergent properties. In many of the neural network models as well as in this thesis, the following simplifications are used (Hopfield (1984)).

1) Since most neurons fire only provided that many action potentials arrive within a short time ($\sim 1 - 10ms$) onto its dendrites, and the neural time constant ($\sim 10ms$ integrating the membrane current to change membrane voltage) is substantially longer than the action potential width, any single action potential and its precise timing are insignificant in these cases. Therefore, a neural output is described by the instantaneous firing rate of the action potentials (short-time average of the number of the action potentials per unit time) instead of the precise time series of action potentials.

2) Each neuron is considered a stationary device (Fig [1.1]) transforming the input voltage u (cell membrane potential state) into an output $V = g(u)$ proportional to the action potential firing rate. $g(u)$ is a sigmoid (Fig. [2.4]), non-decreasing function satisfying $g(-\infty) = 0$, $g'(u) \geq 0$, and $g'(\pm\infty) = 0$.

3) The input current from cell (neuron) j to cell i is seen as proportional to the output V_j of cell j; a transconductance T_{ij} describes the synaptic connection strength from j to i. The input to cell i is $\sum_j T_{ij}V_j + I_i$; I_i represents the external input either from neurons not being considered or from the sensory input such as the current induced by the binding of odor molecules to the receptors.

4) Representing the transmembrane resistance and capacitance of cell i by constants R_i and C_i, the equations of motion for a group of neurons are:

$$C_i \dot{u}_i = \sum_j T_{ij}V_j - u_i/R_i + I_i \qquad u_i = g_i^{-1}(V_i)$$

or taking $T_{ij}/C_i \rightarrow T_{ij}$, $\tau_i = C_i R_i$, and $I_i/C_i \rightarrow I_i$, the equations become

$$\dot{u}_i = \sum_j T_{ij}V_j - u_i/\tau_i + I_i \qquad u_i = g_i^{-1}(V_i). \tag{1.1}$$

Here the sub-indices represent the cells referred to by the variables. This equation will be used in the thesis.

2 Neurobiology Background

2.1 Olfactory Environment

The olfactory system includes the odor-sensing olfactory receptors within the nasal cavity, the olfactory bulb (the output station of the receptors), and the olfactory cortex (receiving inputs from the olfactory bulb, Shepherd 1979, Figure [2.1]). The olfactory system samples the sensory inputs by sniffs. The receptor activities increase during inhalation and decrease during exhalation (Getchell and Shepherd 1978). In the olfactory bulb and cortex, oscillatory neural activities (depending on the odor input) emerge during inhalation and cease during exhalation (Freeman 1978).

The sensory input of the olfactory system is the odorant molecules which bind to the olfactory receptors that lie deep within the nasal cavity (Lancet 1986). The receptor bodies and their short odor-sensing, peripheral processes are confined in a patch called olfactory epithelium, which is $100-200\mu m$ thick and several square centimeters (man and frog) to more than $100cm^2$ (dogs) in area. Each receptor has an unmyelinated axon fiber running from the nasal cavity to the olfactory bulb (Fig[2.2]; myelination is the wrapping of glial cell membranes around an axon to increase the potential signal propagation velocity). Bathed in a layer ($10-30\mu m$ thick) of mucus, through which the odorant molecules diffuse, the olfactory receptive apparatus (termed olfactory cilia) reside at the extented tips of the receptor dendrites, and extend to the surface of the mucosa (Lancet 1986, Getchell et. al. 1984). Each receptor is spontaneously active, and increases its action potential firing rate upon the arrival of odorants (Section 2.3). Different receptors respond differently, and each can respond to more than one type of odorant. The response spectrum of different receptors can also overlap. There can also be more than one type of odorant molecules in the inhaled air, and they cause a response level pattern in the receptor cell population. All odorants are soluble in water, and their equilibrium water/air partition coefficient is $\sim 0-10^3$. Different diffusion constants through the mucus layer result in different temporal response patterns in the receptor-cell population for different odorants (Getchell et. al. 1984).

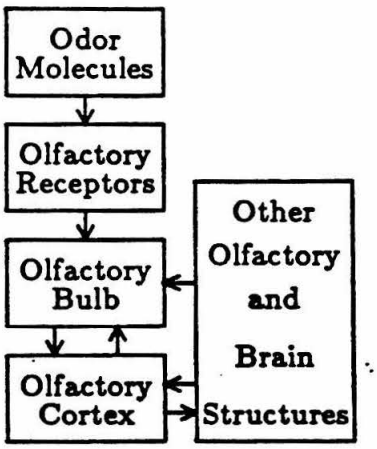

Fig. 2.1 Olfactory systems and its enviroment.

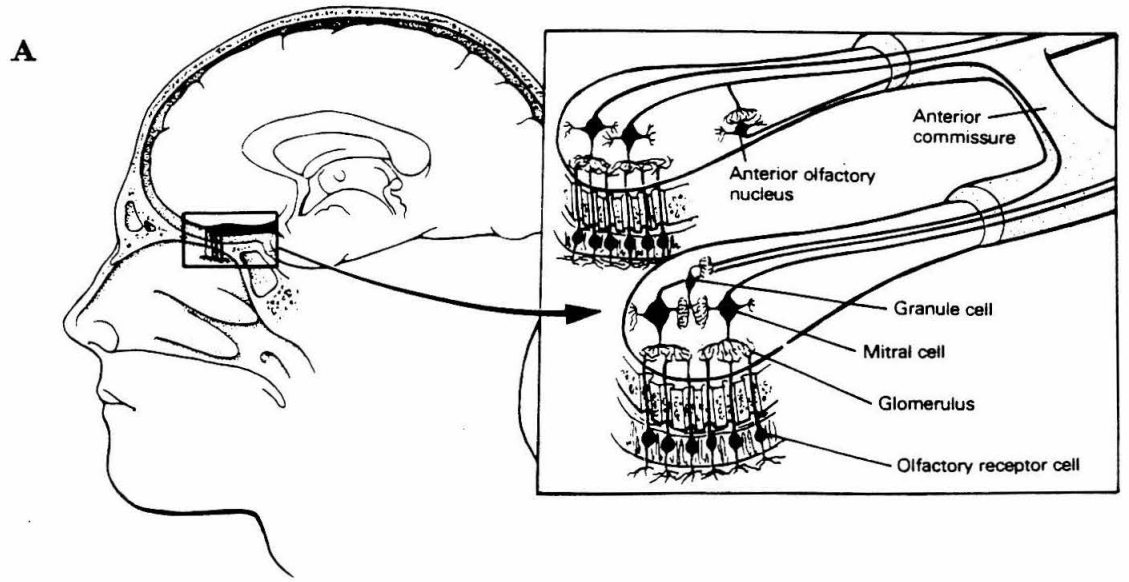

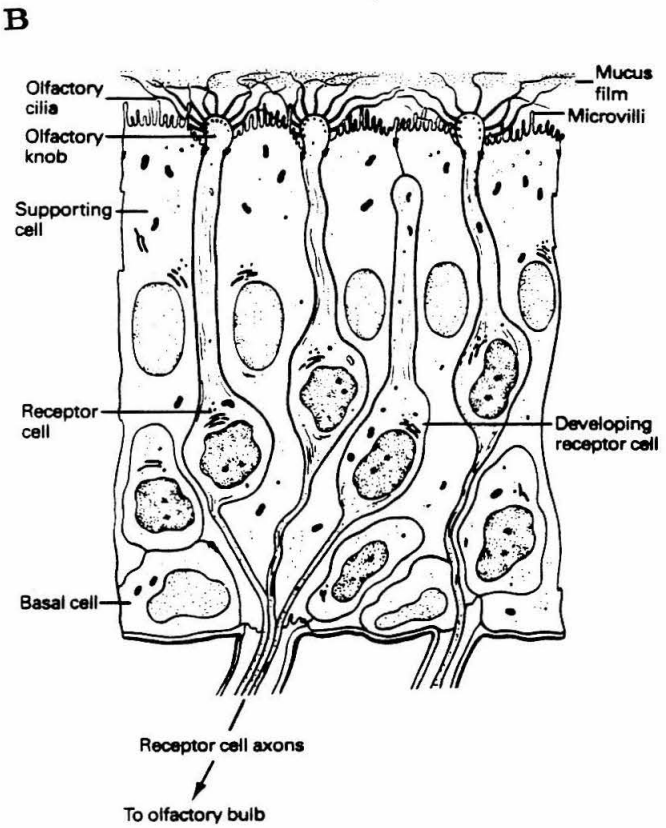

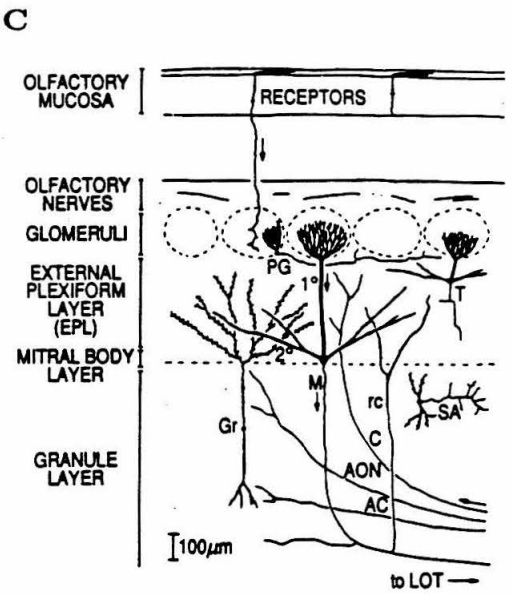

Neuronal elements of the mammalian olfactory bulb. Inputs: olfactory nerves (above) from the receptors; central fibers (C,AON and AC) from the higher centers. Neurons: mitral cell (M), with primary (1°) and secondary dendrites (2°) and recurrent axon collaterals (rc); tufted cell (T), a smaller version of mitral cells; granule cell (Gr); inhibitory cell (PG) in the input layer; deep short axon cells (SA) which are small in number. Outputs: LOT to olfactory cortex. Taken from Shephard 1979.

Fig. 2.2 A: olfactory epithelium and bulb. **B:** olfactory epithelium containing receptors. **C:** olfactory bulb. From Kandel & Schwartz 1985.

The receptor cells output directly to the olfactory bulb, the first processing center of the olfactory system (Shepherd 1979). It is composed chiefly of two layers of locally interacting mitral and granule cells (see later sections for details). Within the bulb, the olfactory receptor axons synapses with various types of cells, particularly the bulbar output cell — the large mitral cells and the smaller tufted cells. The bulb also receives inputs from the olfactory cortex and a region at the base of the brain called the diagonal band. Being the first relay station, the bulb has its input and output pathways more or less separated, making its operation relatively easily understood.

The olfactory cortex, whose main part is the prepyriform cortex (Shepherd 1979), receives bulbar output and interacts with other olfactory structure and parts of the central brain. The bulb and cortex have similar, but different, cortical organizations (Shepherd 1979; Haberly 1985), and both demonstrate $35-90Hz$ rhythmic neural activities (Freeman 1978). Olfactory information is ultimately relayed to the thalamus and the neocortex (Fig [2.1]).

2.2 The Circuitry Organization and Properties of the Olfactory Bulb

The olfactory bulb has several sharply differentiated types of neurons located on different parallel layers. Folded around a fluid-filled cavity called the ventricle, the surface of each layer can be treated as a segment of an ellipsoid, or, in the case of the bulb in the rabbit, as as incomplete sphere (Freeman 1975). Most of the bulbar information is from Shepherd (1979).

Glomerular layer: The receptor nerve axons from the mucosa enter at the bulb surface and terminate in a layer composed of spherical regions of neuropil termed glomeruli. (See Figure [2.2]). Each receptor axon does not branch on its way to (only) one of the glomeruli, but once inside it ramifies, to varying extents, and terminates. Each glomerulus is about $100-200\mu m$ in diameter, and within it, the receptor axon terminals contact the dendritic tufts of the bulbar output neurons, the mitral cells. The periglomerular cells, of inhibitory cell type, also receive input from the receptor terminals in the glomerular layer. These

periglomerular cells have their dendrites and axons radiating in a direction parallel to the glomerular layer. Each periglomerular cell has a short, bushy dendritic tree that arborizes to an extent of $50 - 100\mu m$ within one of the glomeruli, and its axons reach to other glomeruli in the neighborhood. They receive excitation from the neighboring mitral cells by dendrodendritic interactions. (When one neuron gives output from its dendrites to another neuron's dendrites, it is termed dendrodendritic interaction.) They also give inhibitions to neighboring mitral and periglomerular cells (within a distance $\sim 500\mu m$) by both axon-dendritic and dendrodendritic interactions.

Mitral cells: The mitral cell bodies are in a thin sheet about $400\mu m$ below the glomerular layer. Each mitral cell sends an unbranched primary dendrite to a single glomerulus, to terminate there in a tuft of branches, which fills much of the glomerulus it lies within. Each mitral cell also gives rise to several secondary dendrites, which branch sparingly and terminate in the external plexiform layer (EPL) above the mitral cell layer. These secondary dendrites are up to $600\mu m$ or so in length, and can reach into the space of other mitral cells that receive input from several neighboring glomeruli. Within the EPL, the mitral secondary dendrites make (mostly reciprocal) dendrodendritic connections with the dendrites of the numerous small inhibitory cells, termed granule cells. The mitral cell axons carry the bulbar output to the olfactory cortex, and some axon collaterals (axon branches) synapse on the lower dendrites of the granule cells.

Granule cells: The granule cell bodies lie in a thick layer below the mitral cell bodies. Each granule cell has an upper dendritic tree that ramifies and terminates in the EPL. This dendritic tree has a lateral extent of 300-500 um within the EPL. Thus each of them can also reach into the space of the mitral cells that receive input from several neighboring glomeruli. A granule cell also has another dendritic tree, which terminates deeper in the granule layer to receive excitatory input from the mitral cell axon collaterals. The outstanding feature of the granule cells is that they lack morphological axons; the only output is given by their upper dendritic tree in the EPL through the dendrodendritic interaction on the mitral cell secondary dendrites. Over 80% of the dendrodendritic

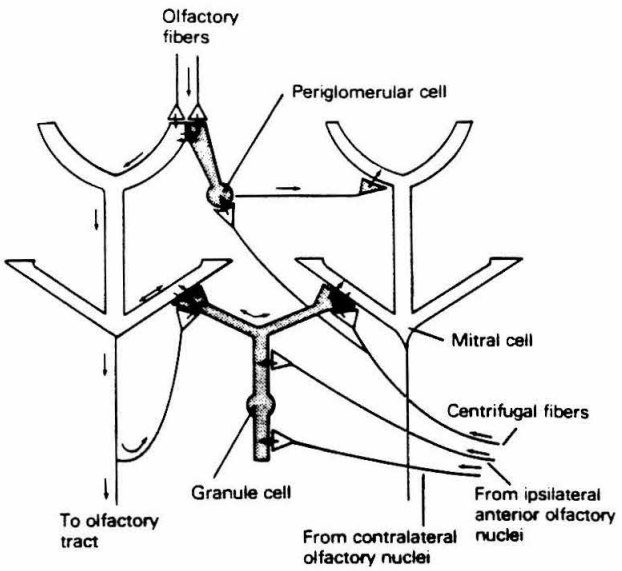

Fig. 2.3 Olfactory fibers carry the receptor inputs while the centrifugal fibers carry the central inputs. The olfactory tract carries the bulbar output. From Shepherd 1979.

interactions in the EPL are reciprocal between the mitral and granule cells.

Other cell types: There are also other cell types in the bulb. Tufted cells, for instance, are just a smaller version of the mitral cells. Short axon cells, found frequently in the granule cell layer, are relatively few in number when compared with granule cells, and have no known specific function for bulbar activity.

Central input: Most central input from other parts of the olfactory system and the brain regions are carried to the granule cell dendrites. One kind of central input fibers that is relatively sparse comes the farthest distance, from a region at the base of the brain called the diagonal band. Other axons, finer and much more numerous, come from a region just posterior to the bulb, the anterior olfactory nucleus. Some input from the diagonal band also synapse on the primary dendrites of the mitral cells.

Output pathway: The output of the bulb is carried by the mitral cell axons, which branch and terminate to the olfactory cortex. The basic neural circuit is now shown in Figure [2.3].

Cell numbers: There are about 50,000,000 receptor cells in the nose. The number of mitral cells is about 50,000, so there is an order of 1000 : 1 convergence from receptor to mitral cells. About 2000 glomeruli are in the olfactory bulb, so there are about 25,000 receptor axons and 25 mitral cells per glomerulus. Approximate estimates of other cell type ratios are: 20 : 1 for the periglomerular cells : mitral cells, 200 : 1 for the granule cells : mitral cells.

Cell properties: The output of a cell increases non-linearly with the input, with both threshold phenomena and saturation. Plots of the local mitral cell firing rates with respect to the bulbar surface EEG wave amplitude (generated mostly by the granule cells, Freeman and Skarda 1985) show a sigmoid-shaped function (Fig [2.4]). Both the mitral and periglomerular cells give axonal action potential output, while the granule cell output is by graded presynaptic depolarization (instead of action potential impulses) at

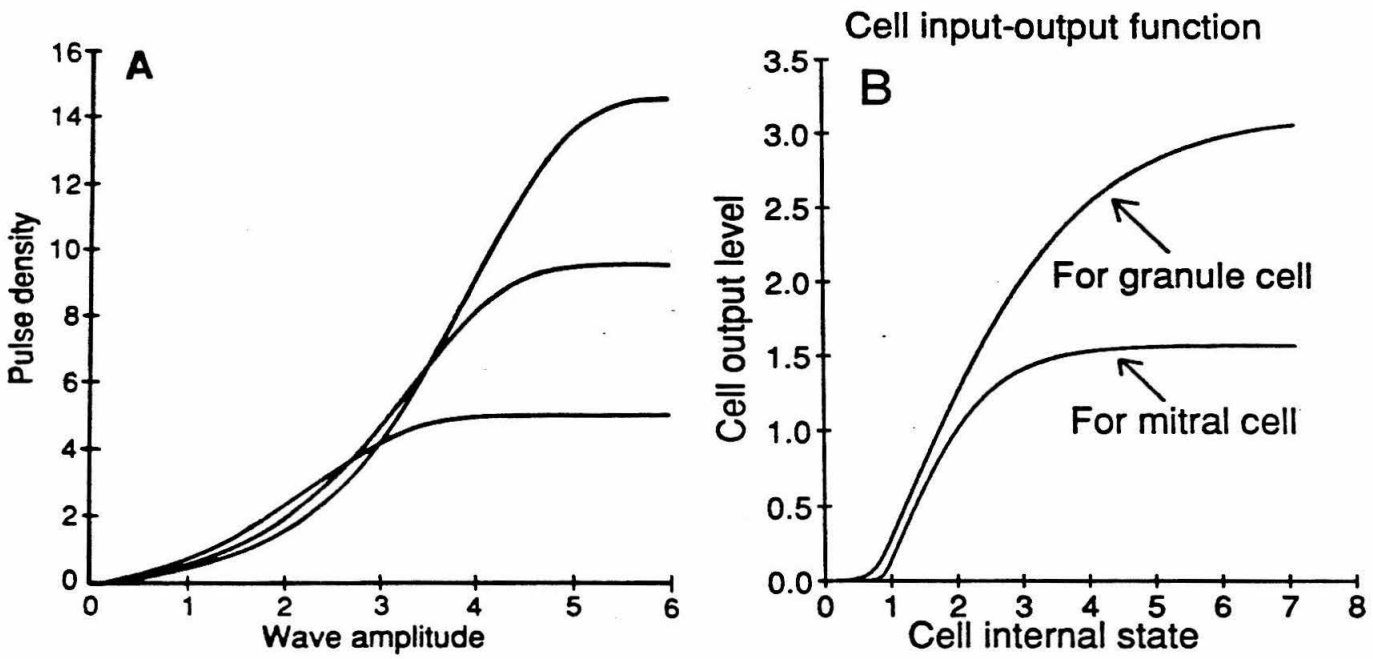

Figure 2.4 — Cell non-linear input-output functions. **A:** three examples of experimentally measured functions in a mass of mitral and granule cells, relating the pulse probability of single or small groups of mitral cells to the EEG wave amplitude originated from the granule cells. Taken from Freeman and Skarda 1985. **B:** the model functions for mitral and granule cells, respectively.

granule- to-mitral dendrodendritic synapses. The dendrodendritic interaction between the periglomerular and mitral cells is also by graded presynaptic depolarization. But the mitral-to-granule dendrodendritic output at the EPL is by the presynaptic impulses. The mitral and granule cells' membrane time constants are $\sim 5 - 10ms$ (Freeman and Skarda 1985, Shepherd 1988). Very little is known about the synaptic strength from one cell to another in the bulb. The granule and mitral cell dendrites have very short electrotonic lengths, mostly less than one, and at most two from a cell body to any parts of the cell dendrites. (When there is current injection at a spot on the cell membrane, the change in membrane voltage decays exponentially with distance from the injection point by length constant λ. A distance measured in the unit of λ is called an electrotonic length.) Therefore, the spread of the current or voltage within a cell is very efficient.

2.3 Inputs to the Olfactory Bulb

Each receptor cell has a background activity of $\leq 1 - 3$ impulses/sec. The impulse firing frequency increases with increasing input odor concentration, and can reach up to 20 impulses/sec. When an odor pulse is delivered to the nose, the pattern of the response consists of a relatively brief latency (of about several hundred millisecond) of onset, a rapid rise in impulse frequency, a continuation of impulse firing during the plateau of the odor pulse, and an abrupt termination of the discharge correlated with the termination of the odor pulse (Getchell and Shepherd 1978). The rapid rise of the receptor firing frequency is approximately linear in time, and lasts for a few hundred milliseconds if the pulse of the input odor lasts longer than that. The firing termination time at the end of the input odor is relatively constant, independent of the odor concentration, and can be as short as $100ms$ (Getchell and Shepherd 1978, Figure [2.5]). For rabbits, the respiratory frequency is about 2-4 Hz (Freeman and Schneider 1982).

Different odor input generates different activity patterns in the receptor cell population. A high-resolution 2-deoxyglucose autoradiography experiment (Lancet *et al* 1982) shows that the odor-specific pattern also exists in the glomerular layer. For an input odor,

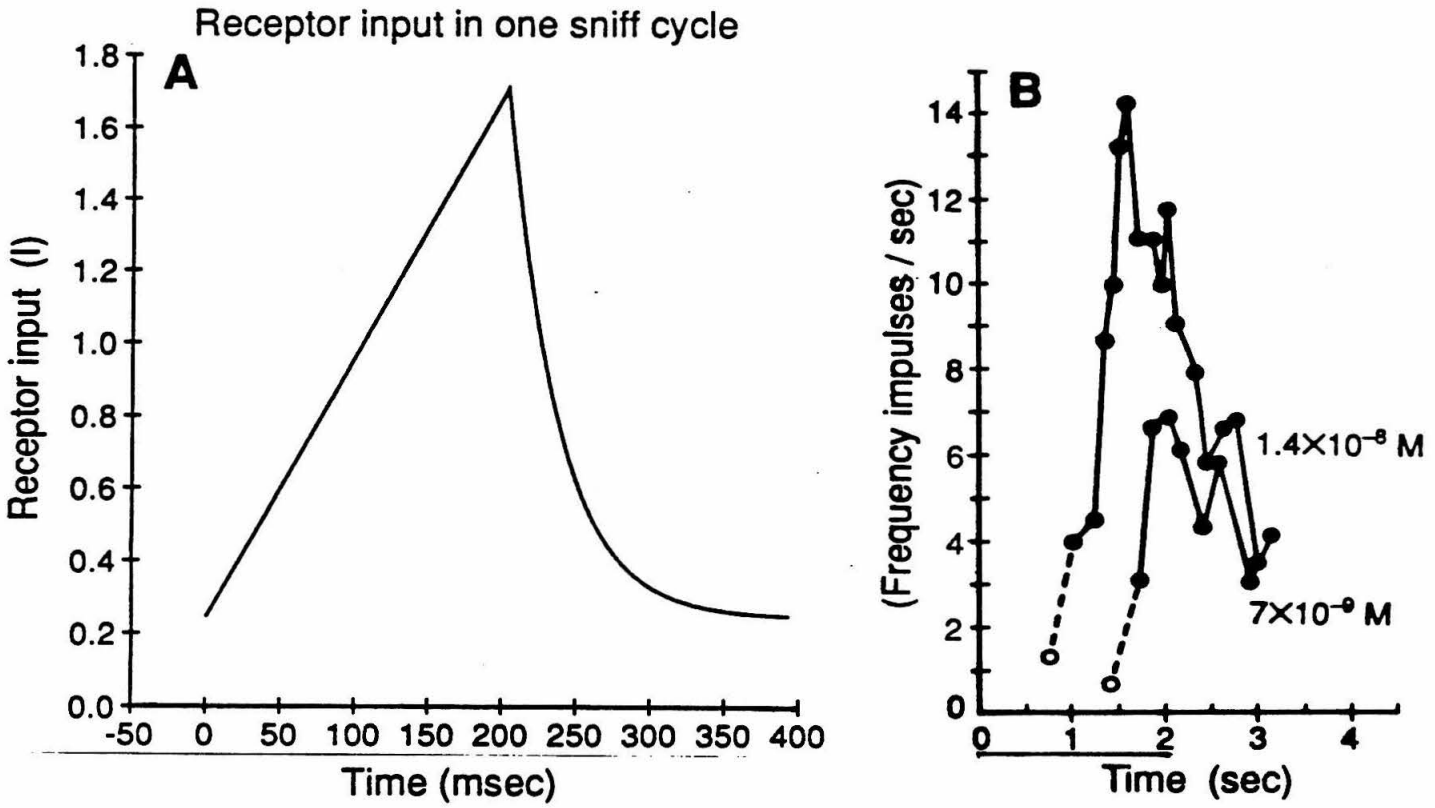

Fig. 2.5 A: model of receptor cell response (input to the bulb) time course to odors in a sniff cycle. B: experimentally measured receptor firing frequency with an odor pulse delivered to the nose, two concentration examples of odor plotted, the line below the time axis indicates the odor pulse duration. Taken from Getchell and Shepherd 1978.

different and even neighboring glomeruli have different activity levels. This level, however, remains relatively uniform within a single glomerulus.

Not much is known about the central input to the granule cells.

2.4 Cell Activities in the Olfactory Bulb

Stimulation with odors, depending on the animal motivation, causes an onset of a high-amplitude bulbar oscillatory activity, which is detected by EEG (electroencephalograph) electrodes at the bulbar surface (Freeman 1978). The oscillations at different parts of bulb have the same frequency, and are coherent with each other. The oscillation is an intrinsic property of the bulb itself, and persists after the central input fibers are cut off (Freeman and Skarda 1985). The oscillation returns to low-amplitude on the cessation of the odor stimulus, and disappears when the nasal air flow is blocked (Freeman and Schneider 1982). Central input (Freeman 1979a; Freeman and Skarda 1985; Baird 1986) influences oscillation onset; the oscillation exists only in motivated animals, and can be present without an input odor (Freeman 1978). The granule cells are the generators of the surface EEG wave, for their morphological structure makes them produce a dipole field, while the mitral cells produce a closed monopole field negligible at the bulbar surface (Freeman 1975). The EEG (Freeman 1978; Freeman and Schneider 1982) shows a high-amplitude oscillation arising during the inhalation and stopping early in the exhalation (Fig [2.6]). The oscillation bursts have a peak frequency of 35-90 H and ride on a slow background wave phase locked with the respiratory wave. Different parts of the bulb have different oscillation amplitudes and phases. A specific odor input will set a specific oscillation pattern across the olfactory bulb (Fig[6.2]).

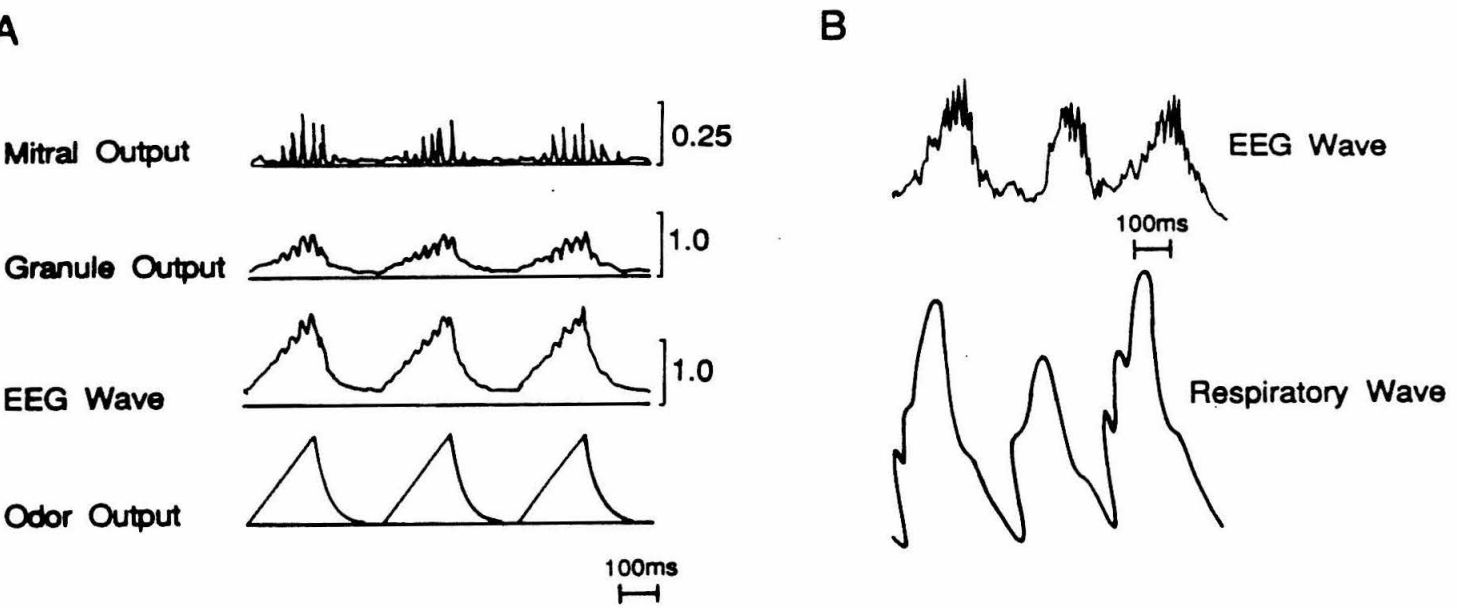

Fig. 2.6 A: simulation result of bulbar response in several sniff cycles. B: experimentally measured EEG waves with odor inputs, taken from Freeman and Schneider 1982. Both the simulated and measured EEG waves are surface negative waves.

3. The Olfactory Bulb Model Organization and Parameters

For comparisons between experiments and theory of the olfactory bulb, it is essential to model with realism. To do the mathematical analysis and simulation necessary to understand collective and statistical properties, it is necessary to disregard superfluous details. The model organization is a compromise between these two considerations.

3.1 Cell Types, Cell Numbers, and Arrangement

Cell types: Only the mitral and granule cells are included in the model. The glomerular layer is assumed to only pass on the input with some processing, and is neglected. The receptor cell input is assumed to be effectively directed onto the mitral cells. Tufted cells are considered the same as the mitral cells, while the short axon cells are neglected for their non-specific functions in bulbar activities. The sources of input to the bulb are considered external and are represented as input parameters in the model.

Cell numbers: There are N mitral and M granule cells in the model. Because of the limited capability in computer simulation, the cell numbers are taken to be much smaller in the simulation than the real cell numbers. Similarly, the ratio $M : N$ is much smaller than that (200 : 1) in the real bulb since, for example, 10 granule cells connected to a mitral cell can be viewed as one granule cell connected to the same mitral cell with synaptic strength 10 times as strong. In the simulation, $N = M = 10$. Since the activity within a single glomerulus is uniform as observed, the mitral cells connected to the same glomerulus receive about the same external input. Assume that the activity level changes very little locally for cells below the same glomerulus; the group of mitral cells connected to the same glomerulus is simplified into a single mitral cell in the simulated model. The number of granule cells M is also reduced by the similar approximation in the simulation. However, the mathematical formulation does not depend on the absolute numbers of the cells and their ratio. The significance of the cell numbers N and M, and their ratio $M : N$, will be discussed in later sections.

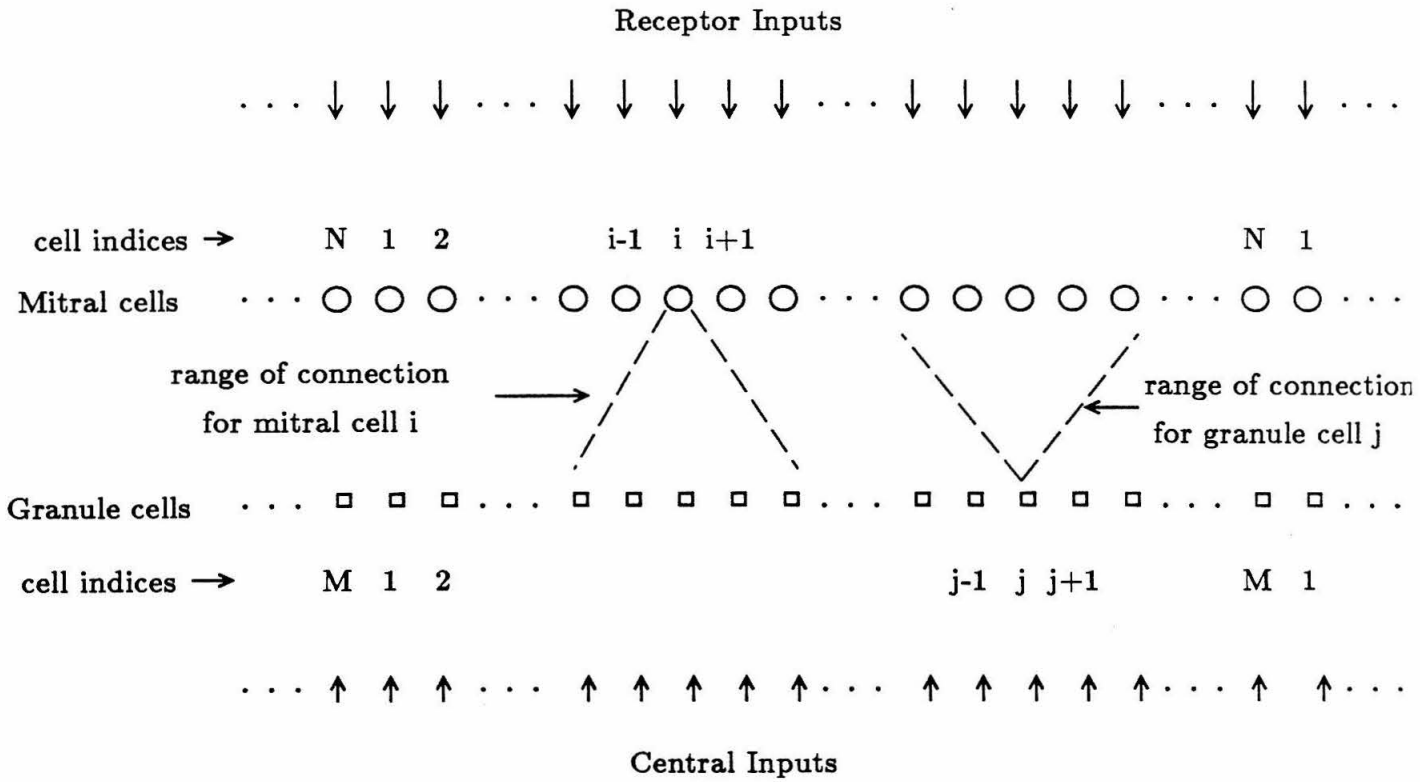

Fig. 3.1 Cell arrangement in the bulbar model

Cell arrangement: Each cell is specified by an index, e.g., i^{th} mitral ($i = 1, 2, \ldots N$), and j^{th} granule cell ($j = 1, 2, \ldots M$). The cells can be considered as sitting on a one-dimensional string with the indices i, j resembling the cell locations on the string. The i^{th} mitral cell is the neighbor of the $i \pm 1^{th}$ mitral cells and the $\frac{i \cdot M}{N}^{th}$ granule cell. The 1^{st} and N^{th} mitral cells are next to each other, and so are the 1^{st} and M^{th} granule cells (Figure [3.1]). So the one-dimensional string of cells has periodic boundary conditions, or the string's end is connected to its beginning. Although the bulb is more like two-dimensional sheets of cells folded into incomplete spheres, the 1-d simplification is helpful for understanding, but is not essential for the model (see Chapter 8).

3.2 The Cell Properties

Cell activity level: Because of the short electrotonic lengths of the mitral and granule cells, the cell membrane potential spreads effectively, and the potentials on different locations of a cell can be simplified as proportional to each other. It is thus justifiable to use only one variable, thought of as proportional to the membrane potential, to describe the internal state level of a single cell (instead of specifying all types of ion channel activities for different compartment of a neuron). As in Section 1.2, each cell is described by an internal state level (or input potential) and an output, which is a continuous sigmoid function of the internal state level.

The internal states of the mitral cells are $X = \{x_1, x_2, \ldots, x_N\}$, and of the granule cells, $Y = \{y_1, y_2, \ldots, y_M\}$. The cell outputs are $G_x(X) \equiv \{g_x(x_1), g_x(x_2), \ldots, g_x(x_N)\}$ for the mitral cells, and $G_y(Y) \equiv \{g_y(y_1), g_y(y_2), \ldots, g_y(y_M)\}$ for the granule cells, where g_x and g_y are the cell output functions for the mitral and granule cells, respectively.

The scales of $x's$, $y's$, g_x, and g_y are set such that

$$Max(dg_x/dx) = (dg_x/dx)\,|_{th} = 1$$

$$Max(dg_y/dy) = (dg_y/dy)\,|_{th} = 1$$

$$th = 1.$$

The function formulae are (Fig [2.4]):

$$g_x(x) = \begin{cases} S'_x + S'_x \cdot tanh(\frac{x-th}{S'_x}), & \text{if } x < th; \\ S'_x + S_x \cdot tanh(\frac{x-th}{S_x}), & \text{if } x \geq th \end{cases} \qquad \begin{matrix} S'_x = 0.14; \\ S_x = 1.4 \end{matrix}$$

$$g_y(y) = \begin{cases} S'_y + S'_y \cdot tanh(\frac{y-th}{S'_y}), & \text{if } y < th; \\ S'_y + S_y \cdot tanh(\frac{y-th}{S_y}), & \text{if } y \geq th \end{cases} \qquad \begin{matrix} S'_y = 0.29; \\ S_y = 2.9. \end{matrix}$$

Note that g_x (org_y) is very non-linear near $x = th$ (or $y = th$). This point can be seen intuitively as the firing threshold of the neurons. The granule cells are modeled with a longer linear range, reflecting that granule cells do not have axons, and thus have a weaker non-linear threshold effect. The non-linear and threshold functions are essential for the bulbar oscillation dynamics (Freeman 1979a; Freeman and Skarda 1985; Baird 1986) to be studied.

The decay time constant $\tau_x \equiv 1/\alpha_x$,and $\tau_y \equiv 1/\alpha_y$ for mitral and granule cells are chosen to be 7 msec.

3.3 The Input Format and Strength in the Olfactory Bulb Model

The external input to i^{th} mitral cell is described by I_i for $1 \leq i \leq N$, and to the j^{th} granule cell, $I_{c,j}$ for $1 \leq j \leq M$. I_i ($I_{c,j}$) is the i^{th} (j^{th}) component of the vector $I = \{I_1, I_2, \ldots, I_N\}$ ($I_c = \{I_{c,1}, I_{c,2}, \ldots, I_{c,M}\}$). Input $I = I_{odor} + I_{background}$ to the mitral cells consists of the background input $I_{background}$ and the odor-induced input I_{odor}. $I_{background}$ includes both the input caused by the spontaneous firings of the olfactory receptors without odor, and the input from the central brain to the mitral cells. From the little knowledge of the central input, and the knowledge that a receptor cell fires at $\leq 1 - 3/sec$ spontaneously up to $20/sec$ at highest odor concentration, $I_{background}$ is considered constant, and I_{odor} ranges from 0 to 10 or 20 times of $I_{background}$. I_c is a constant without considering the central control on the olfactory bulb; it is later to change with time in the model when the central control is studied.

Since the external input synaptic strengths are not known biologically, $I_c = 0.1$ and $I_{background} = 0.243$ are set such that when $I_{odor} = 0$, no large amplitude oscillation exists, as observed physiologically.

I_{odor} changes with time determined by the animal sniff. Since rabbits sniff at frequency of $2 - 4$ Hz, each sniff cycle is modeled to last for $200 - 500$ msec, with inhalation and exhalation taking about half of the cycle. Because of their high water/air partition coefficients, the odorants are assumed to be very little in the exhaled air because of their absorption by the moisturous throat and lungs. It is then assumed that a sniff brings on top of the mucusa an odor pulse, which starts at the beginning of inhalation and terminates at the beginning of the exhalation. Odorant diffusion through the mucous to the receptors should delay the increase in the receptor activities. I_{odor} is modeled to increase slowly, instead of rising abruptly in time during inhalation, as observed in experiments (Getchell and Shepherd 1978). Exhalation is modeled as an exponential return toward the ambient.

Different sensitivities of receptors cause different degrees of responses to an input odor in the receptor population, and thus different input strengths to different mitral cells. For any mitral cell i exposed to odor (Fig [2.5A]),

$$I_{odor,i}(t) = \begin{cases} P_{odor,i} \cdot (t - t^{inhale}) + I_{odor,i}(t^{inhale}), & \text{if } t^{inhale} \leq t \leq t^{exhale}; \\ I_{odor,i}(t^{exhale}) \cdot e^{-(t-t^{exhale})/\tau_{exhale}}, & \text{if } t > t^{exhale}, \end{cases} \tag{3.1}$$

where $\tau_{exhale} = 33\ msec$, t^{inhale} and t^{exhale} are on set times for inhalation and exhalation, $P_{odor,i}$ characterizes the odor concentration and the sensitivities of the receptors that give input to the i^{th} mitral cell. $I_{odor}(t^{inhale}) = 0$ if no odor exists above the epithelium before the inhalation. The vector $P_{odor} = \{P_{odor,1}, P_{odor,2}, \ldots, P_{odor,N}\}$ contains the information of odor identity and concentration, and can be considered the odor image on the mitral cell population. The odor input I_{odor} is taken to be excitatory, and thus P_{odor} has all non-negative components.

More strictly, t^{inhale} represents the onset time of the receptor cell firing with odor input; it is delayed from the beginning of inhalation by a latency that is due chiefly to the

odorant diffusion through the mucous layer (Getchell and Shepherd 1978). This latency is about ten to hundreds of msecs, depending on the odor and its concentration. If only one type of odorant molecules is present, the latency should be the same for all the receptors. If there are more than one odorant, the different diffusion constants for different molecules make different latencies for different odorants. With selective sensitivities of the receptors, the different temporal information in the activities of different receptors can be possibly used for odor information processing, although it is not discussed in this thesis.

3.4 The Synaptic Connection Geometry and Strength

An $M \times N$ matrix W_o is used to represent the synaptic connections from mitral to granule cells. Similarly, an $N \times M$ matrix $-H_o$ represents the connections from granule to mitral cells. Therefore, $W_{o,ji} \geq 0$ and $-H_{o,ij} \leq 0$ are synaptic connection strengths from the i^{th} mitral to the j^{th} granule cell, and vice versa. The minus sign in front of H_o or $H_{o,ij}$ indicates the inhibitory nature of the granule cells.

It is known that mitral and granule cell dendrites extend laterally for $300 - 600\mu m$ in the EPL layer. Since each glomerulus is about $100 - 200\mu m$ in diameter, thus a cell below one glumerulus can connect to cells below several neighboring glomeruli. Therefore, in the simulated model with $N = M = 10$, each mitral (or granule) cell is randomly connected to several $(1 - 5)$ neighboring granule (mitral) cells, with a higher probability of connecting with closer neighbors (Figure [3.1]). Since mitral axon collaterals also connect to the granule cells in a presumably larger neighboring range than that of dendrodendritic connection, extra connections from mitral cells are added randomly and more sparsely to some neighboring granule cells. The matrices used for simulation are (for $N = M = 10$):

$$H_o = \begin{pmatrix} 0.3 & 0.9 & 0 & 0 & 0 & 0 & 0 & 0 & 0 & 0.7 \\ 0.9 & 0.4 & 1.0 & 0 & 0 & 0 & 0 & 0 & 0 & 0 \\ 0 & 0.8 & 0.3 & 0.8 & 0 & 0 & 0 & 0 & 0 & 0 \\ 0 & 0 & 0.7 & 0.5 & 0.9 & 0 & 0 & 0 & 0 & 0 \\ 0 & 0 & 0 & 0.8 & 0.3 & 0.8 & 0 & 0 & 0 & 0 \\ 0 & 0 & 0 & 0 & 0.7 & 0.3 & 0.9 & 0 & 0 & 0 \\ 0 & 0 & 0 & 0 & 0 & 0.7 & 0.4 & 0.9 & 0 & 0 \\ 0 & 0 & 0 & 0 & 0 & 0 & 0.5 & 0.5 & 0.7 & 0 \\ 0 & 0 & 0 & 0 & 0 & 0 & 0 & 0.9 & 0.3 & 0.9 \\ 0.9 & 0 & 0 & 0 & 0 & 0 & 0 & 0 & 0.8 & 0.3 \end{pmatrix} \tag{3.2}$$

$$W_o = \begin{pmatrix} 0.3 & 0.7 & 0 & 0 & 0 & 0 & 0 & 0 & 0.5 & 0.3 \\ 0.3 & 0.2 & 0.5 & 0 & 0 & 0 & 0 & 0 & 0 & 0.7 \\ 0 & 0.1 & 0.3 & 0.5 & 0 & 0 & 0 & 0 & 0 & 0 \\ 0 & 0.5 & 0.2 & 0.2 & 0.5 & 0 & 0 & 0 & 0 & 0 \\ 0.5 & 0 & 0 & 0.5 & 0.1 & 0.9 & 0 & 0 & 0 & 0 \\ 0 & 0 & 0 & 0 & 0.3 & 0.3 & 0.5 & 0.4 & 0 & 0 \\ 0 & 0 & 0 & 0.6 & 0 & 0.2 & 0.3 & 0.5 & 0 & 0 \\ 0 & 0 & 0 & 0 & 0 & 0 & 0.5 & 0.3 & 0.5 & 0 \\ 0 & 0 & 0 & 0 & 0 & 0 & 0 & 0.2 & 0.3 & 0.7 \\ 0.7 & 0 & 0 & 0 & 0 & 0 & 0 & 0.2 & 0.3 & 0.5 \end{pmatrix}$$

Most of the non-zero elements are near the diagonal lines because of the locality of the synaptic connections. The other non-zero elements at the upper-right or the lower-left corners of the matrices originate from the boundary condition that the 1^{st} mitral and granule cells are the neighbors of the N^{th} mitral and the M^{th} granule cells.

No biological data are available for the synaptic strengths (amount of postsynaptic depolarization or hyperpolarization : presynaptic firing rate) in the bulb. Since

$$\textit{postsynaptic input} \;=\; \textit{synaptic strength} \times \textit{presynaptic output},$$

doubling the synaptic strength and at the same time reducing the presynaptic input by half will cause no effect on the postsynaptic side. Therefore, W_o and H_o should be set according to the scales of g_x and g_y used for the mitral and granule cell output functions, respectively. Furthermore, when a mitral cell and a granule cell interact with each other with synaptic strength w and h respectively, the gain of this feedback loop is proportional

to hw. Thus the scale of h (or H_o) should be set appropriately depending on the scale of w (or W_o) to keep the feedback loop gain in a certain range. It is shown in Chapter 4 that this loop gain affects the neural oscillatory frequency. For convenience, H_o and W_o are set to about the same scale, whose value is such that the oscillation in the simulated model has a similar frequency range as that of the real bulb. The individual elements of H_o and W_o are set such that: 1), the connections between the mitral and granule cells are largely reciprocal as the mitral-granule dendrodendritic connections in real bulb; i.e., if $H_{o,ij} \neq 0$, then $W_{o,j,i}$ has a large chance of being non-zero also; 2), although the elements' value in H_o and W_o look quite random, they are carefully chosen such that some input odor patterns can easily induce oscillatory activities within the bulbar cells (see Chapter 6 for mathematical analysis). However, the mathematical formulation does not depend on the exact values of H_o and W_o.

3.5 System of Differential Equations in the Olfactory Bulb Model

The format of the model is summarized here by the system of differential equations:

$$\begin{aligned} \dot{X} &= -H_o G_y(Y) - \alpha_x X + I \\ \dot{Y} &= W_o G_x(X) - \alpha_y Y + I_c \end{aligned} \tag{3.3}$$

where $X = \{x_1, x_2, \ldots, x_N\}$ are mitral cell activities;

$Y = \{y_1, y_2, \ldots, y_M\}$ are granule cell activities;

$G_x(X) = \{g_x(x_1), g_x(x_2), \ldots, g_x(x_N)\}$ are output of the mitral cells;

$G_y(Y) = \{g_y(y_1), g_y(y_2), \ldots, g_y(y_M)\}$ are output of the granule cells;

$I = \{I_1, I_2, \ldots, I_N\}$, are the external input to the mitral cells.

$I_c = \{I_{c1}, I_{c2}, \ldots, I_{cM}\}$, are the central input to the granule cells; W_o and $-H_o$ are the synaptic-strength matrices from mitral cells to granule cells, and vice versa. The matrix elements are: $H_{o,ij} \geq 0$ and $W_{o,ji} \geq 0$ for $i = 1, 2, \ldots, N$, and $j = 1, 2, \ldots, M$. The inhibitory nature of the granule cells are indicated by a minus sign in front of H_o in the equations above; $\alpha_x = 1/\tau_x$ and $\alpha_y = 1/\tau_y$ are decay constants of mitral and granule cells, respectively;

Comparing this equation to Equation (1.1), it can be seen that

$$u_1, u_2, \ldots, u_{N+M} \rightarrow x_1, x_2, \ldots, x_N, y_1, y_2, \ldots, y_M$$

$$V_1, V_2, \ldots, V_{N+M} \rightarrow g_x(x_1), g_x(x_2), \ldots, g_x(x_N), g_y(y_1), g_y(y_2), \ldots, g_y(y_M)$$

$$T \rightarrow \begin{pmatrix} 0 & -H_o \\ W_o & 0 \end{pmatrix}$$

$$I \rightarrow \begin{pmatrix} I \\ I_c \end{pmatrix}.$$

In the simulations, weak random noise with a 7 $msec$ correlation time is added to I and I_c to simulate the fluctuations in the system.

4. Mathematical Analysis

In this chapter, the mechanism for oscillation, pattern formation, and computation processes in the olfactory bulb are studied.

4.1 The Oscillation Mechanism

The origin of the oscillation in the bulb model is a group of oscillators. The intuitive way to see the oscillation mechanism is via a single oscillator.

4.1.1 Single oscillator

An oscillator with frequency ω can be described by the differential equations

$$\begin{aligned} \dot{x} &= -\omega y \\ \dot{y} &= \omega x \end{aligned} \qquad or \qquad \ddot{x} + \omega^2 x = 0 \tag{4.1}$$

with solution:

$$x = r_o sin(\omega t + \phi) \qquad y = -r_o cos(\omega t + \phi),$$

where r_o and ϕ are arbitrary real constants describing the oscillation amplitude and phase, which depend on the initial conditions. The $x(t)$, $y(t)$ trajectory is a circle:

$$x^2 + y^2 = constant.$$

With dissipation, Equation (4.1) becomes

$$\begin{aligned} \dot{x} &= -\omega y - \alpha x \\ \dot{y} &= \omega x - \alpha y \end{aligned} \qquad or \qquad \ddot{x} + 2\alpha\dot{x} + (\omega^2 + \alpha^2)x = 0. \tag{4.2}$$

The solution becomes

$$x = r_o e^{-\alpha t} sin(\omega t + \phi) \qquad y = r_o e^{-\alpha t} sin(\omega t + \phi - \pi/2),$$

where α is the dissipation constant. The solution orbit is no longer a circle, but spirals into the origin as (Fig [4.1A])

$$d(x^2 + y^2)/dt = -2\alpha(x^2 + y^2);$$

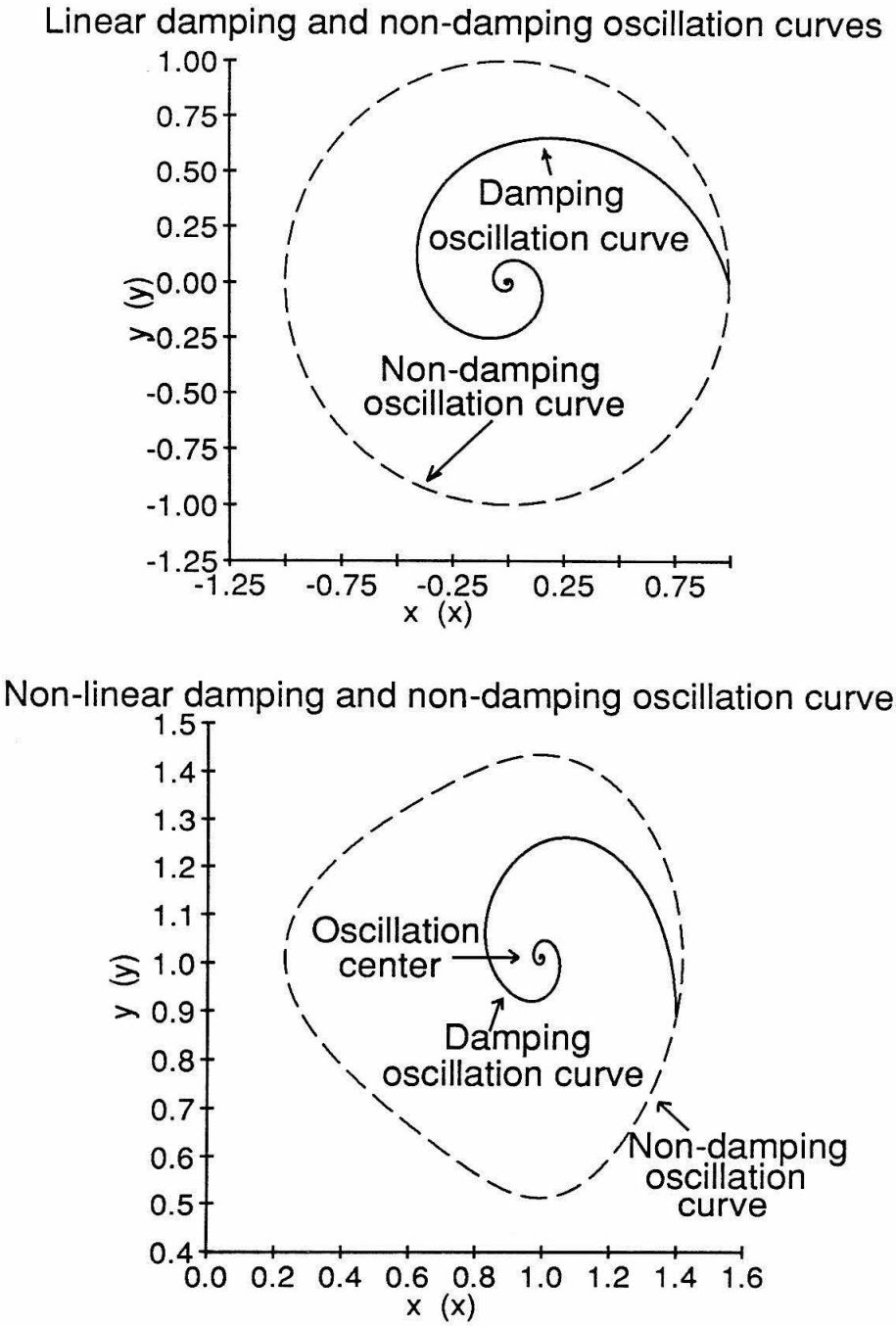

Fig 4.1 oscillation trajectories in linear (upper) and non-linear (lower) oscillations.

i.e., the oscillation amplitude decays.

If a mitral cell and a granule cell are connected to each other (Fig [4.2A]) with connection strength h and w, respectively, and with inputs $i(t)$ and $i_c(t)$, respectively, then

$$\begin{aligned} \dot{x} &= -h \cdot g_y(y) - \alpha_x x + i(t), \\ \dot{y} &= w \cdot g_x(x) - \alpha_y y + i_c(t). \end{aligned} \tag{4.3}$$

This is the scalar version of Equation (3.3) with each upper-case letter representing a vector or matrix replaced by a lower-case letter representing a scalar. It is assumed that $i(t)$ has a much slower time course than x or y, because the frequency of sniffs is considerably lower than the characteristic neural oscillation frequency, and that i_c, input from higher centers, will be kept fixed when the central control is not considered. Use the adiabatic approximation, and define the equilibrium point (x_o, y_o) as

$$\begin{aligned} \dot{x}_o \approx 0 &= -h \cdot g_y(y_o) - \alpha_x x_o + i, \\ \dot{y}_o \approx 0 &= w \cdot g_x(x_o) - \alpha_y y_o + i_c. \end{aligned} \tag{4.4}$$

Define $x' \equiv x - x_o$, $y' \equiv y - y_o$; then

$$\begin{aligned} \dot{x}' &= -h(g_y(y) - g_y(y_o)) - \alpha_x x', \\ \dot{y}' &= w(g_x(x) - g_x(x_o)) - \alpha_y y'. \end{aligned}$$

This is already similar to Equation (4.2). Omitting the dissipation, $\alpha_x = \alpha_y = 0$, the system is a Hamiltonian system. Then, when x' and y' are small, they oscillate along the solution orbit

$$R \equiv \int_{x_o}^{x_o + x'} w(g_x(s) - g_x(x_o))ds + \int_{y_o}^{y_o + y'} h(g_y(s) - g_y(y_o))ds = constant,$$

which is a closed curve (in general, not a circle or ellipse) in the original (x, y) space surrounding the point (x_o, y_o), if R is not too large (Fig [4.1B]). This means that (x, y) oscillates around the point (x_o, y_o), although the oscillation is not sinusoidal when g's are non-linear. (Strictly speaking, If R is too large, the curve could be closed at infinity

$(-\infty, -\infty)$ if $g_x(x), g_y(y) = 0$ for $x, y <, 0$. Also, equilibrium point (x_o, y_o) may not exist if $\alpha_x = \alpha_y = 0$ and $g_x(x) = g_y(y) = 0$ for $x, y < 0$. The above treatment is only to have an intuitive understanding of the oscillation in a pair of interconnected mitral and granule cells.) The oscillation becomes strictly sinusoidal if g's are linear functions, and the solution orbit in the (x, y) space will be an ellipse around (x_o, y_o).

When the dissipation is included, the orbit in (x, y) space will spiral into the point (x_o, y_o):

$$dR/dt = -\alpha_x w(g_x(x) - g_x(x_o))(x - x_o) - \alpha_y h(g_y(y) - g_y(y_o))(y - y_o) \leq 0.$$

Here $dR/dT \leq 0$, because g_x and g_y are non-decreasing. The oscillation amplitude shrinks. Therefore, a connected pair of mitral and granule cells behaves as a damped non-linear oscillator, whose oscillation center (x_o, y_o) is determined by the external inputs i and i_c by Equation (4.4). If the oscillation amplitude is small, then the system can be approximated by a damped, sinusoidal oscillator via linearization around (x_o, y_o):

$$\begin{aligned} \dot{x} &= -h \cdot g_y'(y_o)y - \alpha_x x \\ \dot{y} &= w \cdot g_x'(x_o)x - \alpha_y y, \end{aligned} \tag{4.5}$$

where (x, y) are now the deviation from (x_o, y_o). The solution is

$$x = r_o e^{-\alpha t} sin(\omega t + \phi) \qquad y = r_o e^{-\alpha t} sin(\omega t + \phi - \pi/2),$$

where $\alpha = (\alpha_x + \alpha_y)/2$, and $\omega = \sqrt{hwg_x'(x_o)g_y'(y_o) + (\alpha_x - \alpha_y)^2/4}$. If $\alpha_x = \alpha_y$, which is about right in the bulb, then $\alpha = \alpha_x = \alpha_y$, $\omega = \sqrt{hwg_x'(x_o)g_y'(y_o)}$. Using the bulbar cell time constant and the oscillation frequency from the previous section, $\alpha \approx 0.3\omega$. Notice that x and y differ in oscillation phase by a quarter cycle (cf. Section 4.3). The dependence of oscillation frequency ω on the synaptic strengths h and w shown above is used to choose the scales of h and w (or H_o and W_o), so that the model bulb oscillation frequency agrees with the biological data (Chapter 3). The effect of the input controlled equilibrium point (x_o, y_o) on the frequency ω shown above implies that the oscillation frequency is

modulated by the receptor and central input in the real system. The equilibrium point (x_o, y_o) is always stable; i.e., the non-linear oscillation is always damped, and no sustained oscillation will exist unless an external oscillating input exists.

The larger the oscillation amplitude, the worse the small amplitude approximation, and the more distorted the oscillation waveform from a sinusoidal one. The oscillation can have quite a complex non-sinusoidal waveform if (x_o, y_o) is near a very non-linear region of g's.

4.1.2 Granule cell as a non-linear Leaky Integrator

The mitral cell in the single oscillator system acts back on itself indirectly through a granule cell. Without this granule cell, then the equation for the mitral cell will be:

$$\dot{x} = w' g_x(x) - \alpha_x x,$$

where w' is the mitral cell synaptic strength on itself. This solution for x approaches a fixed value instead of being oscillatory.

An intermediate granule cell integrates the output from the mitral cell and acts back onto the mitral cell, and makes the oscillation possible, although it is not the bulbar output cell. Its self-dissipation makes it a leaky integrator. An analogous oscillatory system is an electric circuit, where an inductance and a capacitor are connected together in a loop (Fig [4.2B]), whose equation of motion is

$$L\dot{I} = -V - I \cdot R_L$$

$$C\dot{V} = I - V/R_C,$$

where L and C are inductance and capacitance, I and V are current and voltage, R_L and R_C are the resistances in the inductor and the capacitor. The mitral cell is like the inductor, whose activity is indicated by the current, and the granule cell is like the capacitor, whose activity is described by the voltage. The capacitor integrates the current from the inductor and feeds back the voltage. The neural non-linearity makes the granule cell here a non-linear, leaky integrator.

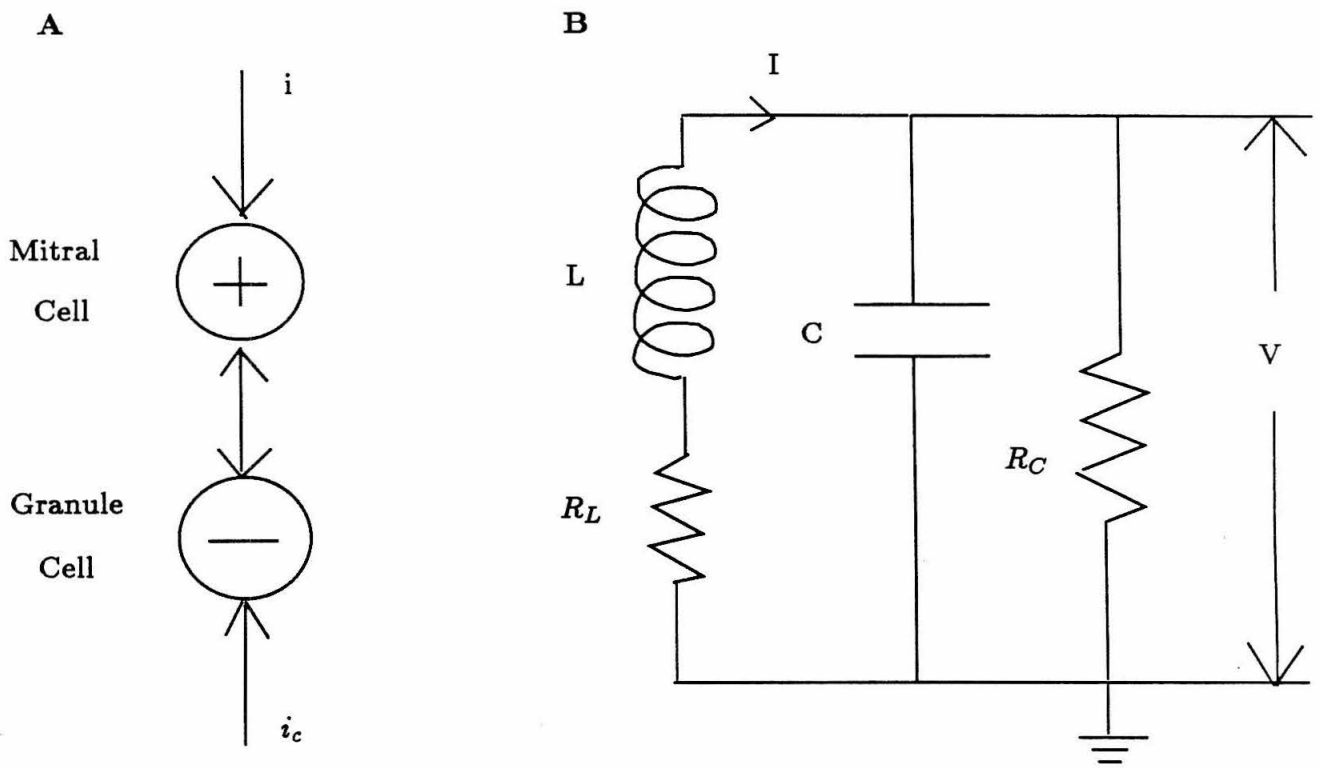

Fig. 4.2 Two oscillatory systems. **A:** a connected pair of mitral and granule cells. **B:** a dissipative LC circuit.

4.1.3 Coupled Non-linear Oscillators

When a group of granule cells replaces the single granule cell in the connected mitral-granule cell pair (since there are many more granule cells than the mitral cells in the real bulb), it can be seen as a single granule cell, whose synaptic strength is as strong as those of all the granule cells in the group combined. Therefore, such a connected mitral and granule cell group is also a non-linear, damped oscillator. Similar argument holds if the number of mitral cells was larger than the number of granule cells. N such mitral-granule pairs without interconnections between the pairs represent a group of N independent, damped, non-linear oscillators. If the cells in one oscillator also connect to cells in the neighboring oscillators, then these oscillators are no longer independent. This is exactly the situation in the olfactory bulb. A granule cell receiving input from a certain mitral cell gives output to other mitral cells as well. Similarly, a mitral cell gives output also to the granule cells that do not give output to this mitral cell. The local bulbar synaptic connections imply the local oscillator couplings. This situation can be quantitatively treated by including many neurons in the mathematical analysis.

Proceed as in the single oscillator case,

$$\begin{aligned} \dot{X} &= -H_o G_y(Y) - \alpha_x X + I, \\ \dot{Y} &= W_o G_x(X) - \alpha_y Y + I_c, \end{aligned} \tag{4.6}$$

where X, Y, I,I_c,$G_x(X)$, and $G_y(Y)$ are now vectors, and H_o and W_o are matrices as described earlier (cf. Equation (4.3)). Use the adiabatic approximation and define the equilibrium point (X_o, Y_o), similar to that of a single oscillator, as:

$$\begin{aligned} \dot{X}_o \approx 0 &= -H_o G_y(Y_o) - \alpha_x X_o + I, \\ \dot{Y}_o \approx 0 &= W_o G_x(X_o) - \alpha_y Y_o + I_c. \end{aligned} \tag{4.7}$$

And

$$\dot{X}_o = \dot{Y}_o = 0 \qquad if \qquad \dot{I} = \dot{I}_c = 0.$$

Linearize around (X_o, Y_o); then

$$\begin{aligned} \dot{X} &= -H_o G'_y(Y_o) Y - \alpha_x X, \\ \dot{Y} &= W_o G'_x(X_o) X - \alpha_y Y, \end{aligned} \tag{4.8}$$

where (X, Y) are now the deviations from (X_o, Y_o), and $G'_x(X_o)$ and $G'_y(Y_o)$ are diagonal matrices

$$G'_x(X_o) = \begin{pmatrix} g'_x(x_{o,1}) & 0 & 0 & \cdots & \cdots & \\ 0 & g'_x(x_{o,2}) & 0 & \cdots & \cdots & \\ \vdots & \vdots & \ddots & \cdots & \cdots & \\ & & \cdots & g'_x(x_{o,i}) & \cdots & \\ \vdots & \vdots & \cdots & \ddots & \cdots & \\ & \cdots & \cdots & \cdots & \cdots & g'_x(x_{o,N}) \end{pmatrix}$$

and

$$G'_y(Y_o) = \begin{pmatrix} g'_y(y_{o,1}) & 0 & 0 & \cdots & \cdots & \\ 0 & g'_y(y_{o,2}) & 0 & \cdots & \cdots & \\ \vdots & \vdots & \ddots & \cdots & \cdots & \\ & & \cdots & g'_y(y_{o,i'}) & \cdots & \\ \vdots & \vdots & \cdots & \ddots & \cdots & \\ & \cdots & \cdots & \cdots & \cdots & g'_y(y_{o,M}) \end{pmatrix}.$$

Define $H \equiv H_o G'_y(Y_o)$, $W \equiv W_o G'_x(X_o)$; then:

$$\begin{aligned} \dot{X} &= -H \cdot Y - \alpha_x X, \\ \dot{Y} &= W \cdot X - \alpha_y Y. \end{aligned} \tag{4.9}$$

To see the picture clearly, first assume $\alpha_x, \alpha_y \ll H, W$. Ignoring the decay terms, it becomes (cf. Equation (4.1))

$$\begin{aligned} \dot{X} &= -H \cdot Y, \\ \dot{Y} &= W \cdot X. \end{aligned} \tag{4.10}$$

Thus

$$\ddot{X} + A \cdot X = 0, \tag{4.11}$$

where $A \equiv HW$ is a $N \times N$ matrix.

The individual components of Equation (4.11) are:

$$\ddot{x}_i + A_{ii} x_i + \sum_{j \neq i} A_{ij} x_j = 0 \tag{4.12}$$

for $i = 1, 2, \ldots N$. Note that since H and W are matrices with non-negative elements, $A_{ij} \geq 0$ for all i, j. In particular, $A_{ii} \geq 0$.

The first two terms in Equation (4.12) represent the dynamics of the i^{th} oscillator (see Equation (4.1)), while the last term in the equation represents the coupling with the other oscillators. If A is a diagonal matrix, the coupling term is zero, and Equation (4.12) describes a group of N independent oscillators.

Since the cells in the olfactory bulb connect only to their neighboring cells, the connection matrices H_o and W_o have most of their non-zero elements near the diagonal lines. It follows that matrix A also has most of its non-zero elements near the diagonal line. Therefore, each oscillator in the system is coupled only to its neighboring oscillators.

The elements of matrix A are

$$A_{ij} = \sum_k H_{o,ik} g'_y(y_{o,k}) W_{o,kj} g'_x(x_{o,j}). \tag{4.13}$$

This means that the coupling from the j^{th} oscillator to the i^{th} oscillator goes through the connection path from the j^{th} mitral cell to the i^{th} mitral cell via all those intermediate granule cells. In particular , A_{ii}, the strength of the i^{th} oscillator, originates from the connection path from i^{th} mitral cell back to itself via the intermediate granule cells. In the particular simulated model as an example, the H_o and W_o (Equation (3.2)) used implies that each cell connects to about three neighboring cells, so from the above argument, each oscillator couples to about 5 neighboring oscillators.

Taking into account the decay terms:

$$\begin{aligned} \dot{X} &= -H \cdot Y - \alpha_x X, \\ \dot{Y} &= W \cdot X - \alpha_y Y. \end{aligned} \tag{4.14}$$

After differentiating, it becomes

$$\ddot{X} = -H \cdot \dot{Y} - \alpha_x \dot{X}$$

$$= -H(W \cdot X - \alpha_y Y) - \alpha_x \dot{X}.$$

Substituting with $Y = -H^{-1}(\dot{X} + \alpha_x X)$, where H^{-1} is the pseudo-inverse of H, and $H^{-1}H = 1$, then

$$\ddot{X} + (\alpha_x + \alpha_y)\dot{X} + (HW + \alpha_x\alpha_y)X = 0$$

or

$$\ddot{X} + (\alpha_x + \alpha_y)\dot{X} + (A + \alpha_x\alpha_y)X = 0. \tag{4.15}$$

This is a generalization of Equation (4.2) for a group of N coupled dissipative oscillators, and a generalization of Equation (4.11) with extra dissipation. The i^{th} oscillator (mitral cell) follows the equation

$$\ddot{x}_i + (\alpha_x + \alpha_y)\dot{x}_i + (A_{ii} + \alpha_x\alpha_y)x_i + \sum_{j \neq i} A_{ij}x_j = 0. \tag{4.16}$$

The first three terms describe a single damped(i^{th}) oscillator (cf. Equation (4.2)), while the last term describes the coupling to other oscillators.

Equation (4.15) is only the small amplitude approximation of Equation (4.6). The non-linear effect shows with larger amplitude oscillations just as in the case for a single oscillator. Therefore Equation (4.6), which is the mathematical model for the olfactory bulb, describes a system of N non-linear dissipative oscillators, each coupled to its neighbors. This explains the mechanism of oscillation in the olfactory bulb.

From oscillation Equation (4.15), it shows that the matrix $A = H_o G'_y(Y_o) W_o G'_x(X_o)$ determines the dynamics. When the scales of H_o, W_o, G_x, and G_y are considered, only their multiplication is important. This means that as long as the scale multiplication is kept constant, their individual scales can be varied. This is how the scales for these parameters are determined in Chapter 3. Of course, for fixed external input I and I_c, the scales of H_o and W_o influence the values of X_o and Y_o by Equation (4.7). This in turn influences the matrix A and the oscillation dynamics. However in this model, the scales for the parameters H_o, W_o, G_x, and G_y are set first before setting the external input scales for appropriate X_o and Y_o (see Chapter 3 and 4).

4.2 Oscillation Pattern Analysis

Consider the non-dissipative equation

$$\ddot{X} + AX = 0. \tag{4.11}$$

If X_k is one of the eigenvectors of A with eigenvalue λ_k, Equation (4.11) has solutions:

$$X \propto X_k e^{\pm i\sqrt{\lambda_k}t} = X_k e^{\pm i\omega_{ko}t} \tag{4.17}$$

for $k = 1, 2 \ldots N$, where $\omega_{ko} \equiv \sqrt{\lambda_k}$. The equation has N such linearly independent oscillation modes. Denote solution $X_k e^{\pm i\sqrt{\lambda_k}t}$ as the k^{th} mode of the system. The oscillation amplitude and phase of the i^{th} mitral cell in the k^{th} mode is determined by the i^{th} component of the complex vector X_k. Note that ω_{ko} is a complex valued frequency; i.e., the oscillation modes can have increasing or decreasing amplitudes as they evolve in time.

Including the dissipation of each oscillator,

$$\ddot{X} + (\alpha_x + \alpha_y)\dot{X} + (A + \alpha_x\alpha_y)X = 0. \tag{4.15}$$

The k^{th} oscillation mode becomes

$$X \propto X_i e^{i\omega_k t} \equiv X_k exp(-\frac{(\alpha_x + \alpha_y)}{2}t \pm i\sqrt{\lambda_k + \frac{(\alpha_x - \alpha_y)^2}{4}}t) \tag{4.18}$$

for $k = 1, 2, \ldots N$, where ω_k is the solution of

$$-\omega_k^2 + i\omega_k(\alpha_x + \alpha_y) + (\lambda_k + \alpha_x\alpha_y) = 0. \tag{4.19}$$

Note that $\omega_k = \omega_{ko} = \sqrt{\lambda_k}$ if $\alpha_x = \alpha_y = 0$. Therefore, extra damping is added to each oscillation mode if dissipation of the oscillators is included. When $\alpha_x = \alpha_y = \alpha$, the oscillation modes become:

$$X \propto X_k e^{-\alpha t \pm i\sqrt{\lambda_k}t} \tag{4.20}$$

for $k = 1, 2, \ldots, N$. From now on, $\alpha_x = \alpha_y = \alpha$ is used in the mathematical expressions, since the time constants of the mitral and granule cells are similar. The equation becomes

$$\ddot{X} + 2\alpha\dot{X} + (A + \alpha^2)X = 0. \tag{4.21}$$

If

$$Re(-\alpha \pm i\sqrt{\lambda_k}) > 0 \tag{4.22}$$

is satisfied for some $k \in 1, 2, \ldots N$, then the oscillation amplitude for k^{th} mode will increase with time. Starting from an initial condition of arbitrary small amplitudes in linear analysis, the mode with the fastest growing amplitude will dominate the output. When there is a single dominating mode, the whole bulb oscillates in the same frequency as observed physiologically (Freeman 1978; Freeman and Schneider 1982) and in the simulation. In large amplitude oscillations, the non-linear effect plays an important role. The oscillation waveform will not be strictly sinusoidal. The N oscillation modes will no longer be independent. The strongest modes will suppress the others. The final activity output will be a single "mode" in a non-linear regime, i.e., a single dominating mode mixed with other non-dominating modes excited by the coupling with the dominating mode.

The collective oscillation mode is a result of coupling. Each oscillator gets external driving "forces" from the neighboring oscillators. The driving "force" for the i^{th} oscillator is $F_i \equiv -\sum_j A_{ij} x_j$. When the oscillators influence each other in harmony, a global oscillation mode results. The oscillation amplitude of the i^{th} oscillator will increase when its driving "force" feeds in more energy than the energy lost through the damping "force" $-(\alpha_x + \alpha_y)\dot{x}_i$ (see Section 4.3.3). An oscillation mode with growing amplitude emerges when each oscillator with substantial amplitude in the mode has enough driving "force" through coupling with other oscillators. It is known that an ordinary coupled oscillator system (e.g., a group of pendulums connected by springs) can not have growing oscillation modes because of energy conservation. This is because when one oscillator drives another oscillator, it gets a reaction force equal to the driving force by Newton's third law. This means that one oscillator feeding energy to another has to lose the same amount of energy. The special coupled oscillator system in this model does not obey Newton's third law; the coupling forces between the i^{th} and j^{th} oscillators, $-A_{ij}x_j$ and $-A_{ji}x_i$, are not necessarily equal. Therefore, the oscillation energy is not conserved, and the growing oscillation modes

are possible. Recall that a single oscillator in this model is always damped; this means that the equilibrium point (x_o, y_o) is always stable. Because of the coupling between the oscillators, the equilibrium point (X_o, Y_o) of a **group** of oscillators **is no longer always stable** with the possibility of growing oscillation modes. (X_o, Y_o) is going to be called operation point or biase sometimes, to avoid confusion.

The only non-zero elements in matrices H_o, W_o, $G'_x(X_o)$, and $G'_y(Y_o)$ are positive valued ones near the diagonal lines. Thus, $A = H_o G'_y(Y_o) W_o G'_x(X_o)$, is also a matrix with its only non-zero elements positive and near the diagonal line. Thus, very few of the eigenvalues of A are expected to have $\lambda_k < 0$ for some $k \in 1, 2 \ldots N$. If $\lambda_k < 0$ for some k, there could be a non-oscillating exponentially growing mode. Since this is not observed in the olfactory bulb, A is assumed to have no negative real eigenvalues in most practical cases of synaptic connections.

In order that some mode X_k can be both growing and oscillatory, λ_k must be complex. For this, a necessary (but not sufficient) condition is that matrix A be non-Hermitian, or non-symmetric in this case of real matrix A. It follows that systems of less than three oscillators will not have growing modes, since a matrix of dimension 1 or 2 (1 or 2 oscillators) with non-negative elements only has real eigenvalues.

4.2.1 Examples of the Oscillation Modes

If H_o is symmetric and W_o is proportional to identity, e.g.,

$$H_o = \begin{pmatrix} h & h' & 0 & 0 & & \ldots & & 0 & h' \\ h' & h & h' & 0 & & \ldots & & 0 & 0 \\ 0 & h' & h & h' & 0 & 0 & \ldots & 0 & 0 \\ \vdots & \vdots & & & & \ldots & \ddots & & \vdots \\ h' & 0 & & & \ldots & & 0 & h' & h \end{pmatrix}$$

$$W_o = \begin{pmatrix} w & 0 & 0 & 0 & & \ldots & & 0 & 0 \\ 0 & w & 0 & 0 & & \ldots & & 0 & 0 \\ 0 & 0 & w & 0 & 0 & 0 & \ldots & 0 & 0 \\ \vdots & \vdots & & & & \ldots & \ddots & & \vdots \\ 0 & 0 & & & \ldots & & 0 & 0 & w \end{pmatrix} \qquad (4.23)$$

This corresponds to each mitral cell's giving output only to the nearest granule cell, and to each granule cell's giving output to the three nearest mitral cells. Moreover, if X_o

and Y_o are vector with identical components, i.e., $x_{o,i} = x_{o,j}$, and $y_{o,i'} = y_{o,j'}$ for all $i \neq j$ and $i' \neq j'$, then both $G'_x(X_o)$ and $G'_y(Y_o)$ are proportional to the identity matrix. $A = H_o G'_y(Y_o) W_o G'_x(X_o)$ should be symmetric and have the form

$$A = \begin{pmatrix} a & b & 0 & 0 & & \dots & & 0 & b \\ b & a & b & 0 & & \dots & & 0 & 0 \\ 0 & b & a & b & 0 & 0 & \dots & 0 & 0 \\ 0 & 0 & b & a & b & 0 & \dots & 0 & 0 \\ \vdots & \vdots & & & & \dots & \ddots & & \vdots \\ 0 & 0 & & & \dots & & b & a & b \\ b & 0 & & & \dots & & 0 & b & a \end{pmatrix}. \tag{4.24}$$

The N oscillation modes for Equation (4.21) will be

$$\begin{pmatrix} sin(k1) \\ sin(k2) \\ \vdots \\ sin(ki) \\ \vdots \\ sin(kN) \end{pmatrix} e^{-\alpha t \pm i\sqrt{\lambda_k}t} \qquad \begin{pmatrix} cos(k1) \\ cos(k2) \\ \vdots \\ cos(ki) \\ \vdots \\ cos(kN) \end{pmatrix} e^{-\alpha t \pm i\sqrt{\lambda_k}t}, \tag{4.25}$$

where $k = \frac{K}{2\pi N}$, K is an integer, $0 \leq K < \frac{N}{2}$, $\lambda_k = a + 2bcos(k)$. For $b < a/2$, $\lambda_k > 0$, all the modes will be damped oscillations with similar frequences close to $\omega = \sqrt{a}$. In each mode, all the oscillators have the same oscillation phase, but different amplitudes.

The same matrix A and thus the same oscillation modes above can be achieved by some different synaptic connection patterns such as, for example (with X_o and Y_o staying the same),

$$H_o = \begin{pmatrix} h & h' & 0 & 0 & & \dots & & 0 & 0 \\ 0 & h & h' & 0 & & \dots & & 0 & 0 \\ 0 & 0 & h & h' & 0 & 0 & \dots & 0 & 0 \\ \vdots & \vdots & & & & \dots & \ddots & & \vdots \\ 0 & 0 & & & \dots & & 0 & h & h' \\ h' & 0 & & & \dots & & 0 & 0 & h \end{pmatrix}$$

$$W_o = \begin{pmatrix} w & 0 & 0 & 0 & & \dots & & 0 & w' \\ w' & w & 0 & 0 & & \dots & & 0 & 0 \\ 0 & w' & w & 0 & 0 & 0 & \dots & 0 & 0 \\ \vdots & \vdots & & & & \dots & \ddots & & \vdots \\ 0 & 0 & & & \dots & & w' & w & 0 \\ 0 & 0 & & & \dots & & 0 & w' & w \end{pmatrix}, \tag{4.26}$$

where $h'w = w'h$. The connection pattern is that each granule cell give output to the nearest and the first mitral cell on the right, and that each mitral cell give output to the nearest and the first granule cell on the left.

Another example is with a non-symmetric matrix

$$A = \begin{pmatrix} a & b & c & 0 & & \cdots & & 0 & 0 \\ 0 & a & b & c & & \cdots & & 0 & 0 \\ 0 & 0 & a & b & c & 0 & \cdots & 0 & 0 \\ \vdots & \vdots & & & & \cdots & \ddots & & \vdots \\ c & 0 & & & \cdots & & 0 & a & b \\ b & c & & & \cdots & & 0 & 0 & a \end{pmatrix}, \tag{4.27}$$

which can be achieved if, for example, each mitral (granule) cell gives output to its nearest and the first granule (mitral) cell on the right with connection pattern

$$H_o = \begin{pmatrix} h & h' & 0 & 0 & & \cdots & & 0 & 0 \\ 0 & h & h' & 0 & & \cdots & & 0 & 0 \\ 0 & 0 & h & h' & 0 & 0 & \cdots & 0 & 0 \\ \vdots & \vdots & & & & \cdots & \ddots & & \vdots \\ 0 & 0 & & & \cdots & & 0 & h & h' \\ h' & 0 & & & \cdots & & 0 & 0 & h \end{pmatrix}$$

$$W_o = \begin{pmatrix} w & w' & 0 & 0 & & \cdots & & 0 & 0 \\ 0 & w & w' & 0 & & \cdots & & 0 & 0 \\ 0 & 0 & w & w' & 0 & 0 & \cdots & 0 & 0 \\ \vdots & \vdots & & & & \cdots & \ddots & & \vdots \\ 0 & 0 & & & \cdots & & 0 & w & w' \\ w' & 0 & & & \cdots & & 0 & 0 & w \end{pmatrix}, \tag{4.28}$$

and with X_o and Y_o proportional to the identity vector.

Then the oscillation pattern will be

$$\begin{pmatrix} e^{i\beta} \\ e^{2i\beta} \\ \vdots \\ e^{im\beta} \\ \vdots \\ e^{iN\beta} \end{pmatrix} e^{-\alpha t \pm i\sqrt{\lambda_\beta}\, t}, \qquad \begin{aligned} &\beta = 2\pi K/N, \\ &K \text{ is an integer}, \\ &0 \le K < N, \\ &\lambda_\beta = a + be^{i\beta} + ce^{2i\beta}. \end{aligned} \tag{4.29}$$

Notice that in this case, λ_β's are non-real complex numbers. It is possible to have growing modes if for some β, $Re(-\alpha \pm i\sqrt{\lambda_\beta}) > 0$. Also notice that the individual oscillators in most modes have different oscillation phases.

4.3 Explanation of the olfactory bulb activities

4.3.1 Oscillation phases for mitral and granule cells

This model predicts that the local mitral cells' oscillation phase leads that of the local granule cells by a quarter cycle, as is clear from the single oscillator analysis (Section 4.1). (This is analogous to the circuit of an inductor and a capacitor, in which the voltage and current differ by a quarter cycle in phase. See Section 4.1.2.) This is confirmed in experiments (Freeman 1975, Eeckman 1988a,1988b, Eeckman and Freeman 1985,1986, 1987), in which the local mitral cell unit activity was compared with the granule cell generated surface EEG waves for phase difference. (Note that the orientation of the granule cell dipole field gives the surface EEG wave an opposite sign to that of granule cell activities (Freeman 1975). Therefore, the sign of the EEG oscillation is reversed before comparing with the local mitral cell oscillation for phase differences.)

4.3.2 Oscillation frequencies

The model also indicates that for any particular stimulus, oscillatory activity should have the same dominant frequency everywhere on the bulb because of the single-mode dominance. This is also true in experiments (Freeman 1978; Freeman and Schneider 1982). Furthermore, the range of oscillation frequencies possible should be narrow. The observed range is $35 - 90$ Hz.

The i^{th} oscillation in the system follows the equation:

$$\ddot{x}_i + 2\alpha\dot{x}_i + (A_{ii} + \alpha^2)x_i = -\sum_{j\neq i} A_{ij}x_j$$

for $i = 1, 2, \ldots N$. The external driving force and the damping force for the oscillator are:

$$F_i \equiv -\sum_{j\neq i} A_{ij}x_j \tag{4.30}$$

and $-2\alpha\dot{x}_i$.

A damped oscillator will not have high-amplitude response unless the frequency of the external driving force is close to the oscillator resonant frequency. Therefore, an

oscillation mode will not be non-damping unless its frequency, which is the frequency of the driving force for every oscillator in the system, is close to the oscillators' resonant frequencies. It can be safely assumed that all the oscillators in the bulb have similar resonant frequencies. This is because the synaptic connection strengths and structure, which determine the frequencies (Section 4.1), are relatively uniform across the bulb. Since only the non-damping oscillation modes will be observable, the oscillation frequencies seen in experiments should be in a narrow spectrum that covers the resonant frequencies of the oscillators.

4.3.3 Oscillation phase gradient across the olfactory bulb

The physiological observation (Freeman 1978; Freeman and Schneider 1982) shows that the oscillations have different phases across the bulb, and thus give a phase gradient field. This phenomenon turns out to be a necessary condition for the existence of oscillation bursts.

For a damped i^{th} oscillator, if the driving force F_i is partially or completely in phase with the oscillator velocity $\dot{x}_i$ to compensate the dissipation, i.e.,

$$\int_{t_o}^{t_o+2\pi/\omega} F_i \dot{x}_i \cdot dt > \int_{t_o}^{t_o+2\pi/\omega} 2\alpha \dot{x}_i^2 \cdot dt > 0, \tag{4.31}$$

where ω is the oscillation frequency, then F_i feeds enough energy into the oscillator and helps to increase the oscillation amplitude. If all the neighboring oscillators x_j coupled to the i^{th} oscillator ($A_{ij} > 0$) are in phase with x_i, the inequality (4.3) can not hold because F_i is perpendicular to $\dot{x}_i$. Thus, the necessary condition for a growing (and thus observable) oscillation mode is that the coupled oscillators are not completely in phase. (This will not be necessarily true if the excitatory-to-excitatory (mitral-to-mitral) connections or other synaptic connections are present, since the nature of oscillator coupling will be different (Section 9.1).) Particularly, for a single mitral cell, the neighboring mitral cells that give output to it through the granule cells should not be all in phase with it in a non-decaying oscillation pattern. This means that the phase of the mitral cell oscillations change within

the range of the cell connections (from one mitral to another via the granule cells): several hundred microns laterally if that is the longest distance of connections. The granule cell oscillation is strongly related to that of the mitral cells, so the phase gradient field also exists in the granule cell population, and gets detected by EEG.

4.3.4 Sniff Control of the Olfaction

The fourth consequence of the model is that the oscillation activity will rise during the inhalation and fall at exhalation, and that the oscillatory wave rides on a slow background baseline shift wave phase locked with the sniff cycles.

Both the physiological observation and the simulation of our model show the bulb activity modulated by sniff input (Fig[2.5], Chapter 6, Freeman 1978, and Freeman and Schneider 1982). The operation point (equilibrium point) (X_o, Y_o) of the bulb is determined by the input (I, I_c) via

$$\begin{aligned} \dot{X}_o &= -H_o G_y(Y_o) - \alpha X_o + I, \\ \dot{Y}_o &= W_o G_x(X_o) - \alpha Y_o + I_c, \end{aligned} \tag{4.7}$$

$$\dot{X}_o = \dot{Y}_o = 0 \quad if \quad \dot{I} = 0 \quad (\dot{I}_c = 0 \quad is\ assumed).$$

Since $I = I_{odor} + I_{background}$, with $I_{background}$ assumed constant, the operation point (X_o, Y_o) will be determined by I_{odor} (the sniff input) alone.

If $I \rightarrow I + \delta I$ and $\delta \dot{I} = 0$, then

$$\begin{aligned} \delta \dot{X}_o &= -H \cdot \delta Y_o - \alpha \delta X_o + \delta I, \\ \delta \dot{Y}_o &= W \cdot \delta X_o - \alpha \delta Y_o. \end{aligned}$$

$\delta \dot{I} = 0$ leads to $\delta \dot{X}_o = \delta \dot{Y}_o = 0$. Thus,

$$\begin{aligned} \delta X_o &= (\alpha + H\alpha^{-1}W)^{-1}\delta I \\ &= (\alpha^2 + HW)^{-1}\alpha \delta I, \\ \delta Y_o &= (H + \alpha W^{-1}\alpha)^{-1}\delta I \\ &= (\alpha^2 + WH)^{-1}W\delta I. \end{aligned} \tag{4.32}$$

To see how the operation point (X_o, Y_o) changes with $\delta\dot{I}$, a differentiation on Equation (4.7) results

$$\begin{aligned}\delta\ddot{X}_o &= -H\delta\dot{Y}_o - \alpha\delta\dot{X}_o + \delta\dot{I} \\ &= -H(W\delta X_o - \alpha\delta Y_o) - \alpha\delta\dot{X}_o + \delta\dot{I} \\ &= -HW\delta X_o + H\alpha\delta Y_o - \alpha\delta\dot{X}_o + \delta\dot{I}.\end{aligned}$$

Similarly

$$\delta\ddot{Y}_o = -WH\delta Y_o - W\alpha\delta X_o - \alpha\delta\dot{Y}_o$$

Since the time scale of a sniff is much longer than the characteristic time of the neurons, adiabatic approximation is used to have

$$\delta\ddot{X}_o = \delta\ddot{Y}_o = \delta\dot{X}_o = \delta\dot{Y}_o = 0.$$

Solving for δX_o and δY_o, we get

$$\begin{aligned}\delta X_o &= (\alpha^2 + HW)^{-1}\delta\dot{I}, \\ \delta Y_o &= -(\alpha^2 + WH)^{-1}\alpha H^{-1}\delta\dot{I}.\end{aligned} \tag{4.33}$$

Combine Equation (4.32) and (4.33):

$$\begin{aligned}dX_o &\approx (\alpha^2 + HW)^{-1}(\alpha dI + d\dot{I}) \\ dY_o &\approx (\alpha^2 + WH)^{-1}(W dI - \alpha H^{-1}d\dot{I})\end{aligned} \tag{4.34}$$

A sniff for odor input takes a time of $\sim 300\ ms$, much longer than $\alpha^{-1} \sim 7\ ms$ and $\alpha(HW)^{-1} \leq \alpha^{-1}$. (Here $(HW)^{-1}$ means the scale of $(HW)^{-1} = A^{-1}$, which is the scale of ${\lambda_k}^{-1}$. $\alpha^2 \leq \lambda_k$ is assumed for the oscillation dissipation time constant α^{-1} is generally longer than the oscillation period $\sim 1/\sqrt{\lambda_k}$.) Therefore, the $d\dot{I}$ terms in equation (4.34) are negligible except at the initial inhalation and exhalation instant. Or

$$\begin{aligned}dX_o &\approx (\alpha^2 + HW)^{-1}\alpha dI \\ dY_o &\approx (\alpha^2 + WH)^{-1}W dI\end{aligned} \tag{4.35}$$

(X_o, Y_o) is the baseline shift or the neural oscillation center of the equation

$$\ddot{X} + 2\alpha\dot{X} + (A + \alpha^2)X = 0 \tag{4.21}$$

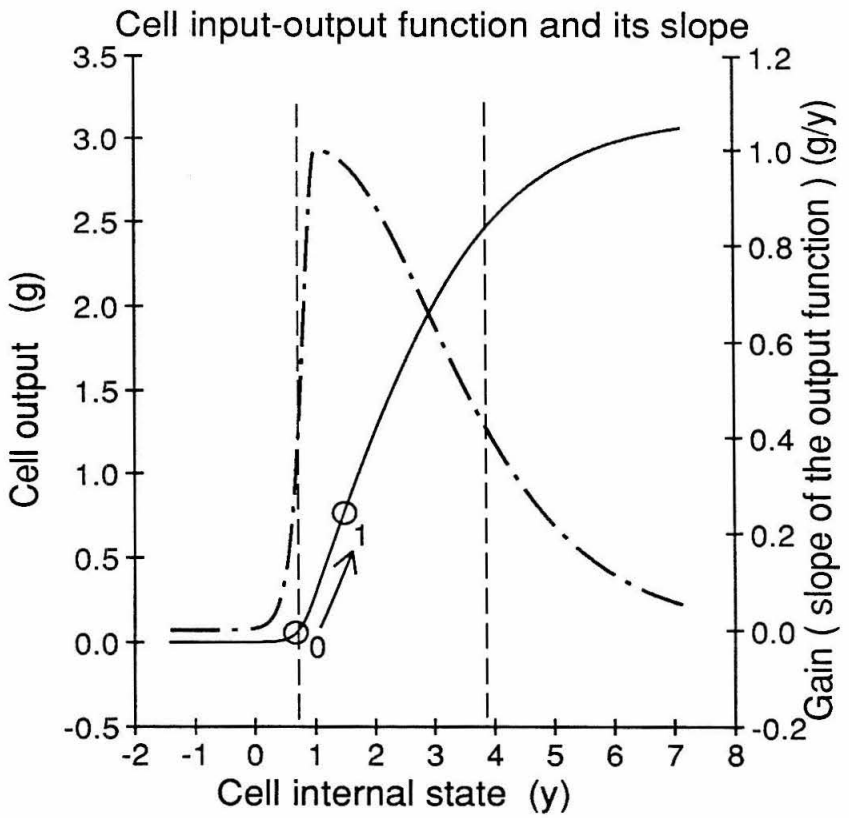

Figure 4.3: This figure illustrates the cell input-output function G (G_x or G_y) with the solid curve and its slope G' with the dotted curve. For the X_o or Y_o value on or outside dashed lines, the cell internal states can be considered either before firing threshold or at saturation regions, the gain G' is too small for the possibility of non-damping oscillation modesr, while for the X_o and Y_o values inside the dashed lines, the gain is larger and non-damping oscillation modes are possible in some circumstances. The circle indicated with "0" is the possible X_o and Y_o locations with no odor input $I_{odor} = 0$, and the circle "1" for possible X_o and Y_o locations during the inhale with odor inputs. The arrow indicates the direction in which the X_o and Y_o are raised by input odors.

Equation (4.35) states that this baseline shift is raised by odor input I during inhalation, when I is increasing, and suppressed by I during the exhalation, i.e., phase locked with the sniff cycles.

Furthermore, the oscillation Equation (4.21) will have a growing oscillation mode only if $Re(-\alpha \pm i\sqrt{\lambda_k}) > 0$ for some k, which means that only if the eigenvalue λ_k is large enough. This requires that the gain $(G'_x(X_o), G'_y(Y_o))$ be high enough to make $A = H_o G'_y(Y_o) W_o G'_x(X_o)$ large. As non-linear functions (Fig.[4.3]), the gains $G'_x(X_o)$ and $G'_y(Y_o)$ are very small when X_o and Y_o are low, and they get larger as (X_o, Y_o) increases before it reaches the saturation parts of the function G_x and G_y. Before inhalation, (X_o, Y_o) is low on the input-output curve and the gains are too small to have emerging oscillation bursts. During the inhalation, the increasing receptor input I raises (X_o, Y_o) towards higher gain points (Fig. [4.3]). When at some point $Re(-\alpha \pm i\sqrt{\lambda_k}) > 0$ is satisfied for some mode k, the oscillation mode emerges from noise. During the exhalation, the receptor input decreases, the process reverses its direction and the oscillation decays away. This explains the rise and fall of the oscillation bursts with the respiratory wave.

5. Computational Features in the Olfactory Bulb

The mathematical exploration on the model revealed the mechanism of oscillation patterns, the oscillation phase and amplitude relationships, the narrow oscillation frequency spectrum, the close relationship between the input sniff and the bulbar activity, etc. The implication of this model on the information processing of the bulb is studied here.

5.1 Information extraction procedure from sniff-input pattern to bulb-output pattern

Sniff-input pattern determines the equilibrium point (X_o, Y_o) of

$$\begin{aligned} \dot{X} &= -H_o G_y(Y) - \alpha X + I, \\ \dot{Y} &= W_o G_x(X) - \alpha Y + I_c \end{aligned} \tag{5.1}$$

(see Equation (4.6)), which describes the dynamics of the bulbar cell. This (X_o, Y_o) determines the mean firing rates of the cells, which are approximately close to $G_x(X_o)$ and $G_y(Y_o)$ for the mitral and granule cells, respectively. Therefore, different input (I, I_c) at least gives different mean output, which is also possibly used for odor information coding. More importantly, the input also sets the stability of (X_o, Y_o) , and defines the local dynamics around (X_o, Y_o) by shaping the parameter matrix $A = H_o G_y'(Y_o) W_o G_x'(X_o)$ of the local oscillation equation

$$\ddot{X} + 2\alpha\dot{X} + (A + \alpha^2)X = 0. \tag{4.21}$$

The resulting growing oscillation modes, if there are any, depend on A and arise from noise.. Thus, different input also gives different oscillatory output superimposed on the mean output level. This completes the information extraction process from sniff-input pattern to bulbar oscillation and baseline output pattern.

(X_o, Y_o) behaves like a high-dimensional knob for the oscillation Equation (4.21) and shapes its behavior, while the input (I, I_c) behaves as the agent that turns the knob. When there is no or little odor input I_{odor}, the point (X_o, Y_o) is stable, and no high-amplitude

oscillation burst occurs because oscillation modes are damped; i.e., $Re(-\alpha \pm i\sqrt{\lambda_k}) < 0$ for all k. Increasing I_{odor} not only raises the mean activity level (X_o, Y_o), but also slowly changes the oscillation modes by structurally changing the oscillation Equation (4.21) through matrix $A = A(X_o, Y_o)$. If the knob (X_o, Y_o) is turned (raised) to such an extent that one of the modes can grow with time, i.e., $Re(-\alpha \pm i\sqrt{\lambda_k}) > 0$ for some k, the equilibrium point (X_o, Y_o) becomes unstable and the k^{th} mode emerges with oscillatory bursts. In these cases, different oscillation modes that emerge are indicative of the different odor-input patterns that control the system parameters (X_o, Y_o). When (X_o, Y_o) is very low, or is raised by non-appropriate receptor input (see Section 5.3), all modes are damped, and only small amplitude oscillations occur, driven by noise and the weak time variation of the odor input.

The stability change (bifurcation) of the equilibrium point (X_o, Y_o) for the oscillation Equation (4.21) has been suggested by others (Freeman and Skarda 1985; Baird 1986; Skarda and Freeman 1987) for olfactory processing. Baird (1986) has showed how single or double Hopf bifurcation in one or two oscillators can make stable (non-damping) cycles occur. Baird used excitatory-to-excitatory connections in the mitral cells to ensure the possibility of the stable cycles, which are otherwise impossible in systems with less than three coupled oscillators (Chapter 4 and 9). The present model shows the multiple (N oscillators) Hopf bifurcations with (Chapter 9) or without requiring excitatory-to-excitatory connections, weak or absent in the olfactory bulb (Nicoll 1971; Shepherd 1979).

The present model system shows the relationship between the odor input and the oscillation mode in terms of the eigenvectors and eigenvalues of matrix A. The oscillation modes that emerge from the bulbar activity with odor input can be thought of as the decision states reached for odor information. The bulb output classifies the odor input by two stages. First, it fails to oscillate appreciably for weak odors (or some particular stronger odors). The absence of oscillation can be interpreted by higher processing centers as the absence of an odor (Skarda and Freeman 1987). Second, when the odor produces

oscillation, the particular pattern of mitral cell activity is specific to an input pattern and its minor variants, the pattern of oscillation classifies odors. This is apparent chiefly when the responses of individual mitral cells are studied, and tends to disappear in the EEG average.

5.2 Necessary Conditions for Significant Bulbar Output

In order for the k^{th} mode $X \propto X_k e^{-\alpha t \pm i\sqrt{\lambda_k} t}$ to be the observable (growing) output mode of the bulb, inequality

$$Re(-\alpha \pm i\sqrt{\lambda_k}) > 0 \tag{4.22}$$

should hold, i.e., λ_k be large enough and be complex (λ_k can never be negative real as assumed). The requires that matrix $A = H_o G'_y(Y_o) W_o G'_x(X_o)$ be large enough in scale and, at the same time, be non-symmetric (non-Hermitian). So the necessary condition for significant bulbar oscillatory output is: 1), Both X_o and Y_o be high enough to give the high gain $G'_x(X_o)$ and $G'_y(Y_o)$ in order to make A large enough. But high gain alone does not ensure the existence of the non-damping mode, so another necessary condition is 2), that A be non-symmetric.

Inequality (4.22) shows that the bulbar cell dissipation α puts a threshold in selecting λ_k or the growing oscillation modes. Two examples in the next section will show the implication of A's being non-symmetric as the necessary condition for bulbar oscillatory response.

5.3 How to Enhance Sensitivity or to Be Responsive to a Particular Search Pattern

First case: Consider the situation when the synaptic connection in the bulb is directionally symmetric, i.e., when each cell connects to its left neighbor(s) in the same strength(s) as to its right neighbor(s), and furthermore, if the connection is also uniform across the bulb, i.e., one part of the bulb has exactly the same connections as any other

part. The connection pattern

$$H_o = \begin{pmatrix} h & h' & h'' & & & \cdots & & h'' & h' \\ h' & h & h' & h'' & & \cdots & & & h'' \\ h'' & h' & h & h' & h'' & & \cdots & & \\ \vdots & \vdots & & & & \cdots & \ddots & & \vdots \\ h' & h'' & & & \cdots & & h'' & h' & h \end{pmatrix}$$

$$W_o = \begin{pmatrix} w & w' & w'' & & & \cdots & & w'' & w' \\ w' & w & w' & w'' & & \cdots & & & w'' \\ w'' & w' & w & w' & w'' & & \cdots & & \\ \vdots & \vdots & & & & \cdots & \ddots & & \vdots \\ w' & w'' & & & \cdots & & w'' & w' & w \end{pmatrix}$$

and Equation (4.23) are examples of these situations. Moreover, if the central input I_c and receptor background input $I_{background}$ are also uniform across the bulb, i.e., $I_{ci} = I_{cj}$, and $I_{background,i'} = I_{background,j'}$ for all $i \neq j$ and $i' \neq j'$, then this bulb network will be insensitive to a uniform input I_{odor} from the receptors as shown below.

If I_{odor} is uniform too, then the equilibrium point (X_o, Y_o) will also be uniform by obvious symmetry. The matrices $G'_x(X_o)$ and $G'_y(Y_o)$ are now proportional to the identity matrix. By symmetry, $A = H_o G'_y(Y_o) W_o G'_x(X_o)$ will be symmetric and have the form

$$A = \begin{pmatrix} a & b & c & & & \cdots & & c & b \\ b & a & b & c & & \cdots & & & c \\ c & b & a & b & c & & \cdots & & \\ \vdots & \vdots & & & & \cdots & \ddots & & \vdots \\ b & c & & & \cdots & & c & b & a \end{pmatrix}.$$

(Matrix A in Equation (4.24) is an example of this.) According to the necessary condition discussed in the last section, no significant oscillation mode output arises from the bulb. (See the example in Section 4.2.1.) Therefore, this particular bulb structure will be non-responsive to uniform receptor input I_{odor}, no matter how strong it is, and no matter how high the gain $(G'_x(X_o), G'_y(Y_o))$ is raised by I_{odor}.

Such a bulb, however, may respond to certain non-uniform input I_{odor}, which destroys the uniformity of (X_o, Y_o) and causes a non-symmetric matrix $A = H_o G'_y(Y_o) W_o G'_x(X_o)$. A decision-state, oscillatory output may be reached if the input I is sufficiently non-uniform (i.e., the odor selectively excites different mitral cells).

Second case: Olfaction, however, is different from vision. The visual system extracts information from contrasts and disregards the brightness of the input, while the olfactory system needs to recognize both the odor identity and intensity (concentration). Therefore, I believe that the olfactory system should have some sensitivity to uniform input. A possible bulb network that is sensitive to uniform input is described below.

If the synaptic connection is uniform across the bulb but non-symmetric in the directions, e.g., each neuron gives output to its left neighbor(s) but not the right neighbors as in Equation (4.26),

$$H_o = \begin{pmatrix} h & h' & 0 & 0 & & \cdots & & 0 & 0 \\ 0 & h & h' & 0 & & \cdots & & 0 & 0 \\ 0 & 0 & h & h' & 0 & 0 & \cdots & 0 & 0 \\ \vdots & \vdots & & & & \cdots & \ddots & & \vdots \\ h' & 0 & & & \cdots & & 0 & 0 & h \end{pmatrix}$$

$$W_o = \begin{pmatrix} w & w' & 0 & 0 & & \cdots & & 0 & 0 \\ 0 & w & w' & 0 & & \cdots & & 0 & 0 \\ 0 & 0 & w & w' & 0 & 0 & \cdots & 0 & 0 \\ \vdots & \vdots & & & & \cdots & \ddots & & \vdots \\ w' & 0 & & & \cdots & & 0 & 0 & w \end{pmatrix}.$$

If everything else in this network stays the same as in the previous case, A matrix for uniform input I_{odor} will is

$$A = \begin{pmatrix} a & b & c & 0 & & \cdots & & 0 & 0 \\ 0 & a & b & c & & \cdots & & 0 & 0 \\ 0 & 0 & a & b & c & 0 & \cdots & 0 & 0 \\ \vdots & \vdots & & & & \cdots & \ddots & & \vdots \\ c & 0 & & & \cdots & & 0 & a & b \\ b & c & & & \cdots & & 0 & 0 & a \end{pmatrix},$$

which is non-symmetric. Section (4.2.1) shows that this system will have possible oscillatory growing modes. Thus, a bulb with this structure can be responsive to uniform receptor input pattern if it is strong enough. Note that since $G'_x(X_o)$ and $G'_y(Y_o)$ are diagonal matrices, the matrix $A = H_o G'_y(Y_o) W_o G'_x(X_o)$ with above H_o and W_o will always be non-symmetric even for non-uniform input I_{odor}. This network is therefore sensitive to both uniform and non-uniform receptor input I_{odor}.

These two examples demonstrate that the bulbar synaptic connection pattern determines the input patterns to which the bulb selectively responds and thus fulfills pattern classification.

The real biological olfactory bulb suggests that its structure stays in between these two example structures. In the EPL layer of the bulb, the dendrodendritic connections between the mitral and granule cells are dominantly reciprocal. If synaptic strength differences are ignored, this suggests that $W_o^T \approx H_o$, where W_o^T is the transverse of the matrix W_o, and implies the symmetric matrix A for uniform input. But since the mitral cells also have extra axon collaterals that connect to the granule cells in their deeper dendritic trees, $W_o^T = H_o + extra\ \ connections$, which has less reason to be thought symmetric. This confirms the conjecture that the olfactory bulb is possibly responsive to uniform receptor input patterns.

5.4 Performance Optimization and Feature Extraction in the Bulb

5.4.1 Ready for the Next Sniff

An active mammalian olfactory system samples the input by sniffs, each lasting 200 msec to 1 sec in rabbits. The olfactory system should make itself ready for the next sniff, which may contain different odor information from the previous sniff. If (X,Y) is the initial deviation of the system from the equilibrium point (X_o,Y_o), then the degree to which the k^{th} oscillation mode gets excited in the beginning of inhalation is proportional to $< XX_k >$. $X = 0$ corresponds to no excitation to any modes, while X as a random noise corresponds to equal chances of excitation to all the modes. Terminating the oscillation during the exhalation leaves only random noise and minimum information contamination from the previous sniff in the system. It therefore helps the bulb to reach an unbiased decision state (oscillation mode) on the odor information for the next sniff. Furthermore, exhalation also changes the operation point (X_o,Y_o) back to the original value before the inhalation (Section (4.3.4)), making the system ready for the next sniff.

5.4.2 Motivation level control

The initial operation point (X_o, Y_o) before a sniff input should be controlled by the motivation level of the animal. If (X_o, Y_o) is very low initially, a strong input I_{odor} is needed to raise the bias (X_o, Y_o) high enough for an oscillation-burst output. Less strong input I_{odor} would be required for an initially higher bias. Since the initial bias (X_o, Y_o) is determined by $I_{background}$ and the central input I_c by Equation (4.7), it seems likely that the motivation level of the animal will be controlled by the input from higher centers. The simulation value for $I_{background}$ and I_c are set such that the (X_o, Y_o) with $I_{odor} = 0$ is just below the maximum gain point on the non-linear input-output curves (Section 3.3, Fig[4.5]). This corresponds to a motivated state; a small amount of odor input can raise the gain to maximum values. Physiologically, the bulbar oscillatory bursts are observed to occur only in the motivated animals (Freeman 1978; Freeman and Schneider 1982). The experimental measured gain (defined as the change in the mitral firing rate with respect to the change in EEG amplitude) for bulb neural mass is shown to be higher in the motivated states (Freeman 1979a), which can be achieved by raising $I_{background}$ through the central input. Experiments even show the existence of oscillations without the odor input with nasal breathing in motivated animals (Freeman and Schneider 1982).

The central input I_c is also likely to participate in other olfactory functions such as odor-masking or sensitivity-enhancing for particular odors (see also Freeman and Schneider 1982). This issue will be studied in Chapter 7.

6. Simulation of the Bulb Model without Central Control

The computer simulation of the model has been done on a special case of $N = M = 10$. The parameters used in the simulated model are described in Chapter 3. Here the central control from the higher olfactory and brain centers are not considered. Thus the central input I_c to the granule cells are kept fixed and considered a background input. The simulations start with initial cell internal states close to the background states when no odor input is present. Different odor input patterns are represented by different I_{odor}, i.e., different P_{odor} (see Equation (3.1)). Appendix A gives the sample computer program written in C for the simulation.

6.1 General Model Response

Response to odor input: When a particular input I_{odor} is present for several sniff cycles,

$$I_{odor}(t) = \begin{cases} P_{odor}(t - t_j^{inhale}) + I_{odor}(t_j^{inhale}), & \text{if } t_j^{inhale} < t \leq t_j^{exhale}; \\ I_{odor}(t_j^{exhale}) \cdot e^{-(t-t_j^{exhale})/\tau_{exhale}}, & \text{if } t_j^{exhale} < t \leq t_{j+1}^{inhale}. \end{cases},$$

where t_j^{inhale} and t_j^{exhale} are the onset time of the inhalation and exhalation on the j^{th} sniff. The model bulb oscillates with about the same frequency as that of the real bulb. The oscillation bursts, which ride on the slow baseline shift wave phase locked with the respiratory wave (Figure [2.6]), set up during inhalation and drop at the early part of the exhalation. The baseline shift is more obvious in the granule cells than the mitral cells.

The oscillation amplitude, phase and baseline activity level can vary from cell to cell. The responses of all cells constitute a response pattern for an odor input. Figure [6.1] shows an example of a response pattern for an input pattern during one sniff of 370 miliseconds, the first 180 miliseconds of which is inhalation. Both the internal states of the cells and mitral cell output $G_x(X)$ are plotted in the figure. From the figure, one can see that the internal states (corresponding to the cell membrane potentials) of mitral cells 1, 3, 7, and 9 oscillate with higher amplitudes, while those of mitral cell 4 and 10 oscillate with lower

Fig. 6.1 Internal states of mitral and granule cells and the outputs of the mitral cells in one sniff cycle with odor input I_{odor_1}. The cells are arranged in the normal reading sequence, i.e., from left to right and from top to bottom.

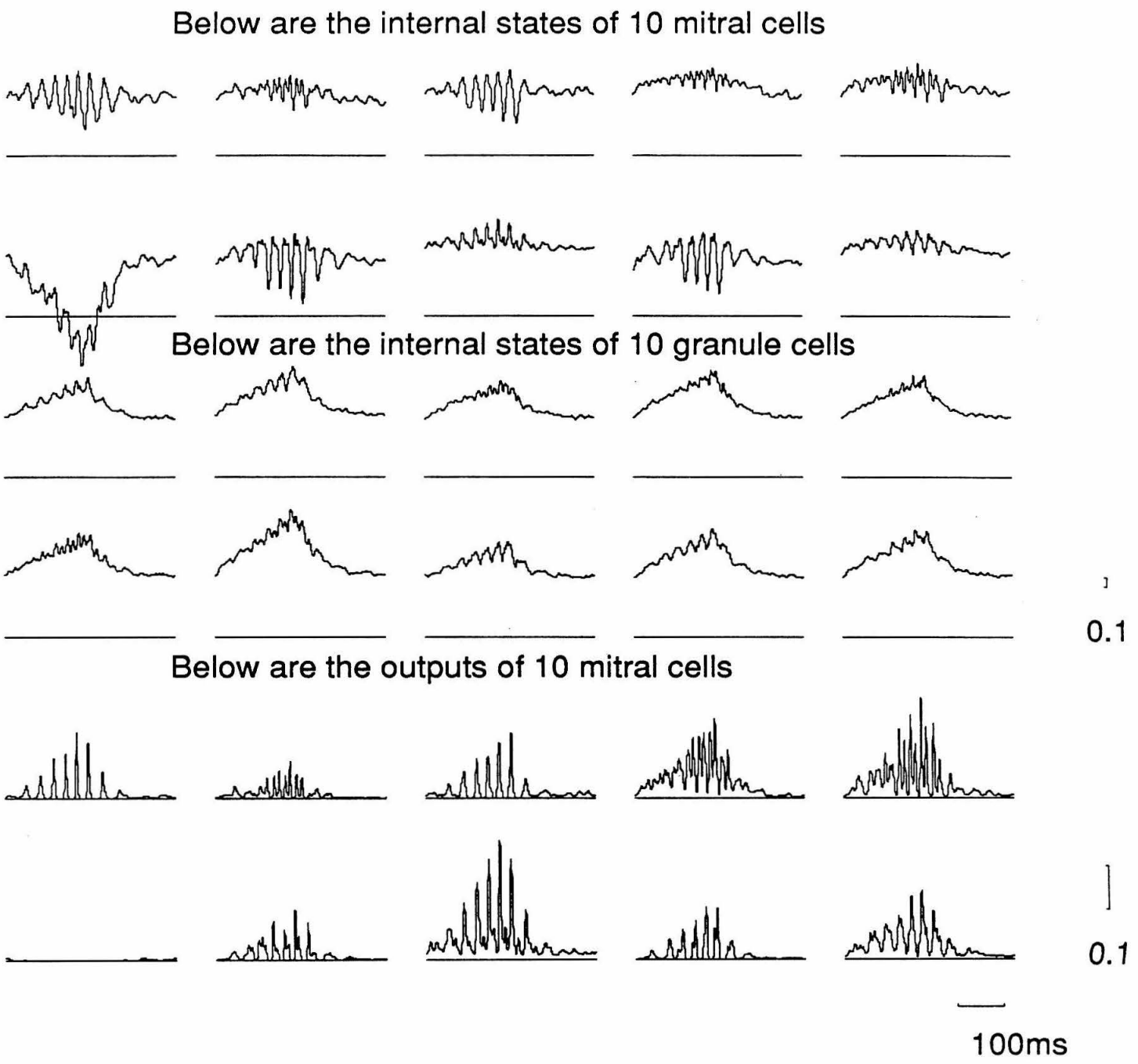

amplitudes. Mitral cell 6 has low baseline shifts and therefore has small output although its internal state oscillation amplitude is quite substantial. (This implies that although some cell membrane potentials are oscillating with high amplitudes, they seldom exceed the cell firing thresholds to give substantial action potential output.) Actually, mitral cell 6 has its baseline shift suppressed by the odor input, and decreases its firing rate by odor stimulation as is sometimes observed in biology (Shepherd 1979). Mitral cells 3, 4, 8, and 10 give more substantial oscillation output. Although mitral cells 4 and 10 have smaller amplitudes internal states oscillations, they oscillate near the neuron firing thresholds, which amplifies their output by the threshold non-linearity. Furthermore, all the cells with substantial amplitudes oscillate with about the same peak frequency but different phases (see later sections for calculations of frequencies and phases). Higher frequency components are also visible in the activities, and they make the activity waveforms look complex. Since the mitral cell output is the only information sent to the higher olfactory centers, it will be often referred to later in the thesis as the bulbar response.

Response to zero-odor input: In agreement with the experimental observations, there is very little or no large amplitude oscillatory activity other than some transient ones generated by noise (Figure [6.3D]) when $I_{odor} = 0$. In fact, such model response is achieved by setting the values of $I_{background}$ and I_c appropriately (as already mentioned in Chapter 3) to agree with the experimental result.

EEG Explained: The cell activities generate electrical current, which flows from individual neurons in the extracellular spaces in and around the olfactory bulb, and gives rise to summed extracellular potentials recorded by EEG. When the EEG probe is at the bulbar surface on or above the glomerular layer, the granule cells, which generate a dipole field, can have their potential field detected by EEG measurement, while the monopole field generated by the mitral cells because of their morphology can not be detected (Freeman 1975). EEG measurement therefore represents the average activities of the local granule cells in the bulb. Here the approximation by Freeman (1980) is used to calculate the surface EEG

as a weighted sum of the granule cell output according to cell distances to the electrode. Simultaneous measurements of EEG at multiple spots on the bulbar surface give the EEG response pattern to an odor input (Figure [6.2]). Such multi-channel measurement of surface EEG waves (Freeman 1978), though originating from the externally invisible granule cell activities, also displays an odor information pattern in the multi-dimensions.

6.2 The pattern classification properties of the model

An odor input pattern of one sniff

$$I_{odor}(t) = \begin{cases} P_{odor} \cdot (t - t^{inhale}) + I_{odor}(t^{inhale}), & \text{if } t^{inhale} \leq t < t^{exhale}; \\ I_{odor}(t^{exhale}) \cdot e^{-(t-t^{exhale})/\tau_{exhale}}, & \text{if } t \geq t^{exhale}. \end{cases}$$

with $I_{odor} = 0$ at t^{inhale}, and t^{exhale} fixed is determined by P_{odor}. For a sniff cycle lasting 370 $msec$ with inhalation taking 180 $msec$, some P_{odor} induce oscillation, while others do not, and different P_{odor} induce different oscillation patterns (Figure [6.3]). This means that the bulb model shows the capability of a pattern classifier. (What patterns drive the bulb well is as yet arbitrary in the model, for there is no relation between the particular connections and the odor used.) As the only bulbar information output, mitral output patterns are studied for the pattern classification properties.

Some measures have been defined to describe the difference between different patterns. The mitral output $G_x(X(t))$ were filtered above 20 Hz to obtain the oscillatory signal $S_h(t)$, and below 20 Hz for for baseline shift $S_l(t)$. Both $S_h(t) = \{s_{h,1}(t), s_{h,2}(t), \ldots, s_{h,N}(t)\}$ and $S_l(t) = \{s_{l,1}(t), s_{l,2}(t), \ldots, s_{l,N}(t)\}$ have N (= number of mitral cells) components to describe all the mitral cells. The oscillation period T is the time lag ≥ 5 $msec$ that gives the largest auto-correlation for $S_h(t)$. Similar operations are done to the different components of $S_h(t)$ to obtain the individual cell oscillation frequencies. Similarly, oscillation phase differences between the mitral cells are calculated by cross-correlating the different components of $S_h(t)$ after the higher frequency components ($f > 1.3/T$) are removed (to eliminate noise). The phase differences are measured with respect to the first cell. The oscillation amplitude of i^{th} cell is the root-mean-square of $s_{h,i}(t)$ averaged in time. The

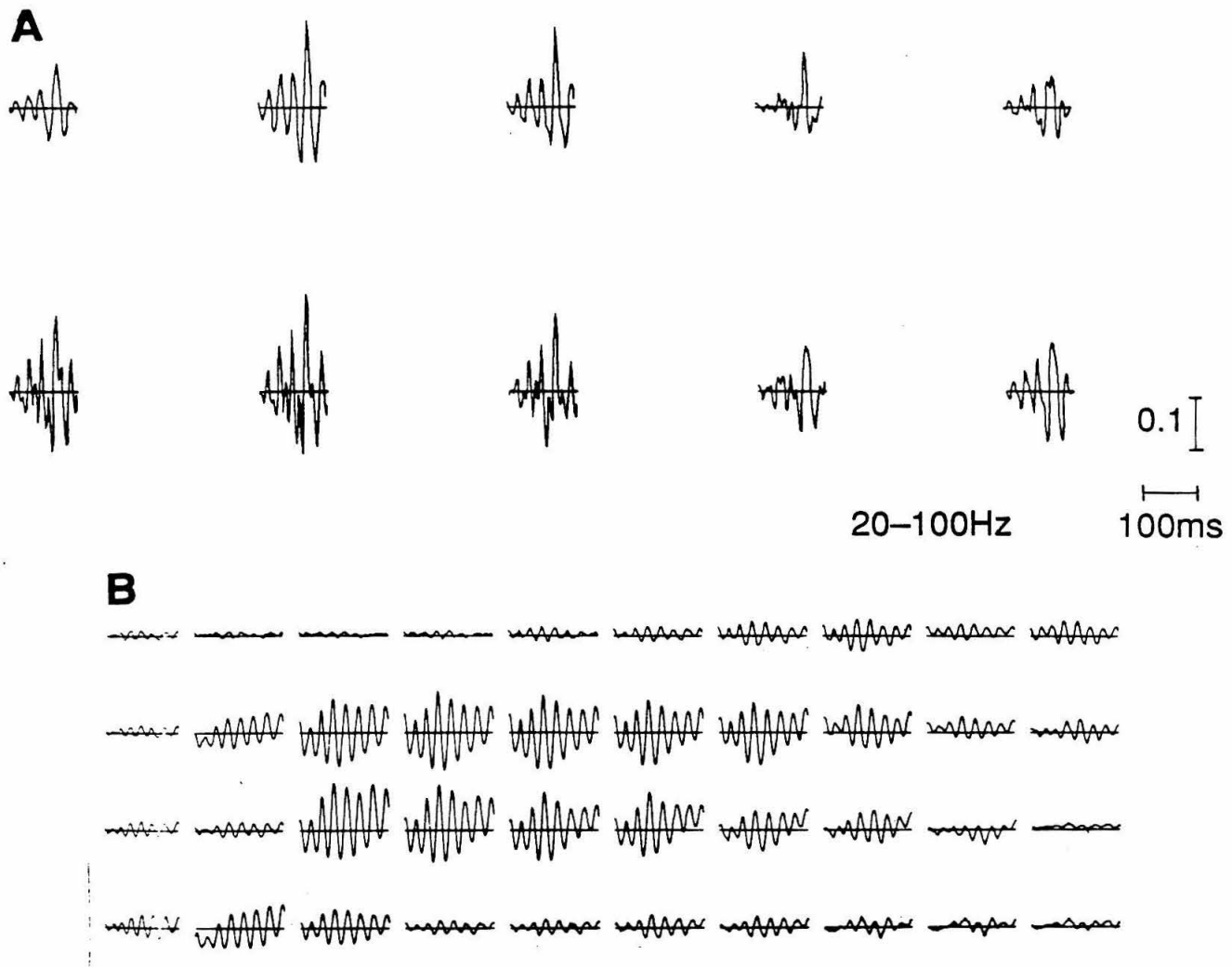

Fig. 6.2 A: A segment of a simulated surface EEG wave pattern during the oscillatory bursts with the odor input I_{odor_1}. **B:** Multi-channel recorded bulbar surface EEG wave pattern during 100 msec of bursts, taken from Freeman 1978. Both signals in A and B are band-pass filtered.

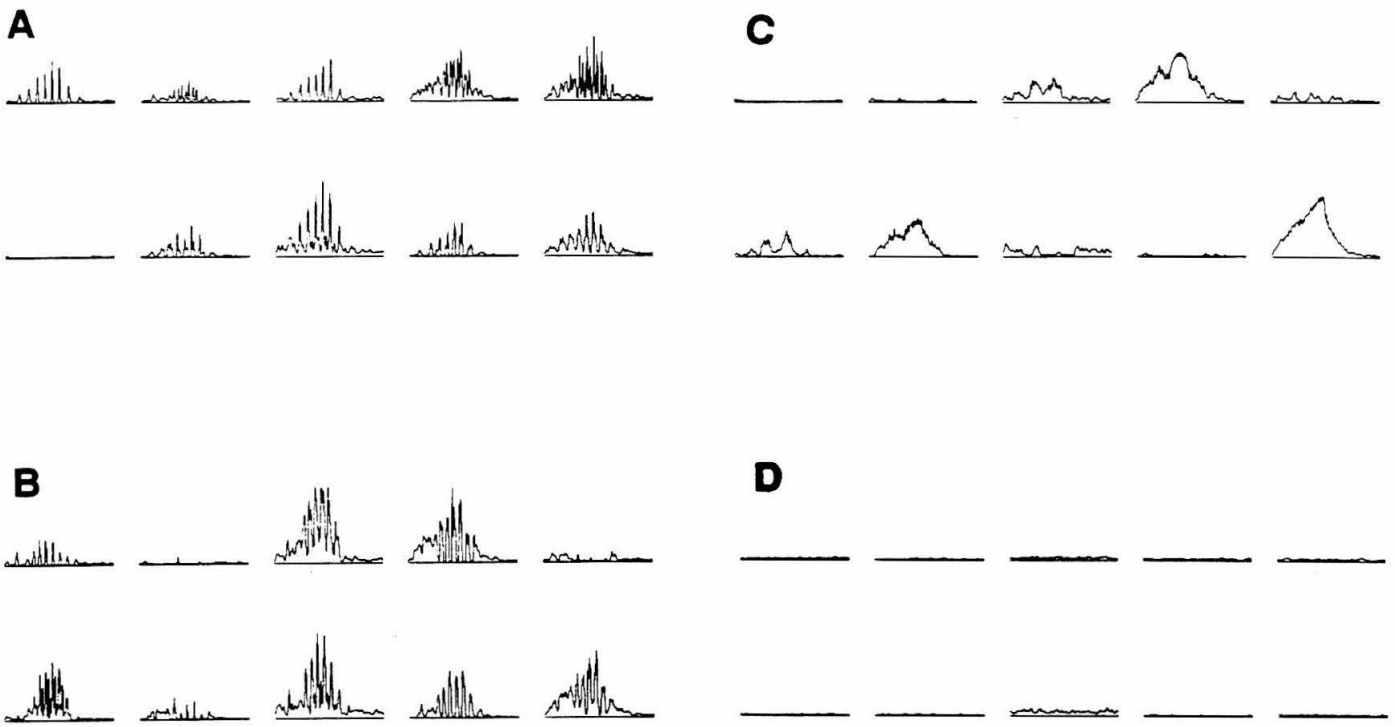

Fig. 6.3 Mitral output response patterns for different inputs I_{odor} of one sniff cycle lasting 370 msec. A,B: oscillatory responses for two different inputs. C: non-oscillatory response for an input. D: response for no odor inputs.

results show that for each response, cells with substantial oscillation amplitudes have frequencies within 1 Hz of each other. Define

O_{osci}: an N-dimensional complex vector whose i^{th} component has its amplitude and phase equal to the amplitude and phase of the i^{th} mitral cell oscillation;

O_{mean}: an N-dimensional real vector describing the baseline activities above the background level $(S_l(t) - S_l|_{P_{odor}=0})$ averaged over the sniff cycle;

$\bar{O}_{mean}$ and $\bar{O}_{osci}$: scalars describing the root-mean-square averages of the components of O_{mean} and O_{osci}, respectively; i.e., they are proportional to the lengths of the vectors O_{mean} and O_{osci}, respectively.

These quantities are used to define the similarity or difference between response patterns. For two response patterns a and b indicated by superindices, possible distance measures are:

$$\begin{aligned} d_1(a,b) &= 1 - \frac{< O^a_{mean} O^b_{mean} >}{|O^a_{mean}||O^b_{mean}|} & d_2(a,b) &= 1 - \frac{|< O^a_{osci} O^b_{osci} >|}{|O^a_{osci}||O^b_{osci}|} \\ d_3(a,b) &= \frac{\bar{O}^a_{mean} - \bar{O}^b_{mean}}{\bar{O}^a_{mean} + \bar{O}^b_{mean}} & d_4(a,b) &= \frac{\bar{O}^a_{osci} - \bar{O}^b_{osci}}{\bar{O}^a_{osci} + \bar{O}^b_{osci}} \end{aligned} , \qquad (6.1)$$

where $< UV >$ means the dot product of vectors U and V, and $|U|$ is the absolute value or the length of U. d_1 and d_2 give differences in the response pattern forms, while d_3 and d_4 give differences in the response levels. $d_1, d_2, |d_3|, |d_4| \ll 1$ suggests the similarity between two response patterns. $d_3(a,b), d_4(a,b) > 0$ could suggest that the response level in a is higher than that in b. This choice of difference measure is certainly not the only possible one. For instance, the frequencies of response patterns are not accounted for in this measure.

Using the responses to three different odor inputs I_{odor_1}, I_{odor_2} and I_{odor_3} (or P_{odor_1}, P_{odor_2} and P_{odor_3}) of three presumably different odor types, Table [6.1] gives the differences measured between them, compared with differences between two responses with the same I_{odor_a} for $a = 1,2,3$ input but different system noises. These examples show that the three odor inputs are easily distinguishable, while the same odor input

Table [6.1]

Differences between responses to different odor inputs and between responses to the same odor inputs with different noises and between the input patterns

	$i =$	$j =$	$d_1(a,b)$	$d_2(a,b)$	$d_3(a,b)$	$d_4(a,b)$	$d_1^{in}(a,b)$	$d_3^{in}(a,b)$
a, b: responses to same odor inputs but different system noises	1	1	0.001	0.068	0.002	-0.016	0	0
	2	2	0.001	0.008	-0.001	0.010	0	0
	3	3	0.000	0.092	-0.012	0.098	0	0
a: response to I_{odor_i} b: response to I_{odor_j}	1	2	0.253	0.243	-0.210	-0.112	0.014	-0.247
	1	3	0.226	0.556	-0.180	0.321	0.031	-0.060
	2	3	0.486	0.474	0.031	0.419	0.032	0.190

with different system noises induces similar responses. The three odor vectors used in the simulations have their P_{odor}, respectively:

$$\begin{aligned} P_{odor\_1} &= 1/70\{0.3, 0.3, 0.3, 0.3, 0.3, 0.3, 0.3, 0.3, 0.3, 0.3\} \\ P_{odor\_2} &= 1/70\{0.6, 0.5, 0.5, 0.5, 0.3, 0.6, 0.4, 0.5, 0.5, 0.5\} \\ P_{odor\_3} &= 4/700\{0.7, 0.8, 0.5, 1.2, 0.7, 1.2, 0.8, 0.7, 0.8, 0.8\} \end{aligned} \quad . \tag{6.2}$$

The differences between the input patterns P_{odor_a} for $a = 1, 2, 3$ can be calculated by replacing O_{mean} with P_{odor} in Equation (6.1) for d_1 and d_3 to get the corresponding d_1^{in} and d_3^{in}, respectively. That is,

$$\begin{aligned} d_1^{in}(a,b) &= 1 - \frac{< P_{odor\_a} P_{odor\_b} >}{|P_{odor\_a}||P_{odor\_b}|} \\ d_3^{in}(a,b) &= \frac{\bar{P}_{odor\_a} - \bar{P}_{odor\_b}}{\bar{P}_{odor\_a} + \bar{P}_{odor\_b}} \end{aligned} \quad . \tag{6.3}$$

d_1^{in} indicates the difference in form (not amplitude) of the input patterns P_{odor}, while d_3^{in} indicates their level or amplitude difference. Table [6.1] shows that the bulb amplifies the differences in input vector P_{odor} to give output vectors O_{osci} and O_{mean} (compare d_3^{in} with d_1 and d_2). The vector P_{odor} has all non-negative components, while O_{mean} can have both positive and negative components. The bulb also creates the oscillatory response O_{osci} from the non-oscillatory (not counting the low frequency respiratory part) odor input.

7 A model of olfactory adaptation and sensitivity enhancement in the olfactory bulb

An application of this bulb model is shown in this chapter. Appropriate inputs from the higher centers can enhance or suppress the sensitivity to particular odors. Psychophysical phenomena such as olfactory adaptation (Pryor et al. 1970; Steinmetz et al. 1970), sensitivity enhancement in odor searching can be understood from these arguments (Li, 1989).

7.1 The Problem

The olfactory system needs to solve two problems: 1) What is the identity of the input odor? 2) What is the intensity of the input odor object? If there is only one odor type ("odor object") in the actual sensory input, the computation will be straightforward. But when there are odor mixtures in the input, the problem becomes complex, and the olfactory system often cannot tell the individual odor subcomponents (Moncrieff 1967). Since most receptor cells respond to more than one odor types (Lancet 1986; Sicard and Holley 1984), and a given odor may contain a mixture of molecules that bind predominantly to different receptors, the information about any one odor object may be distributed across the whole receptor population. Therefore, it will generally be inappropriate to focus attention on a small subset of receptors to search for a particular odor object. The integrative processing done by olfactory centers must be responsible for identifying individual odor objects, separating multiple objects if possible, or sensing an odor mixture as a whole new odor type. (Odor mixtures have a complex psychophysics. For example, two substances odorous singly may be inodorous together — counteraction; or only one odor type is sensed when two are mixed — masking (Moncrieff 1967).)

Since the major olfactory problem of an animal in a rich olfactory environment is to identify odor objects, it would be desirable if the olfactory system could detect individual odors in a mixture. Olfactory adaptation may be a strategy used to detect individual odor components. It should not be understood as an olfactory fatigue, but as an active

mechanism used by the olfactory system to screen out a pre-existing odor object, which has already been detected, and to stay sensitive to new odors mixed with the pre-existing odors. For example, after a human adapts to vanillin, a mixture of vanillin and coumarin smells only of coumarin (Moncrieff 1967). Without adaptation, the new odors may be masked or counteracted by the pre-existing odors and not detected as the appropriate odor object.

If the olfactory system can reduce its sensitivity to particular odors in adaptation, it is reasonable to expect that it may also be able to increase the sensitivity to certain odors in, for instance, odor searching. Psychophysical experiments are not generally done on the olfactory sensitivity enhancement by motivation since the subject is not as easy to handle as olfactory adaptation. Enhanced sensitivity to a particular stimulus is evident in other sensory systems such as vision and audition — attention can be focused on a particular object in a large input image to eyes, or a particular speaker in a noisy cocktail party. It is not surprising that the olfactory system can also focus its attention on a particular odor stimulus.

What is the mechanism for olfactory adaptation or enhancement? It is known that the olfactory adaptation is not due simply to the exhaustion of receptor cells (Moncrieff 1967). The receptor cells keep firing, but within a second, change from phasic to tonic response during continuous stimulus (Getchell and Shepherd 1978; Lancet 1986), while the olfactory adaptation occurs in the time order of minutes (Pryor et al. 1970; Steinmetz et al. 1970). So the olfactory structure responsible must then be at the bulb or higher in the olfactory pathway. Physiological experiments (Chaput and Panhuber 1982) show that the bulbar mitral cells' firing decreases with long exposure to (a single) odor, suggesting the bulb's involvement in olfactory adaptation.

There are several theoretical reasons suggesting that the feedback signal from higher olfactory centers to the olfactory bulb is the source for bulbar adaptation. First, bulbar cell exhaustion should not be the source for adaptation since the sensitivity to new odor inputs

remains intact after adaptation to the pre-existing odor. Second, with the same odor input and no bulbar cell exhaustion, the bulbar response should not change from one sniff to another unless the other bulbar input, namely, the central input, changes in time. Third, the selectivity of the sensitivity reduction to only the pre-existing odors suggests that the bulb is instructed by a well-computed information signal, which is only available from higher centers. Fourth, the signals from the higher centers should serve some information processing purpose by their existence. Olfactory adaptation as one of the processes used to detect new odors, may very likely have the central signal involved in it.

Here a possible mechanism for a central signal to participate in the adaptation is suggested as follows. After the pre-existing odor object is detected, the higher olfactory centers have a good knowledge about this odor. They can then send a computed signal to the bulb to cancel the effect of this particular odor object input on the bulb output. If the cancellation is complete and exact, the bulb output would ideally be as if no such odor existed. Because of the selectivity of the cancelling, a new input odor object mixed with the pre-existing and cancelled odor object could be detected by the bulb as if it were the only component in the odor input mixture.

We can extend our suggestion to olfactory enhancement. If the higher olfactory centers can send signals to the bulb to reduce its response level to a particular odor object, it is reasonable to expect that they can also send some signals to increase the response level to a particular odor object. If a signal S from higher centers can cancel the effect of a particular input odor on the bulb output, an opposite of this signal (i.e., $-S$, the enhancing signal,) may increase the effect of this particular odor. In this case, we have a sensitivity enhancement to this odor object. The higher centers should have a knowledge of the odor in order to send a right enhancing signal. This requires that the odor information be known either through genetics and development or by experience.

If this suggested mechanism for olfactory adaptation and enhancement is correct, there will be the following consequences. Suppose we have a situation when an odor object is

detected, and adaptation is set up such that a cancelling signal is sent for this pre-existing odor object in every sniff. If in the next sniff, a new odor object is introduced and at the same time the pre-existing odor object is withdrawn, then the cancelling signal can not find the odor object it is supposed to cancel. This also means that the pre-existing odor object is not there to cancel the effect of this central control signal on the bulbar output. Therefore, the cancelling signal will affect and impair the bulbar sensitivity and detectability to this new odor object. This is known as cross-adaptation and is psychophysically observed (Cain and Engen 1969). Experiments show that after sniffing one odor, another odor at the next sniff smells weaker than it would be and even smells different sometimes (Moncrieff 1967). (The recovery from olfactory adaptation after the pre-existing odor is removed takes a few minutes (Pryor et al. 1970; Steinmetz et al. 1970). Therefore, if there is such a cancelling signal, it will not disappear as soon as the pre-existing odor is removed.) The cross-adaptation is observed to depend on both the pre-existing and the new odor types, and it is non-symmetric on the odor types (Cain and Engen 1969); i.e., the extent to which one odor in cross-adapted by another is different from the extent of vice versa. Another consequence is analogous to the cross-adaptation. Suppose an animal is motivated to search for an odor object; therefore, an enhancing signal is sent from the higher centers to the bulb to enhance the sensitivity to that particular odor. If a different object instead of the interested odor object is inhaled, the enhancing signal will distort the bulbar response to this odor object because of the effort to enhance the interested odor response. We will call this cross-enhancement. There are no experimental data on the cross-enhancement.

This chapter is to show how the olfactory adaptation and enhancement mechanism suggested above can be realized in the bulbar model studied, and confirmed by simulation.

7.2 A model of central control on bulbar response

In this model of the olfactory bulb, the mitral cell output has an oscillatory part determined by X in Equation (4.21), and a baseline shift part determined by X_o which is the oscillation center or the equilibrium point. The granule cell response also has a

baseline shift state level Y_o and an oscillatory part Y determined by Equation (4.6) and (4.7), although this activity is invisible outside bulb. (The mitral cells are the only output neurons of the bulb.)

The oscillatory response X is determined by (X_o, Y_o) via matrix A; thus (X_o, Y_o) completely determines the bulbar oscillatory. By Equation (4.34), the receptor input I determines the bulbar output provided that the central input I_c stay fixed. When the central input I_c is not fixed, it can also control the bulbar output by shifting (X_o, Y_o). Calculations show that:

$$\begin{aligned} dX_o &\approx (\alpha^2 + HW)^{-1}(-H\,dI_c + \alpha W^{-1} d\dot{I}_c) \\ dY_o &\approx (\alpha^2 + WH)^{-1}(\alpha dI_c + d\dot{I}_c) \end{aligned} \quad . \tag{7.1}$$

This equation can be obtained simply by interchanging $X_o \iff Y_o$, $I \iff I_c$ and $-H \iff W$ in the derivation for Equation (4.34). Therefore, we have

$$\begin{aligned} dX_o &\approx (\alpha^2 + HW)^{-1}(\alpha dI + d\dot{I} - H\,dI_c + \alpha W^{-1} d\dot{I}_c) \\ dY_o &\approx (\alpha^2 + WH)^{-1}(W\,dI - \alpha H^{-1} d\dot{I} + \alpha dI_c + d\dot{I}_c) \end{aligned} \quad . \tag{7.2}$$

Let

$$I_c \equiv I_{c,background} + I_{c,control}, \tag{7.3}$$

where $I_{c,background}$ is the central background input, which does not change during a sniff and controls the motivation level such as sleeping, resting, hunger states, while $I_{c,control}$ is the control signal, which changes during a sniff. I_{odor} and $I_{c,control}$ determine the bulbar output activities during a sniff.

Suppose for a particular odor input I_{odor} that there is a central control signal $I_{c,control}$ which cancels the effect of I_{odor} on (X_o, Y_o), such that (X_o, Y_o) stays the same as if neither I_{odor} nor $I_{c,control}$ exists — cancelling, i.e.,

$$\begin{aligned} dX_o &\approx (\alpha^2 + HW)^{-1}(\alpha dI_{odor} + d\dot{I}_{odor} - H\,dI_{c,control} + \alpha W^{-1} d\dot{I}_{c,control}) = 0 \\ dY_o &\approx (\alpha^2 + WH)^{-1}(W\,dI_{odor} - \alpha H^{-1} d\dot{I}_{odor} + \alpha dI_{c,control} + d\dot{I}_{c,control}) = 0 \end{aligned} \quad . \tag{7.4}$$

Then not only the baseline bulbar response X_o, but also the oscillatory X by its dependency on (X_o, Y_o) in Equation (4.21) stay the same as if no odor input exists. In this case, a complete self-adaptation to that odor input is achieved, and we will denote the control signal as I_c^{cancel}.

When $(\Delta X_o, \Delta Y_o)$ depends linearly on $(I_{odor}, I_{c,control})$, a central control signal

$$I_c^{enhance} \equiv -\gamma I_c^{cancel} \qquad for \quad \gamma > 0$$

will enhance rather than cancel the effect of I_{odor}, and thus enhance the bulbar output level or the sensitivity to that particular input odor. Since $H = H_o G_y(Y_o)$ and $W = W_o G_x(X_o)$, Equation (7.2) is a non-linear equation. Thus, such an enhancing signal is certain to work when (X_o, Y_o) is in a near linear range of the gain curves G_x and G_y with I_{odor}. Physiological experiments show that when the oscillation signals are small, the bulbar system operates in a near linear range (Freeman 1979a) with odor input. When the near linear approximation is not valid, the enhancing signal can not simply be a negative constant times the cancelling signal.

An absolute self-adaptation signal I_c^{cancel} satisfying Equation (7.4) for odor input I_{odor} can not be achieved generally. Since X_o and Y_o are N and M dimensional vectors, respectively, Equation (7.4) is a system of $N + M$ equations. This number of equations is too many for solving M unknown components of an M dimensional vector I_c^{cancel}. Therefore, no cancelling signal I_c^{cancel} will satisfy Equation (7.4) for a given odor I_{odor}, generally.

We can compromise by modifying I_c^{cancel} (and thus $I_c^{enhance}$) such that weaker requirements for cancelling are satisfied. Since the mitral cells are the only output cells of the bulb, we need only demand that the mitral cell activity induced by I_{odor} be cancelled, while the granule cell activity can be different from the no-odor input case. To have the baseline response X_o raised by I_{odor} be cancelled (suppressed) by I_c^{cancel}, we have

$$dX_o \approx (\alpha^2 + HW)^{-1}(\alpha dI_{odor} + d\dot{I}_{odor} - H dI_c^{cancel} + \alpha W^{-1} d\dot{I}_c^{cancel}) = 0. \qquad (7.5)$$

We already know from Chapter 4 and 5 that the necessary condition for oscillatory response is to have both X_o and Y_o be high enough. Therefore, the above suppressed baseline response X_o also makes the non-damped oscillatory mode impossible, as if no odor input exists. An effectively complete self-adaptation is therefore fulfilled. Such an I_c^{cancel}, however, cannot cancel the effect of I_{odor} on the baseline shift of the granule cells Y_o. A solution of Equation (7.5) for I_c^{cancel} with M unknown variables will generally exist, since the number of equations N, which is number of the mitral cells, is much smaller than M, which is the number of the granule cells (Shepherd 1979).

It is not easy to calculate the I_c^{cancel}, since Equation (7.5) is non-linear (H and W depend on (X_o, Y_o)). In the computer simulation, a simplification is used. If the inputs (I, I_c) change in a time scale much longer than $1/\alpha \approx 7\ mesc$, then Equation (7.2) becomes (see Chapter 4)

$$\begin{aligned} dX_o &\approx (\alpha^2 + HW)^{-1}(\alpha dI - H dI_c) \\ dY_o &\approx (\alpha^2 + WH)^{-1}(W dI + \alpha dI_c) \end{aligned} . \tag{7.6}$$

And Equation (7.5) becomes

$$dX_o \approx (\alpha^2 + HW)^{-1}(\alpha dI_{odor} - H dI_c^{cancel}) = 0. \tag{7.7}$$

This is true for I since a sniff cycle is about a few hundred milliseconds, and it is reasonable to assume that the central control I_c is also modulated in a time scale of a sniff cycle. By Equation (7.7), $dI_c^{cancel} = H^{-1}\alpha dI_{odor}$, suggesting that I_c^{cancel} will change in about the same time scale as I_{odor}. Therefore, the approximation is self-consistent. (It can be noticed in deriving Equation (7.1) that I and I_c are analogous. So it is to be expected that I_{odor} and I_c^{cancel} should change in the same time scale.)

Now if we have

$$I_c^{enhance} = -\gamma I_c^{cancel}, \tag{7.8}$$

we have response enhancement. Instead of suppressing X_o, which is being raised by I_{odor}, $I_c^{enhance}$ helps I_{odor} to raise X_o in the same direction. To the mitral cells, it is almost

as if the odor input is stronger in concentration than it actually is. If Y_o is also raised to the extent as if a stronger input odor were inhaled, then the oscillatory bulbar output determined by (X_o, Y_o) will be enhanced as if a stronger input odor were inhaled. But on the contrary, Y_o is being suppressed by the $I_c^{enhance}$ while being raised by I_{odor}. By Equation (7.6), (7.7) and (7.8),

$$dY_o \approx (\alpha^2 + WH)^{-1}(W\,dI_{odor} - \gamma\alpha^2 H^{-1} dI_{odor}). \tag{7.9}$$

The larger the $I_c^{enhance}$ (or γ), the more Y_o is suppressed.

We now examine closely the role of Y_o and how odor enhancement works. The (weak) odor input I_{odor} raises (X_o, Y_o) to higher a gain $(G'_x(X_o), G'_y(Y_o))$ point. Let us denote this Y_o as $Y_o^{weaker-odor}$ (which can be raised further to $Y_o^{stronger-odor} > Y_o^{weaker-odor}$ if a stronger odor is inhaled). The negative central control signal $I_c^{enhance}$ lowers the central input $I_c = I_{c,background} + I_c^{enhance}$ to the granule cells, and thus lowers Y_o to $Y_o^{enhance} < Y_o^{weaker-odor}$ (Fig.[7.1]). This effectively reduces the granule inhibitory drive to the mitral cells and raises X_o, as if a stronger odor is inhaled for the mitral cells. But for granule cells, $Y_o^{enhance} < Y_o^{stronger-odor}$, so enhancing is <u>not</u> exactly equivalent to inhaling a stronger odor. Since granule cells affect the bulbar oscillatory response by the gain $G'_y(Y_o)$, thus as long as $Y_o^{enhance}$ and $Y_o^{stronger-odor}$ are in about the same linear range on the gain curve $G_y(Y_o)$, the mitral cell output will be insensitive to the exact Y_o. In such cases, X_o will be the only important factor to determine bulbar output, and it will appear as if a stronger odor is inhaled because of the raised X_o. Y_o without odor input is in a very non-linear range of $G_y(Y_o)$, and has a gain $G'_y(Y_o)$ too low for oscillatory bulbar response. Therefore, two necessary conditions for olfactory enhancement are: *a*): $I_c^{enhance}$ to lower Y_o and thus raise X_o to a higher level; *b*): $I_c^{enhance}$ should not be so strong as to make $Y_o^{enhance}$ lower than Y_o without odor inputs such that $G'_y(Y_o^{enhance})$ is too small. By Equations (7.6) and (7.9), condition *b* means

$$\alpha|dI_c^{enhance}| < W\,dI_{odor} \qquad or \quad \gamma\alpha^2 H^{-1} < W. \tag{7.10}$$

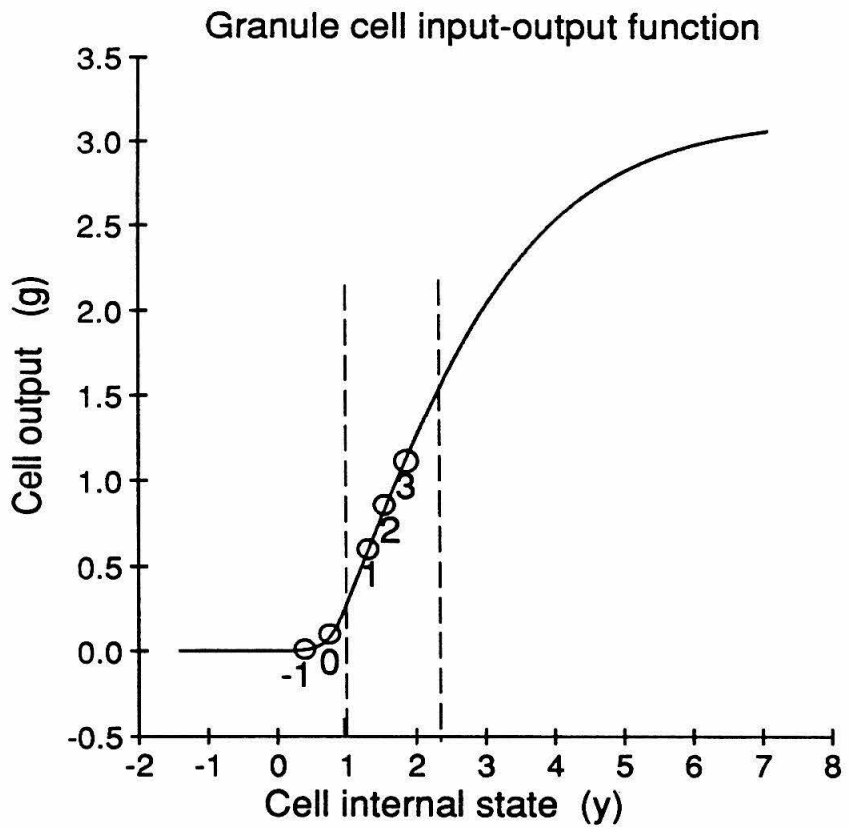

Fig. 7.1 This figure illustrates the possible positions of Y_o indicated by circles on the input-output curve G_y under different circumstances. The circle numbered "0" is the Y_o with no odor input $I_{odor} = 0$, "2" with inhaled odor without enhancing, "1" with the same odor input with enhancing, "3" with a stronger odor input, "-1" without odor input while with enhancing. The region inside the dashed lines is the linear region of G_y where the oscillation output is insensitive to the exact position of Y_o.

Since the scales of α, H and W satisfy the relation (Chapter 4) $\alpha^2 \leq HW = A$, Y_o will be raised as the combined effect of I_{odor} and $I_c^{enhance}$ as long as γ is not too much larger than unity. It is argued in Chapter 3 that G_y (for the granule cells) has a relatively long linear range. Thus, with a not too strong enhancing signal, an enhanced baseline shift bulbar output $G_x(X_o)$ will enhance the oscillatory part of the output as well.

A consequence of this argument is that no odor will be detected (no oscillation) if no odor exists even if sensitivity enhancement is going on for a particular odor. When $I_{odor} = 0$, the condition b mentioned above or inequality (7.10) is violated, and non-damping oscillation bulbar output becomes impossible, although the baseline shift output determined by X_o is raised by the enhancing signal. Since it appears that the oscillation pattern output carries the essential part of the odor information, a higher baseline output without oscillation means no odor information inputs to the olfactory cortex.

The central input to the bulb during enhancement is $I_c \equiv I_{c,background} + I_c^{enhance}$; since $I_c^{enhance}$ is negative, enhancing corresponds to lowering the central input from the background level. For biological synapses of a definite sign (excitatory), $I_c \geq 0$ or $|I_c^{enhance}| \leq I_{c,background}$ should always be satisfied. This implies that $I_c^{enhance}$ amplitude is restricted below a maximum value. For a not too weak odor input, a small $I_c^{enhance}$ is enough to enhance the output to be observable. For too weak an odor input, inequality (7.10) implies that too strong an $I_c^{enhance}$ would not help the enhancement. Thus, in most cases for the purpose of enhancement, only $|I_c^{enhance}| \leq I_{c,background}$ is needed.

Cross-adaptation and cross-enhancement automatically follow by the argument above. For odor a, denote $I_c^{cancel\_a}$ and $I_c^{enhance\_a}$ as the cancelling and enhancing central signal, respectively, for its receptor input I_{odor_a}. The cancelling signal $I_c^{cancel\_a}$ for odor a can not cancel quite completely odor input I_{odor_b} for odor $b \neq a$. However, $I_c^{cancel\_a}$ will impair the bulbar response for I_{odor_b} since $I_c^{cancel\_a}$ does actually suppress the mitral baseline X_o (Eq. 7.6), although not quite as if a weaker odor b is inhaled. Similarly, an enhancing signal $I_c^{enhance\_a}$ for odor a can only distort the bulbar response to odor input I_{odor_b}.

Even though $I_c^{enhance-a}$ raises X_o, it does not raise it in the same direction as if a stronger input of odor b is inhaled. The bulbar output will be an information mixing or distortion of odor a and b.

7.3 Simulations

Computer simulation is done to verify the olfactory adaptation and enhancement in the olfactory bulb. The simulated model with all its parameters is the same as described in Chapters 3 and 6. To solve for the cancelling signal I_c^{cancel} for odor input I_{odor}, use equation

$$dX_o \approx (\alpha^2 + HW)^{-1}(\alpha dI_{odor} - H dI_c^{cancel}) = 0.$$

It follows that:

$$dI_c^{cancel} \approx H^{-1}\alpha dI_{odor} = (H_o G_y'(Y_o))^{-1}\alpha dI_{odor}. \tag{7.11}$$

This is very difficult to solve since H depends on Y_o, which changes with time as

$$dY_o \approx (\alpha^2 + WH)^{-1}(W dI_{odor} + \alpha dI_c^{cancel}). \tag{7.12}$$

Further approximations are used in the simulation to calculate I_c^{cancel}. First neglect the change of Y_o (or H) with time and take

$$H(t) = H_o G_y'(Y_o(t)) \approx H(t=0) = H_o G_y'(Y_o(t=0)) = constant, \tag{7.13}$$

where $Y_o(t=0)$ and $H(t=0)$ are, respectively, Y_o and H at the beginning of the inhalation $t=0$, when $I_{odor} = I_c^{cancel} = 0$. Thus,

$$I_c^{cancel}(t) \approx H(t=0)^{-1}\alpha I_{odor}(t). \tag{7.14}$$

But such an approximation works well only when I_{odor} is small. So the second stage of the approximation is to take

$$I_c^{cancel} \approx \beta H(t=0)^{-1}\alpha I_{odor}, \tag{7.15}$$

where β is a constant that is tuned in the simulation until a best cancellation is achieved. Here the better cancellation means not only the bulbar output $G_x(X)$, but also the oscillation equation operation point X_o is closer to that of the no-odor input, such that an inhalation of a new odor input mixed with the pre-existing odor induces a response closer to the response to the new odor alone. The best cancellation case is a compromise between these two requirements judged by visual inspection. The final value is $\beta = 0.452$ for a sniff cycle of 370 msec, during the first 180 msecs of which is inhalation.

With such an approximated cancelling signal, the enhancing signal is

$$I_c^{enhance} \approx -\gamma I_c^{cancel} \qquad \gamma > 0. \tag{7.16}$$

The value of γ used in most of the simulation is 0.5. Other values can be used to make the olfactory enhancing signal stronger or weaker. This ad hoc procedure generates an adequate cancellation and enhancement, but not as good a signal as could in principle be done with less approximations. In order to see the effect of cancelling and enhancing, I use the same measures as in Chapter 6 (Equation (6.1) to see the difference between the two bulbar response patterns in a sniff cycle. Note that $d_3(a,b), d_4(a,b) > 0$ implies that the response level in a is higher than that in b. The three different odor inputs I_{odor_1}, I_{odor_2}, and I_{odor_3} (Equation (6.2)) are used in the simulations for olfactory adaptation and enhancement.

Simulation of self-adaptation (self-cancelling) shows that

$$I_c^{cancel\_i} \equiv \beta H(t=0)^{-1} \alpha I_{odor\_i}$$

diminishes quite well the bulbar response to the odor I_{odor_i} for $i = 1, 2, 3$. Application of half of the cancelling signal, i.e., $I_{c,control} = 0.5 I_c^{cancel\_i}$, reduces the response level of the bulb to input I_{odor_i}, while the response pattern waveform is still similar to the original response without cancelling. This implies that the response signal to odor is less strong with non-complete adaptation than it would be without adaptation, and that a stronger

input of the pre-existing and adapted odor type will still be detected by the bulb although it would smell less strong. Fig [7.2] shows an example of self-adaptation, and Table [7.1] gives the measured differences between the adapted and non-adapted responses to odors. Notice that $d_3, d_4 \approx 1$ between the original response and self-adapted response means that a complete self-adaptation is achieved. d_3 and d_4 between the simulated original and fully adapted responses are $\approx 0.6 - 0.8$; this is partly because the granule cells are raised to highly responsive internal state Y_o, which enhances the system noise and raises up the $\bar{O}_{osci}$ and $\bar{O}_{mean}$ levels. Another reason is that the cancelling signal used is an approximation. The fully adapted response waveform, which is mostly amplified system noise, is very different from that of the original response.

Simulations also show that the model bulb can remain sensitive to new odor inputs I_{odor_j} after being completely self-adapted to the pre-existing odor I_{odor_i} for $i \neq j$. Assume that the total receptor input to the bulb is a linear sum of the odor components in a mixture:

$$I_{odor} = I_{odor\_i} + I_{odor\_j}. \tag{7.17}$$

Since the bulb is adapted to I_{odor_i}, the cancelling signal $I_c^{cancel\_i}$ is sent to the bulb from the higher centers. Simulations show that both the response waveform and the response level in this situation look quite similar to the response to only I_{odor_j} without adaptation (Fig [7.2], Table[7.2]).

In the simulation for olfactory enhancement, $I_c^{enhance\_i} = -\gamma I_c^{cancel\_i}$ is taken with $\gamma = 0.5$ for $i = 1,2,3$. Figure [7.3] compares the bulbar response to an odor example of half the input strength, i.e., $I_{odor} = 0.5 I_{odor\_i}$, with and without enhancing. Enhancing raises the response to half-strength-input to about the level of original response, while the response waveform stays similar to the original response (Table [7.3]). Similar simulations can be done with an even weaker odor input or with different strength-enhancing signals (different γ values). Since the quality of the enhancing relies on the linearity of the granule cells, the weaker the enhancing signal, the more likely the Y_o value stays in the same linear

Table [7.1] Difference between adapted and non-adapted responses

	odor number	$d_1(a,b)$	$d_2(a,b)$	$d_3(a,b)$	$d_4(a,b)$
a: Non-adapted response b: Half-adapted response	1	0.003	0.039	0.271	0.399
	2	0.014	0.041	0.274	0.471
	3	0.012	0.078	0.309	0.313
a: Non-adapted response b: Fully adapted response	1	0.144	0.803	0.690	0.728
	2	0.166	0.736	0.743	0.770
	3	0.642	0.788	0.774	0.589

Figure 7.2 — Demonstration of olfactory adaptation. **A,E:** Original responses to I_{odor_1} and I_{odor_2}, respectively. **B,C:** Half-adapted and fully adapted responses to I_{odor_1}. **D:** Response to no odor input without adaptation. **F:** Response to $I_{odor\_1} + I_{odor\_2}$ without adaptation. **G:** Response to $I_{odor\_1} + I_{odor\_2}$ with full adaptation to I_{odor_2}.

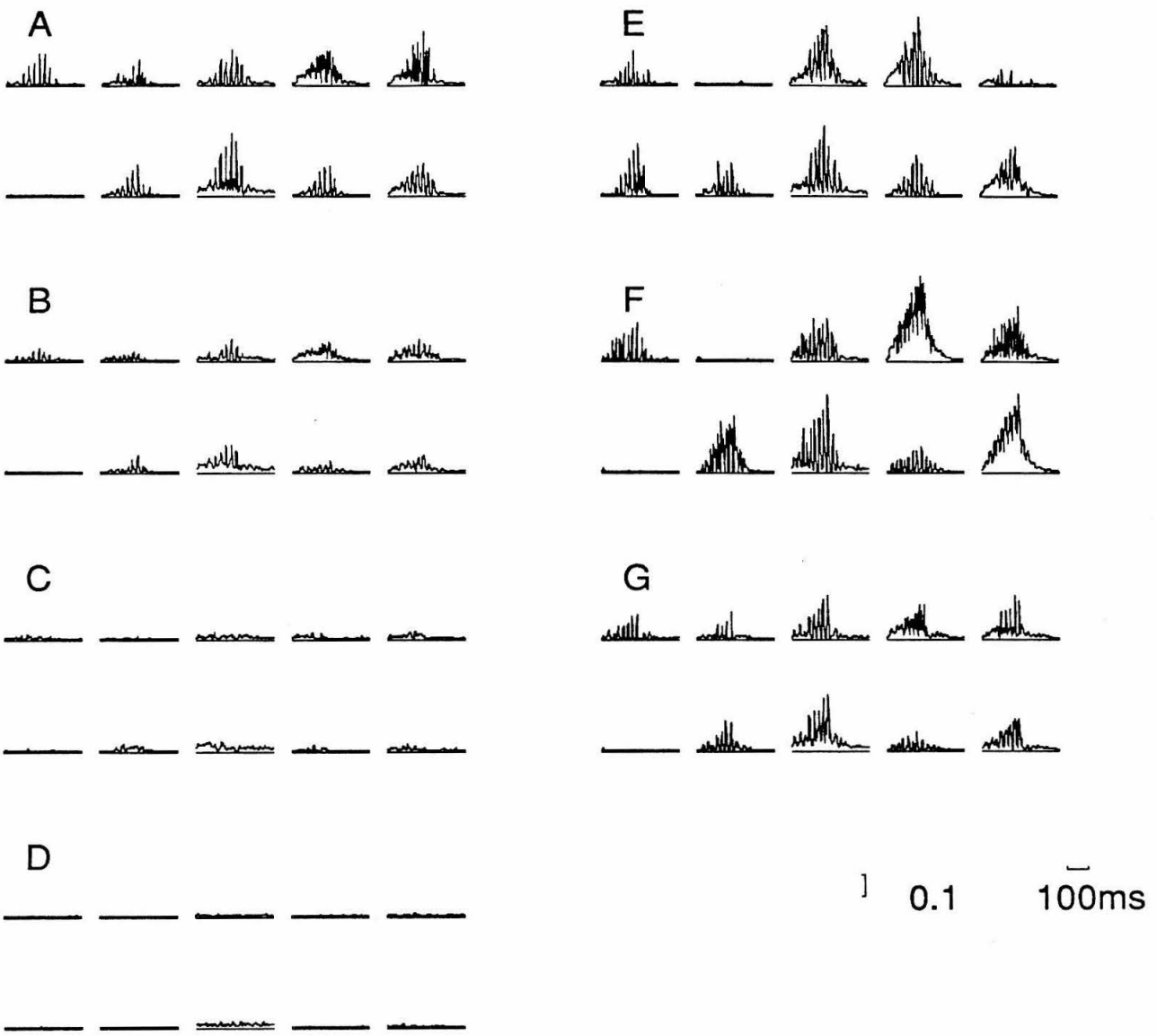

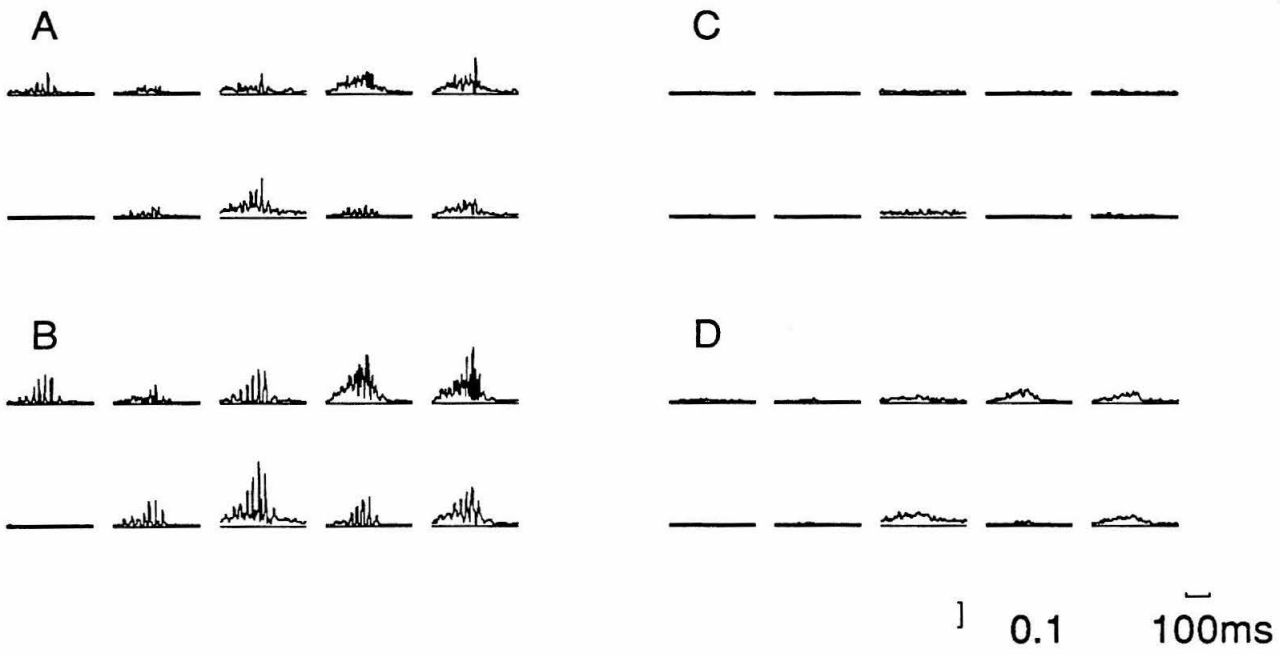

Figure 7.3 — Demonstration of olfactory enhancement. **A,B:** Responses to $0.5I_{odor\_1}$ without and with enhancement, respectively. **C,D:** Responses to no odor input without and with enhancement for I_{odor_1}, respectively.

Table [7.2]

Differences between the original response to an odor and the response to this odor after fully adapted to another odor

Response a: the original response to I_{odor_i} for all i

Response b: the response to $I_{odor} = I_{odor\_i} + I_{odor\_j}$ with cancelling signal $I_c^{cancel\_j}$ for $j \neq i$

$i =$	$j =$	$d_1(a,b)$	$d_2(a,b)$	$d_3(a,b)$	$d_4(a,b)$
1	2	0.025	0.039	0.010	0.070
	3	0.016	0.013	0.008	0.065
2	1	0.030	0.038	-0.029	0.087
	3	0.022	0.009	-0.023	0.027
3	1	0.006	0.029	0.005	0.151
	2	0.009	0.037	0.021	-0.002

Table [7.3] **Differences between the enhanced and non-enhanced responses**

	odor number	$d_1(a,b)$	$d_2(a,b)$	$d_3(a,b)$	$d_4(a,b)$
a: Non-enhanced original response b: Non-enhanced response to half-strength input	1	0.001	0.083	0.272	0.423
	2	0.013	0.048	0.286	0.420
	3	0.001	0.045	0.272	0.399
a: Non-enhanced original response b: Enhanced response to half-strength input	1	0.003	0.014	0.010	0.081
	2	0.002	0.007	-0.001	-0.009
	3	0.005	0.023	0.006	0.165

region, and the less distortion in the enhanced response, although a weaker enhancing signal results in less response level enhancement. Caution should be taken always to have $I_c \geq 0$. Violating the inequality (7.10) or having too strong an enhancing signal implies no oscillatory response.

Cross-adaptation or cross-enhancement can be simulated as well. Among the simulated examples are those with odor input I_{odor_i} and the cancelling $\delta I_c^{cancel\_j}$ for cross-adaptation, and those with odor input $0.5I_{odor\_i}$ and enhancing signal $-\delta I_c^{cancel\_j}$ for cross-enhancement for $i \neq j$. δ is a positive number whose value is taken as 0.5. Other strengths of the input odors and the cancelling or enhancing signals can be used for simulations as well. Different degrees of information mixing and distortion are seen in both the cross-adaptation and cross-enhancement, and they depend on the odor pair; i.e., odor i can be cross-adapted or cross-enhanced by odor j to a different extent as the extent of vice versa. For instance, response to $0.5I_{odor\_1}$ with enhancing for I_{odor_2} is quite similar to the original response to I_{odor_1}, while the response to $0.5I_{odor\_2}$ is more distorted by enhancing for I_{odor_1}, and resembles the original response to I_{odor_1}, even though the strength of I_{odor_1} is weaker than that of I_{odor_2}. Non-linearity of the system presumably plays an important role in the asymmetry between the two odors in a pair for cross-adaptation and cross-enhancement. Tables [7.4], [7,5] and Figure [7.4] show the differences between the cross-adapted or cross-enhanced responses and the original responses.

7.4 Self-adaptation and recovery time courses

Psychophysical experiments (Pryor et al. 1970; Steinmetz et al. 1970) show that olfactory adaptation set up slowly in a time period of several minutes. An odor exposed to the nose smells less and less strong until no odor perception or a constant faint odor perception is reached. The perceived odor strength $S(t)$ can be thought of as following an exponentially decaying curve described by (Fig [7.5]):

$$S(t) = (S_i - S_f)e^{-(t-t_o)/\tau} + S_f, \tag{7.18}$$

Table [7.4]

Differences between the original responses and the cross-adapted responses

Cross-adapted response is response to odor input I_{odor_i} with cancelling signal $0.5I_c^{cancel\_j}$

	$i=$	$j=$	$d_1(a,b)$	$d_2(a,b)$	$d_3(a,b)$	$d_4(a,b)$
a: Original response to I_{odor_i}	1	2	0.246	0.595	0.320	0.646
		3	0.272	0.266	0.118	0.421
b: Cross-adapted response to I_{odor_i}	2	1	0.072	0.131	0.095	0.188
		3	0.106	0.115	0.040	0.575
	3	1	0.015	0.755	0.189	0.362
		2	0.038	0.266	0.296	0.490

Table [7.5]

Differences between the original and cross-enhanced responses

Cross-enhanced response is response to $0.5I_{odor\_i}$
with enhancing signal $0.5I_c^{enhance\_j}$ for $i \neq j$

	$i=$	$j=$	$d_1(a,b)$	$d_2(a,b)$	$d_3(a,b)$	$d_4(a,b)$
a: Original response to I_{odor_i} b: Cross-enhanced response to $0.5I_{odor\_i}$	1	2	0.050	0.046	-0.102	0.184
		3	0.177	0.316	-0.091	0.560
	2	1	0.121	0.126	0.079	0.239
		3	0.291	0.356	-0.005	0.330
	3	1	0.008	0.036	0.076	0.107
		2	0.012	0.042	-0.019	0.100
a: Original response to I_{odor_j} b: Cross-enhanced response to $0.5I_{odor\_i}$	1	2	0.134	0.175	-0.089	-0.290
		3	0.017	0.250	-0.088	-0.321
	2	1	0.065	0.095	0.112	-0.131
		3	0.019	0.061	0.018	0.070
	3	1	0.193	0.559	0.103	-0.386
		2	0.310	0.403	0.006	-0.473

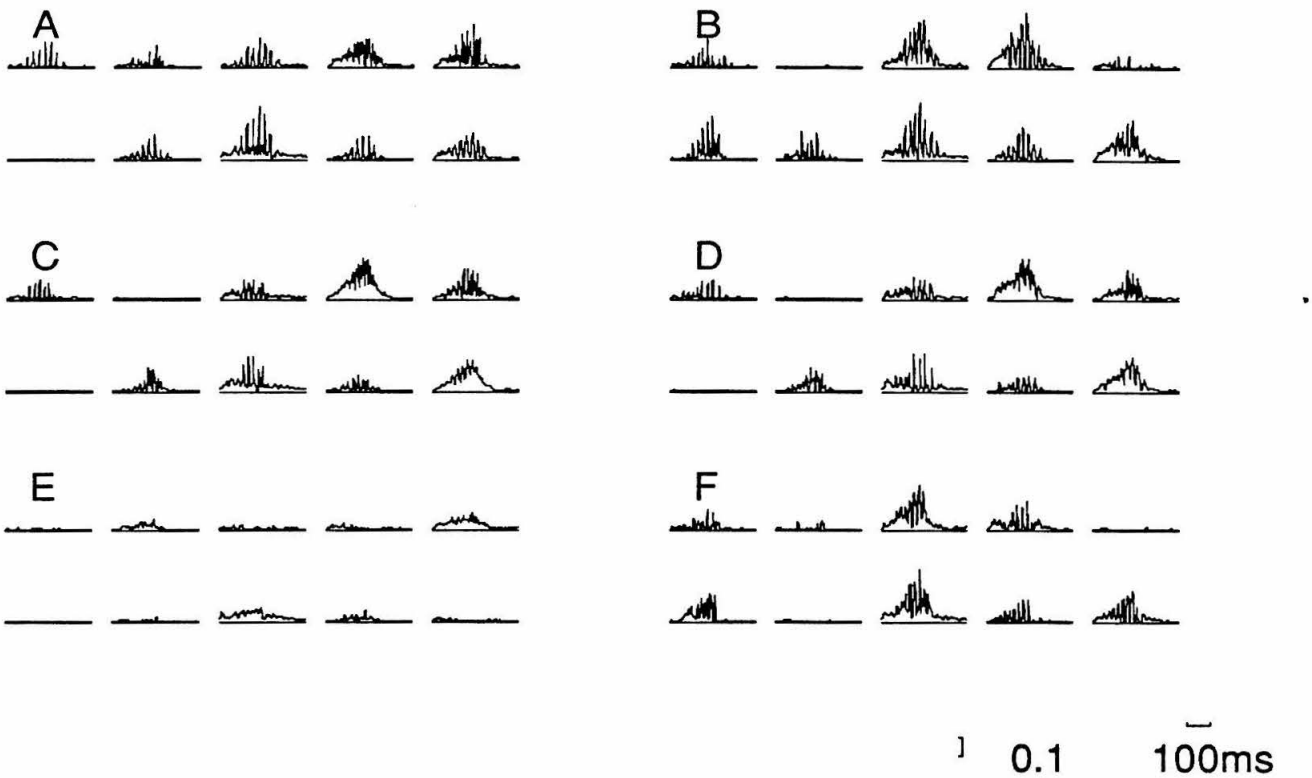

Figure 7.4 — Demonstration of cross-adaptation and cross-enhancement. **A,B:** Original responses to I_{odor_1} and I_{odor_2}, respectively. **C:** Response to $0.5I_{odor\_1}$ with enhancement for I_{odor_2}. **D:** Response to $0.5I_{odor\_2}$ with enhancement for I_{odor_1}. **E:** Response to I_{odor_1} with half-adaptation to I_{odor_2}. **F:** Response to I_{odor_2} with half-adaptation to I_{odor_1}.

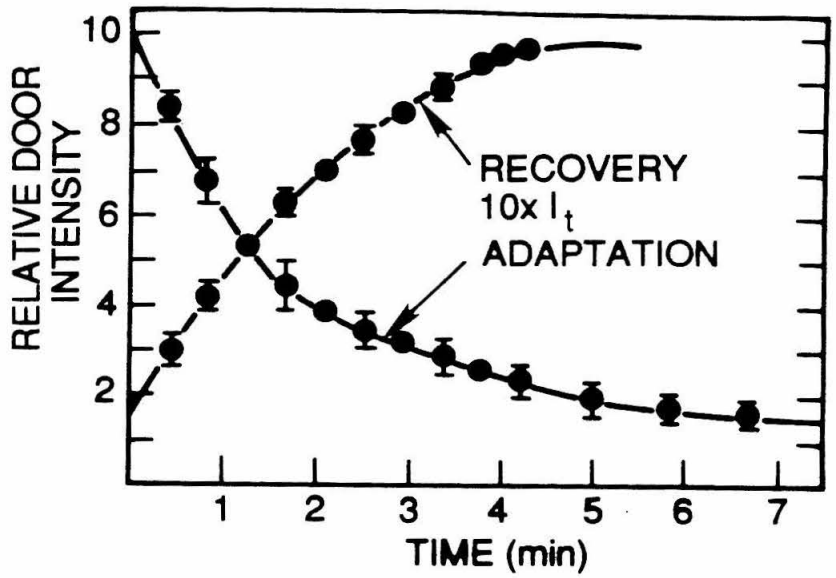

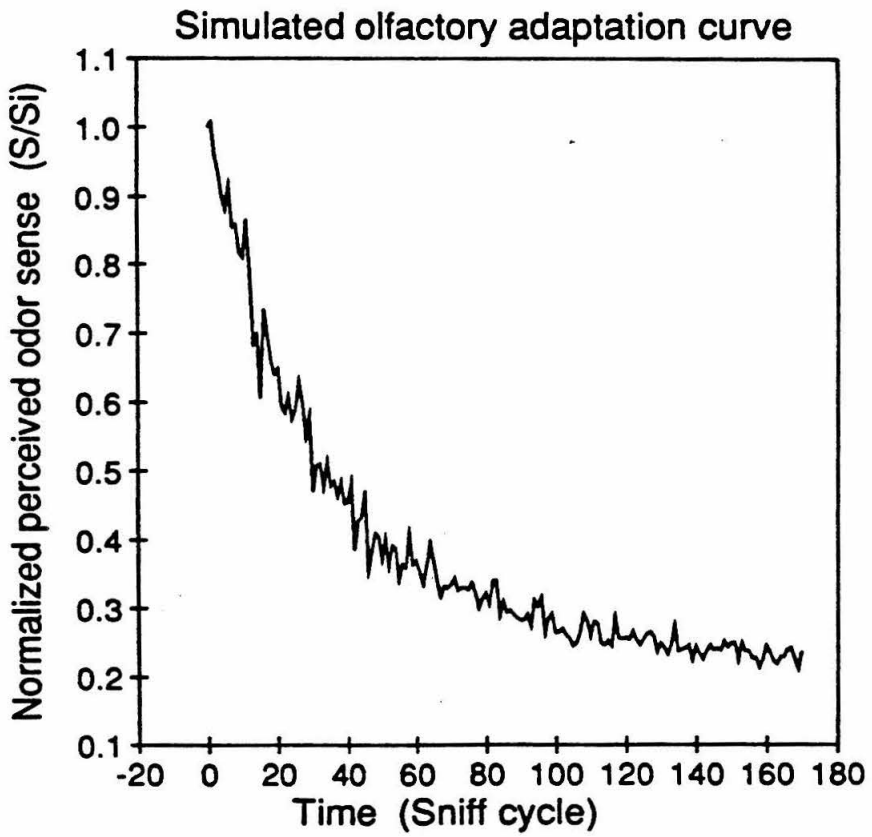

Figure 7.5 — The upper figure shows the experimental adaptation and recovery curves (Steinmetz et al. 1970). The lower illustrates the simulated olfactory adaptation curve. The vertical axis is S/S_i; the horizontal axis is time in the unit of a sniff cycle. The initial odor detection and adaptation start at time = 0 sniff cycle. Odor input is I_{odor_2}, $S_f = 0.2S_i$, $\tau \approx 33.3$.

where S_i and S_f are the initial and final perceived odor strength, and the adaptation starts at $t = t_o$ which is assumed to be the time when the odor is initially detected, τ is the time decay constant of the perceived odor strength with time. The perceived strength $S(t)$ can be thought of as proportional to the $\bar{O}_{mean}$ and $\bar{O}_{osci}$ described in Chapter 6; i.e., $S \equiv c\bar{O}_{mean} + (1-c)\bar{O}_{osci}$. S_f and τ may depend on the odor type and concentration.

Olfactory recovery occurs after the odor is withdrawn. The sensitivity to the adapted odor gradually increases and saturates at the original sensitivity before adaptation (Figure [7.5]). The sensitivity recovery takes about the same time as it is for the adaptation, suggesting that the olfactory adaptation and recovery may or may not use the same underlying mechanism in the brain. The model can, however, be used to explain the self-adaptation time course.

Suppose that the central brain sends an extra cancelling signal ΔI_c if the odor is perceived at the last sniff; i.e., $I_c \rightarrow I_c + \Delta I_c$. The original I_c is the sum of the background central input $I_{c,background}$ and any other central controlling signal which existed at the last sniff, for instance, some (non-complete) cancelling signal already sent at the last sniff for the existing odor. Assume that at the present sniff:

$$\Delta I_c = 1/\tau \frac{S - S_f}{S_i} I_c^{cancel}, \tag{7.19}$$

where S is the perceived odor strength at the last sniff. Encouraged by the result of the linear approximation for the cancelling, I assume that

$$\Delta S \approx -\frac{\Delta I_c}{I_c^{cancel}} S_i, \tag{7.20}$$

where ΔS is the difference of the perceived odor strength between the last and present sniff. It follows that

$$\Delta S \approx (S - S_f)/\tau. \tag{7.21}$$

This process will continue for the next sniff, and finally Equation (7.18) results, where the time t can be thought of as the discrete time for the odor perception at discrete sniffs.

Adjusting the adaptation speed with τ in Equation (7.18) causes different adaptation time scales. Simulation is done (Figure [7.5]) with $c = 0.5$, $S_f = 0.2S_i$ and $\tau = 33.3$ sniff cycles. The simulated adaptation curve is not very smooth partly because of the different system noises in the different sniffs.

When the odor is suddenly withdrawn, it can no longer be perceived and the cancelling signal will then decay, which may involve some other mechanism.

8. Conclusions and discussion on the olfactory bulb model

The present model of the olfactory bulb is a simplification of the known anatomy and physiology. The net of the mitral and granule cells simulates a group of coupled non-linear oscillators, which are the sources of the rhythmic activities in the bulb. The coupling makes the oscillation coherent across the whole bulb surface with a single frequency for each sniff but different amplitudes and phases for different mitral cells. The model suggests, in agreement with Freeman and coworkers, that stability-change bifurcation is used for the bulbar oscillator system to decide primitively on the relevance of the receptor input information. Different non-damping oscillation modes that emerged from the bifurcation are used to distinguish the different odor input information, which is the driving source for the bifurcations. These oscillation modes are approximately thought of as the decision states of the system for the odor information. The coupling between the oscillators implies that information from different parts of the bulb is combined to make the coherent output oscillation mode, and thus a unitary decision. In Chapter 9, more general cases with more complicated cell connections will be analyzed.

This model bulb encodes the non-oscillatory input in the oscillatory "AC" output. Since the oscillation is intrinsic in the bulb, the model amplifies the weak odor input by transforming it to the oscillatory output. Consequently, whether or not an oscillatory mode exists indicates whether an odor is present. With the extra information represented in the oscillation phases of the cells, the bulb emphasizes the differences between different input patterns (Chapter 6). Both the analysis and simulation show that the bulb is selectively, i.e., non-uniformly, sensitive to different receptor input patterns. This selectivity as well as the motivation level of the animal could also be modulated from higher centers (Chapter 5). The information encoding scheme suggests that to extract information from the oscillation amplitudes and phases, the mitral cells, rather than the EEG waves (in which the detailed amplitude and phase information tend to be averaged out), should be looked at. Within this model, the information is carried by the detailed pattern of activity of the individual

mitral cells; the spatial EEG pattern is an information epiphenomenon. This model does not exclude the possibility that the information is coded in the non-oscillatory slow wave X_o, since X_o is also determined by the odor input.

The chief behaviors do not depend on the number of cells in the model. The frequencies of the oscillation modes are close to the resonant frequency of a single oscillator in the system and are independent of the size of the model. However, since the number of the possible oscillation modes is the same as the number of the mitral cells, the simulated model with less cells has fewer oscillation modes or decision states, and it therefore has smaller memory capacity than the real bulb. The simulated bulb does not respond oscillatorily to most randomly selected input patterns P_{odor}.

This model uses a continuous input-output function, instead of discrete spikes generated by neurons, to describe the neuron output. Since the continuous output value is meant to simulate the average of the firing rate of the neurons, unaveraged discrete spike output should chiefly introduce more fluctuations in the system. If the biological system had approximately equivalent close by neurons, then a continuous output would be a good approximation to the group average. Simulation was also done on a model, in which each cell in the original model was replaced by a group of cells that generated action potentials rather than continuous valued output (Figure [8.1]). Oscillatory behavior is obvious in the summed spike trains of groups of local cells. But the spike train of a single cell appears very noisy and sparse with barely recognized oscillatory behavior. In the physiological experiment, each mitral cell fires on the average about once in 100 ms (Freeman and Skarda 1985), making it hard to recognize an oscillation with a period of 25 ms in the spike train of a single cell. On the other hand, the EEG wave is clearly oscillatory since it is from the averaged activities of many local granule cells.

The simulation is done on a one-dimensional ring of mitral and granule cells, while the real bulb has cells sitting on two-dimensional segments of a sphere. The dimension

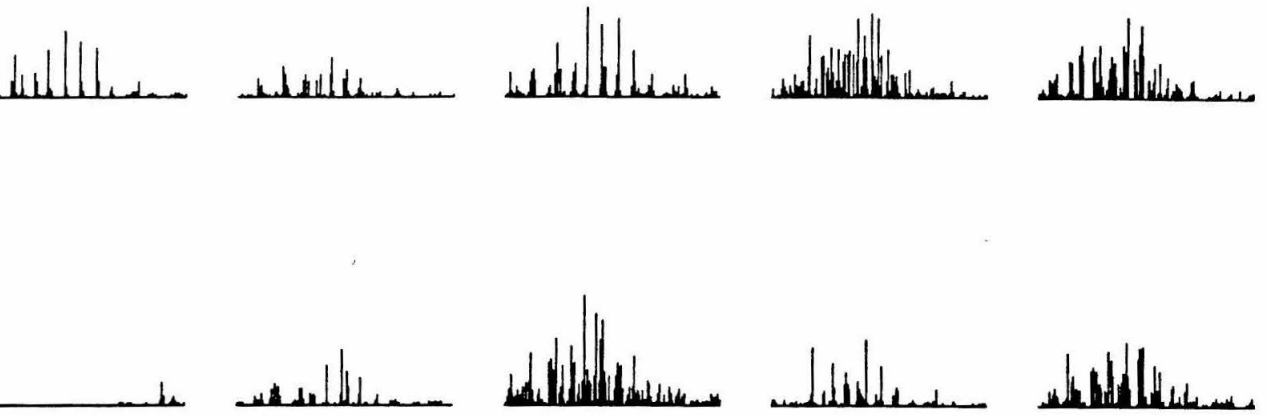

Firing histograms of local clusters of mitral cells

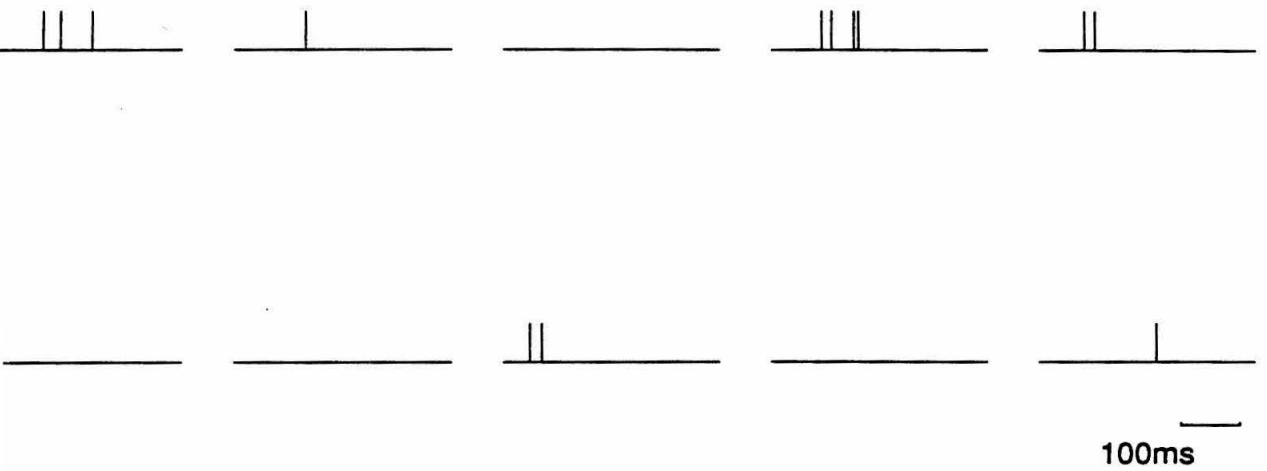

Spike trains of one mitral cell in each local cluster

Figure 8.1 — Simulated bulbar mitral cell response pattern corresponding to Fig.6.A. Each cell is modeled to have discrete action potential firings of maximum rate about 300/sec. Each cluster has about 310 mitral cells, and thus a maximum firing rate of 93,000/s.

of the cell arrangement is not crucial in the model. One simulation was done on a two-dimensional surface of the cells to mimic the real bulb, and the basic oscillation phenomena were very similar to those of the one-dimensional rings.

This model is successfully used to explain the observed psychophysical phenomena of both the self-adaptation and cross-adaptation. The model bulb can remain sensitive to new odor input, including a stronger input of the pre-existing odor type, after being adapted to the pre-existing odor input. Distorted and reduced response is seen for an odor input that replaces the pre-existing and adapted odor input before recovery (cross-adaptation). Furthermore, sensitivity enhancement by central control is postulated for the olfactory bulb. It produces response level enhancement when sniffing a weaker odor (self-enhancement). The model bulb does not respond oscillatorily (or sensibly) to no odor input even if the olfactory enhancement signal is sent from the central brain for a particular odor. Different degrees of odor information mixing and distortion can be seen if the bulb has its sensitivity enhanced for one odor while another odor is inhaled (cross-enhancement). This can also be considered reasonable since it is analogous to the cross-adaptation, which is psychophysically observed. Physiological experiments demonstrate that when the central input to the bulb is blocked, the neural oscillatory activity induced by breathing is increased substantially (Gray and Skinner 1988). This model of olfactory enhancement agrees with this experimental result by showing that reducing the central input enhances the bulbar (oscillatory) response to the odor input. The time course of olfactory adaptation can also be explained in the model.

The adapting and enhancing signals in the computer simulation are calculated with several stages of approximations: the slow input approximation described in Section 7.2, and the linear approximation in Section 7.3. The simulated results are quite satisfactory with these approximated signals. The linear approximation works better with smaller signals. I believe that if these signals are calculated with less approximations, the simulated results would be better.

A necessary condition for the higher olfactory centers to send an adapting (cancelling) or enhancing signal for a particular odor is that they have enough information about that odor to send the appropriate signal. This condition is easily fulfilled in the adaptation process since the adaptation is triggered after the odor is detected, and the higher centers will then have a memory of the recent input odor. To enhance the sensitivity to a particular odor (which may or may not be present), the higher centers must already know the odor either from long-term memory of experience or genetically inherited information.

9. Beyond the Olfactory Bulb

9.1 Generalization to the Olfactory Cortex and Other Parts of the Brain

This model of the olfactory bulb can be generalized to other masses of interacting excitatory and inhibitory cells such as those in the olfactory cortex, neocortex, and hippocampus (Shepherd 1979; Singer et al. 1988; Eckhorn et al. 1988), where there may be connections between the excitatory cells as well as the inhibitory cells, as is claimed by some for the olfactory bulb (Nicoll 1971; Freeman 1975, 1979b, 1979c). One can use the same formulation as in the bulb model, with mitral cells generalized to N excitatory cells and granule cells to M inhibitory cells, add B_o and C_o to represent excitatory-to-excitatory and inhibitory-to-inhibitory connection matrices, respectively. Then Equation (4.6) becomes:

$$\begin{aligned} \dot{X} &= -H_o G_y(Y) - \alpha_x X + B_o G_x(X) + I(t), \\ \dot{Y} &= W_o G_x(X) - \alpha_y Y - C_o G_y(Y) + I_c(t). \end{aligned} \tag{9.1}$$

9.1.1 Adiabatic Non-linear Coupled Oscillator System

If the inputs (I, I_c) for these systems also change very slowly in a time scale much longer than with the characteristic neural dynamic time constant (e.g., the oscillation period), then the adiabatic approximation can again be used, and a similar equilibrium point (X_o, Y_o) follows the equation (cf. Equation (4.7):

$$\begin{aligned} \dot{X}_o \approx 0 &= -H_o G_y(Y_o) - \alpha_x X_o + B_o G_x(X_o) + I(t), \\ \dot{Y}_o \approx 0 &= W_o G_x(X_o) - \alpha_y Y_o - C_o G_y(Y_o) + I_c(t). \end{aligned} \tag{9.2}$$

Linearizing around (X_o, Y_o) (cf. Equation (4.9)),

$$\begin{aligned} \dot{X} &= -HY - \alpha_x X + BX, \\ \dot{Y} &= WX - \alpha_y Y - C'Y. \end{aligned} \tag{9.3}$$

where (X, Y) is the deviation from (X_o, Y_o), H and W are the same as those defined in Chapter 4, $B \equiv B_o G_x'(X_o)$, and $C' \equiv C_o G_y'(Y_o)$. Eliminating Y leads to (cf. Equation (4.15))

$$\ddot{X} + (\alpha_x - B + \alpha_y + C)\dot{X} + (A + (\alpha_x - B)(\alpha_y + C))X = 0, \tag{9.4}$$

where $C = HC'H^{-1} = HC_oG_y'(Y_o)H^{-1}$. This is a system of N coupled oscillators with the i^{th} oscillator following the equation

$$\ddot{x}_i+(\alpha_x - B_{ii} + \alpha_y + C_{ii})\dot{x}_i + (A_{ii} + \alpha_x\alpha_y - \alpha_y B_{ii} + \alpha_x C_{ii} - (BC)_{ii})x_i$$
$$= \sum_{j\neq i}(B_{ij} - C_{ij})\dot{x}_j - \sum_{j\neq i}(A_{ij} + \alpha_y B_{ij} - \alpha_x C_{ij} + (BC)_{ij})x_j \quad , \tag{9.5}$$

where $(BC)_{ij}$ means the corresponding matrix element of the matrix product BC. The left-hand side describes a damped oscillator, while the right-hand side describes the couplings from other oscillators. The oscillator couplings are more complicated in this system; even the dissipations in oscillators are coupled (see the $\dot{x}_j$ terms above).

Replacing α_x by $\alpha_x - B$, and α_y by $\alpha_y + C$, Equation(4.15) becomes Equation (9.4). This means that if coupling B and C is local (i.e., B and C are almost diagonal), having excitatory connections B_o is like reducing dissipation for oscillators, while having the inhibitory connections is like adding some oscillator dissipation. Strong enough local excitatory-to-excitatory connections B_o can reduce the oscillator dissipations so much that the net can oscillate even without much input I as is simulated by Freeman (1979b, 1979c). This is, however, not necessarily true if the connection B_o is non-local (as in the olfactory cortex, Haberly 1985). This is because neighboring oscillators i and j for $i \approx j$ are more likely to oscillate in phase; therefore, with local connections B_o, the coupling $B_{ij}\dot{x}_j$ from the neighboring j^{th} oscillator to the i^{th} oscillator is more likely to be in phase with $\dot{x}_i$; this feeds the energy to the i^{th} oscillator (see Chapter 4). A negative dissipation introduced by a local excitatory-to-excitatory connection B_o can become positive non-locally when the two oscillators coupled by B are oscillating with opposite phases.

A more compact way to write Equation (9.4) is

$$\ddot{X} + B'\dot{X} + A'X = 0, \tag{9.6}$$

where $A' \equiv A + (\alpha_x - B)(\alpha_y + C)$, and $B' \equiv \alpha_x - B + \alpha_y + C$. Equation (9.5) becomes

$$\ddot{x}_i + B'_{ii}\dot{x}_i + A'_{ii}x_i = -\sum_{j\neq i} B'_{ij}\dot{x}_j - \sum_{j\neq i} A'_{ij}x_j. \tag{9.7}$$

In such a system, the oscillation modes are no longer the eigenvectors of matrix A or A' (cf. Equation (4.18). To obtain the oscillation modes, define $(N + M)$ dimensional vector $Z \equiv \begin{pmatrix} X \\ Y \end{pmatrix}$, and $(N + M) \times (N + M)$ matrix $P \equiv \begin{pmatrix} -\alpha_x + B & -H \\ W & -\alpha_y - C' \end{pmatrix}$, and Equation (9.3) will be

$$\dot{Z} = P \cdot Z. \tag{9.8}$$

The system has $(N + M)$ solution modes. For eigenvector Z_k of matrix P with eigenvalue λ_k, the k^{th} mode is

$$Z \propto Z_k e^{\lambda_k t} \tag{9.9}$$

for $k = 1, 2 \ldots, N, N+1, N+2, \ldots, N+M$. λ_k is a complex valued number. If $Im(\lambda_k) \neq 0$ (Im means the imaginary part of a complex number), then the k^{th} mode will be an oscillation mode. Not all the modes actually oscillate. In the special case when $B = 0$ and $C = 0$, for example, there are $(M - N)$ non-oscillatory modes

$$Z \propto \begin{pmatrix} X = 0 \\ Y_{k'} \end{pmatrix} e^{-\alpha_y t}, \tag{9.10}$$

where $Y_{k'}$ satisfies $HY_{k'} = 0$ for $k' = 1, 2, \ldots, (M - N)$. These $(M - N)$ modes have the Y components decoupled from the X components, and are therefore not available from Equation (9.4) (or (4.15) in the special case). The rest of the $(N + M)$ modes ($2N$ of them) involve non-zero X components. Since P is a real matrix, all its non-real eigenvalues come as complex conjugate pairs. Therefore, these $2N$ modes are actually N pairs of modes. They are the modes of Equation (9.4) (or (4.15) in the special example). (Notice that the solution (4.21) comes with the pair $X_k e^{-\alpha t + i\sqrt{\lambda_k} t}$ and $X_k e^{-\alpha t - i\sqrt{\lambda_k} t}$ for all modes k.)

For those oscillatory modes ($Im(\lambda_k) \neq 0$), the oscillation amplitudes will increase with time if

$$Re(\lambda_k) > 0. \tag{9.11}$$

Again, as in the case for the olfactory bulb, whether the system will have sustained oscillation patterns, and which oscillation modes shape the output will be determined by the

equilibrium point $Z_o \equiv (X_o, Y_o)$, which is determined by the input (I, I_c). In other words, the oscillator sytem is adiabatically changed by the external input (I, I_c). When the oscillation amplitude is large, the non-linear effect is visible again, and the waveform will be complex. When the output is carried by the principal excitatory cells (as in most brain structures), only the first N components of $Z = \begin{pmatrix} X \\ Y \end{pmatrix}$ are important for an output pattern.

9.1.2 Externally Driven Non-linear Coupled Oscillator system

The model can be generalized further to the cases when adiabatic approximations can not be used; i.e., the external input (I, I_c) does not change slowly enough compared with the neural dynamics. The olfactory cortex, for example, receives olfactory bulb output, which oscillates with about the same frequency as that of the olfactory cortex activities (Freeman 1978). In these cases, the external input can be separated into fast and slow components. Suppose $I(t) \equiv I^{slow}(t) + I^{fast}(t)$ and $I_c(t) \equiv I_c^{slow}(t) + I_c^{fast}(t)$, where the superindices indicate the fast and slow input components, respectively. $I^{slow}(t)$ and $I_c^{slow}(t)$ are assumed to change very slowly compared with the neural dynamics. The "equilibrium point" (X_o, Y_o) can be calculated as (cf. Equation (9.2)):

$$\begin{aligned} \dot{X}_o \approx 0 &= -H_o G_y(Y_o) - \alpha_x X_o + B_o G_x(X_o) + I^{slow}(t), \\ \dot{Y}_o \approx 0 &= W_o G_x(X_o) - \alpha_y Y_o - C_o G_y(Y_o) + I_c^{slow}(t). \end{aligned} \tag{9.12}$$

Here the adiabatic approximation is used only on the slow input components, and the "equilibrium point" is no longer actually in equilibrium because of the extra driving forces $I^{fast}(t)$ and $I_c^{fast}(t)$. Linearizing around (X_o, Y_o) (cf. Equation (9.3)), then

$$\begin{aligned} \dot{X} &= -HY - \alpha_x X + BX + I^{fast}(t), \\ \dot{Y} &= WX - \alpha_y Y - C'Y + I_c^{fast}(t). \end{aligned} \tag{9.13}$$

where all the variables and parameters have the same definition as in Equation (9.3) except for the extra external fast input. Eliminating Y as before (cf. Equation (9.4)),

$$\ddot{X} + (\alpha_x - B + \alpha_y + C)\dot{X} + (A + (\alpha_x - B)(\alpha_y + C))X = (\alpha_y + C)I^{fast}(t) - H I_c^{fast}(t) + \dot{I}^{fast}(t), \tag{9.14}$$

where C is the same as in Equation (9.4). Or

$$\ddot{X} + B'\dot{X} + A'X = F(t), \tag{9.15}$$

where $F \equiv (\alpha_y + C)I^{fast}(t) - H\,I_c^{fast}(t) + \dot{I}^{fast}(t)$. This is a system of coupled oscillators driven by the external force $F(t)$.

9.2 Discussions and Speculations on Future Research

This thesis has focused on the modeling of the olfactory bulb which has the characteristic rhythmic neural activities. Recently, similar high frequency oscillations have been found in visual neocortex (Singer et al. 1988; Eckhorn et al. 1988). Shepherd (1979) has argued that the brain is organized in similar principles in many different areas. Since the mathematical model in this thesis does not depend crucially on the olfactory environment, the oscillatory network model can also be applied to these other brain areas, as sketched in Section 9.1. Of course, the computational function of the oscillation may be quite different in other areas.

The neural oscillatory activities can be conceivably used in many different processing algorithms. The oscillation phase information can be used for temporal information. Since the high frequency brain waves have frequencies on the order of 40 Hz, the resolution of the collective temporal information can be much more accurate than 25 milliseconds. The oscillatory dynamics is also structurally stable against saturations (exponential growth in neural activity with time) when nonlinearity is included. Using limit cycles as memory or classification states can take advantage of the sensitive dynamics, and thus may be more sensitive to external input than a memory mechanisms using system fixed points as memories. This is true since most of the fixed points so far studied are in the saturation regions of the neural states and therefore sacrifice the sensitivity. An oscillatory memory system may have smaller basins of attraction for most memory states than those of the static memory systems. Of course, by using a gentler nonlinearity, a similar sensitivity might also be generated at limit points. But the new variable phase is present only in the oscillatory system, and allows a richer description of attractor states.

The application of this model to olfactory adaptation and enhancement could also be used in other brain areas. It could be used as one of the mechanisms in the brain for attention control. The (rhythmic) thalamus in the brain, for instance, receive sensory inputs from all the major sensory systems. Each sensory pathway has its specific thalamic nucleus. Each part of the thalamus, in turn, receives fibers from the area of cortex to which it projects (Shepherd 1979). As the gateway to the neocortex for the sensory inputs, the attention control is probably needed there. The olfactory adaptation and enhancement model in the bulb uses the fact that the numbers of intrinsic neurons (granule cells) or central input fibers are much larger than that of the principal neurons (mitral cells). The thalamus structure for visual inputs — lateral geniculate nucleus (LGN) — has, however (up to the knowledge of today), less intrinsic neurons than the principal neurons. So these attention control mechanisms may have to be of modified versions. However, LGN does receive more central feedback fibers from the visual cortex than the number of feedforward fibers to the cortex. The reticular complex may be involved in attention control for LGN (Crick 1984).

In order for an oscillatory mechanism to be useful in information processing, presumably several periods of oscillations are needed before the information can be deciphered. For oscillations of 40 Hz frequency, it takes about 0.2 second for 8 periods. This is about the right timescale for the shortest of human perceptions. Higher level intelligent functions take longer.

Resonance phenomena can be another advantage of the oscillation systems. It provides a mechanism for specific couplings between successive information processing centers. The later stages of brain areas in the information pathway can respond to the sensible inputs from previous stages by resonance locking to the input, while no resonance may exist if the inputs do not have a proper frequency, oscillation phases, and amplitude pattern — the generalization of the resonance phenomena from a single driven oscillator to a group of coupled oscillators driven by external oscillatory input patterns (see Section 9.1). This

may also be used conceivably for attention control or feature selection. The central brain area can focus its attention on one sensory input or set of features by resonance-locking to that input source only and ignoring the others. A way of decoupling from resonance can be provided by the slower rhythms, like the sniff rhythm, to allow attention shifts.

References

Baird B. Nonlinear dynamics of pattern formation and pattern recognition in rabbit olfactory bulb. *Physica* **22D,** 150-175 (1986).

Bressler S. Relation of olfactory bulb and cortex I: Spatial variation of bulbo-cortical interdependence. *Brain Research* **409,** 285-293 (1987).

Cain W.S. and Engen T. Olfactory adaptation and the scaling of odor intensity. *Olfaction and Taste,*C. Pfaffmann (Ed.) New York, Rockefeller Press 1969 pp.127-141.

Chaput M.A. and Panhuber H. Effects of long duration odor exposure on the unit activity of olfactory bulb cells in awake rabbits. *Brain Research***250** (1982)41-52.

Crick F. Function of the thalamic reticular complex — the searchlight hypothesis. *Proc. Natl. Acad. Sci.* 81(14):4586-4590 (1984).

Eckhorn, R., Bauer, R., Jordan, W., Brosch, M., Kruse, W., Munk, M. and Reitboeck, H.J. Coherent oscillations: a mechanism of feature linking in the visual cortex? *Biol. Cybern.*60, 121-130 (1988).

Eeckman F.H. Statistical Correlations between Unit-Firing and Cortical EEG. Thesis, University of California, Berkeley, 1988a.

Eeckman F.H. Personnal communication, 1988b.

Eeckman F.H. and Freeman W.J. Mitral-granule cell interactions underlie rat olfactory bulbar EEG. *Soc. Neurosci Abstract* 356.6 (1985) (15^{th} Ann. Meeting Dallas, TX).

Eeckman F.H. and Freeman W.J. Cell interactions in the olfactory bulb of the awake rat. *Soc. Neurosci Abstract*#370.5(1986)(16^{th} Ann. Meeting. Wash. D.C.).

Eeckman F.H. and Freeman W.J. Correlations between multi-unit spikes and EEG in rat olfactory cortex. *Soc. Neurosci. Abstract*387.8(1987) (17^{th} Ann. Meeting New Orleans, LA).

Freeman W.J.*Mass Action in the Nervous System.* New York: Academic Press 1975.

Freeman W.J. Spatial properties of an EEG event in the olfactory bulb and cortex. *Electroencephalogr. Clin. Neurophysiol.***44,** 586-605 (1978).

Freeman W.J. Nonlinear Gain mediating cortical stimulus-response relations. *Biol. Cybernetics***33,** 237-247 (1979a).

Freeman W.J. Nonlinear dynamics of paleocortex manifested in the olfactory EEG. *Biol. Cybernetics***35,** 21-37 (1979b).

Freeman W.J. EEG analysis gives model of neuronal template-matching mechanism for sensory search with olfactory bulb.*Biol. Cybernetics* **35,** 221-234 (1979c).

Freeman W.J. Use of spatial deconvolution to compensate for distortion of EEG by volume conduction. *IEEE Trans. Biomed. Engineering* **27,** 421-429 (1980).

Freeman W.J., Schneider W.S. Changes in spatial patterns of rabbit olfactory EEG with conditioning to odors. *Psychophysiology* **19,** 44-56 (1982).

Freeman W.J., Skarda C.A. Spatial EEG patterns, non-linear dynamics and perception: the Neo-Sherringtonian view. *Brain Res.*Rev. **10,** 147-175 (1985).

Getchell T.V., Margolis F.L. and Getchell M.L. Perireceptor and receptor events in vertebrate olfaction.*Progress in Neurobiology* Vol. 23.pp.317- 345. (1984).

Getchell T.V., Shepherd G.M. Responses of olfactory receptor cells to step pulses of odor at different concentrations in the salamender. *J. Physiol.* **282,** 521-540 (1978).

Gray C.M. and Skinner J.E. Centrifugal regulation of neuronal activity in the olfactory bulb of the waking rabbit as revealed by reversible cryogenic blockade.*Exp. Brain. Res.* (1988)**69**: 378-386.

Haberly L.B. Neuronal circuitry in olfactory cortex: anatomy and functional implications.*Chemical Senses* **10,** no.2 219-238 (1985).

Hopfield J.J. Neurons with graded response have collective computational properties like those of two-state neurons. *Proc. Natl. Acad. Sci. USA*Vol. 81. pp.3088-3092 (1984).

Jahr C.E., Nicoll R.A. Dendrodendritic inhibition: demonstration with intracellular recording.*Science* **207,** 1473-1475 (1980).

Kandel E.R. and Schwartz J.H.*Principles of Neural Science.*Second edition. Elsevier Science Publishing Co. (1985).

Lancet D. Vertebrate olfactory reception *Ann. Rev. Neurosci.* **9,** 329-355 (1986).

Lancet D. Greet C.A. Kauer J.S. and Shepherd G.M. Mapping of odor-related neuronal activity in the olfactory bulb by high-resolution 2-deoxyglucose autoradiography.*Proc. Natl. Acad. Sci. USA* **79,** 670-674 (1982).

Li Z., Hopfield J.J. Modeling the olfactory bulb and its oscillatory processings. To be published in*Biological Cybernetics* (1989).

Li Z., A model of olfactory adaptation and sensitivity enhancement in the olfactory bulb. Submitted to *Biological Cybernetics* (1989). Moncrieff R.W.*The Chemical Senses,* 1967 CRC Press.

Mori K., Kishi K. The morphology and physiology of the granule cells in the rabbit olfactory bulb revealed by intracellular recording and HRP injection. *Brain Res.* **247,** 129-133 (1982).

Nicoll R.A. Recurrent excitation of secondary olfactory neurons: a possible mechanism for signal amplication. *Science* **171,** 824-825 (1971).

Pryor G.T., Steinmetz G. and Stone H. Changes in absolute detection threshold and in subjective intensity of suprathreshold stimuli during olfactory adaptation and recovery.*Perception & Psychophysics* (1970) Vol.8**(5B)** 331-335.

Scott J.W. The olfactory bulb and central pathways. *Experientia* **42,** 223-232 (1986).

Shepherd G.M.*The Synaptic Organization of the Brain.* New York: Oxford University Press 1979.

Shepherd G.M. Private communication. (1988).

Sicard G., Holley A. Receptor Cell Responses to Odorants: Similarities and Differences among Odorants. *Brain Research* **292,** 283-296 (1984).

Singer, W., Gray, C.M., Engel, A. and Konig, P. Spatio-temporal distribution of stimulus specific oscillations in the cat visual cortex I: local interactions. Spatio-

temporal distribution of stimulus specific oscillations in the cat visual cortex II: global interactions. Presented at the 1988 Neuroscience Meeting in Toronto.

Skarda C.A., Freeman W.J. How brains make chaos in order to make sense of the world. *Behavioral and Brain Sciences* **10,** 161-195 (1987).

Steinmetz G., Pryor G.T., and Stone H. Olfactory adaptation and recovery in man as measured by two psychophysical techniques.*Perception & Psychophysics*(1970) Vol.**8(5B)** 327-330.

Appendix A

This appendix contains the source codes used to run the simulation on the SUN computer. Languange C is used. The codes contains the following programs (files) and the input file:

dy_externs.h — for the external variables;
main.c — main source code controlling the simulation;
init.c — to read in the simulation parameters;
incextra.c — used when central control is needed;
netforthesis — input for init.c and incextra.c;
initoutput.c — to initialize the output data file;
stepforward.c — simulation run after initialization;
derivative.c — used in stepforward.c;
celloutput.c — used in derivative.c;
extract.c — to extract information from the data;
realft.c — FFT routine, used in extract.c;
fft.c — FFT routine, used in realft.c.

These codes are compiled and linked together to run the simulation. They will be sequentially listed below by the order listed above. The routines "init.c" and "incextra.c" will read simulation parameters from the input file "netforthesis." The simulated data describing cell activities are outputed to the file called "datafile," and oscillation information is extracted from these data by "extract.c," and this extracted information is outputed to the file "extractout."

dy_externs.h:

```
/*
** Global variable declarations
*/

#define         NMAX         100         /*** Maximum dimension of y vector
                           --- the number of neurons ***/

extern int         nmitral, ngranule; /** numbers of mitral and granule
                  cells, respectively.  Can be substituted for any
                  excitatory and inhibitory cell types.  **/
extern int         ndim;          /** =nmitral+ngranule**/
```

```
extern double        initt,t_exhale,finalt,inity[NMAX],resty[NMAX];
               /***   initt: initial time, when inhalation starts;
                        t_exhale: time when exhalation starts;
                            finalt: end of exhalation time.
                       inity[NMAX]: the initial values of the
                        neural internal states.
                      inity[0], inity[1]...inity[nmitral-1] for
                      mitral cells, corresponds to initial value
                      of vector X in Equation (3.3);
                      inity[nmitral], inity[nmitral+1]...
                       inity[ndim-1] for granule cells;
                      corresponds to initial value of
                      vector Y in Equation (3.3)
                     resty is similar to inity, it is the resting
                     (or background) values of vector X and Y in
                       Equation (3.3) when no odor input
                      exists. Usually inity=resty.  ***/
extern int         nstep;        /*** number of steps or time intervals
           in the simulation of the differential Equation (3.3)*/
/*** For mitral (excitatory) cells**/
extern double        Sx, Sx2;   /** Sx, and Sx', respectively, defined in
                              Section (3.2), characteristics of
                         the excitatory cell gain functions ***/
/*** For granule (inhibitory) cells**/
extern double        Sy, Sy2;   /** Sy, and Sy', respectively, defined in
                            Section (3.2), characteristics of
                       the inhibitory cell gain functions ***/
extern double        threshold;          /** defined as "th" in Section
                       (3.2) , maximum slope point in the cell
                          gain functions --- like a threshold
                            of the cells ***/
extern double        exhalespeed;          /**  Defined as 1/tau_exhale
                     in Equation (3.1), characteristic of
                           the exhalation  speed**/
extern double        noise[NMAX];   /* noise in individual neuron input,
                       added to I and I_c in Equation  (3.3) **/
extern double        noiselevel;          /* noiselevel in the noise[] */
```

```
extern double        noisewidth;   /* "correlation time" of noise[] */
extern double  lastnoise[NMAX];        /** initial time of the last
                                  noise pulse**/
extern double        alpha[NMAX];         /** decay constants of neurons,
                        defined as alpha in Equation (3.3) **/
extern double        init_in[NMAX];         /** initial external inputs
                              I and I_c (Equation 3.3) to neurons**/
extern double        P_odor[NMAX];         /**  Defined as P_odor in
                    Equation (3.1). Characteristic of odor input***/
extern double        connection[NMAX][NMAX]; /** connection between
                        neurons. In olfactory bulb model,
                         used for -H_o and W_o in Equation (3.3).
                        connection[i][j] = -H_o[i][j-nmitral]
                        for i<nmitral, j>= nmitral;
                        connection[j][i] =  W_o[j-nmitral][i]
                                          for i<nmitral, j>= nmitral;
                           connection[i][j] = 0 for i>=nmitral,
                                   j<nmitral in the special case of
                           olfactory bulb model (Equation (3.3)).  **/
/**  For olfactory  central control **/
extern double Icontrol[NMAX];        /* Central control,Equation (7.3)*/
extern int         yescontrol;        /**  When there is central control
                                  yescontrol = 1;
                                  otherwise, yescontrol = 0; ***/
extern double Icdecay;        /* decay constant of Icontrol at exhalation,
                           Supposedly Icdecay = exhalespeed by eq.(7.15) **/
/** data handling **/
extern FILE    *fppattern;   /*** simulation data output file ***/
extern char        datafile[20]; /*** contain the name of the
                                  output data file ***/
```

main.c:

```
/*
** main:        This  file contains all of the
```

```
**                declarations for global variables used.
**                Contains code to  control the simulation process.
*/

#include        <stdio.h>
#include        <math.h>

/*** below are those in dy_externs.h, see that file for
                detailed comments.***/
#define         NMAX        100         /*** Maximum dimension of y vector
                (the number of neurons )***/

int         nmitral, ngranule, ndim,nstep,yescontrol;
double          initt,t_exhale,finalt,inity[NMAX],resty[NMAX];
double          Sx, Sx2,Sy, Sy2,threshold;
double          noise[NMAX],noiselevel,noisewidth, lastnoise[NMAX];
double          exhalespeed,alpha[NMAX],init_in[NMAX],P_odor[NMAX],
        Icontrol[NMAX], Icdecay,connection[NMAX][NMAX];
FILE    *fppattern;
char        datafile[20];

/*
** main:        simulation control
*/

main(argc, argv)
        int         argc;   /*** program arguments are : 1.  filename
                            of a file containing informations for the
                            system. This file is "netforthesis" here
                            in the Appendix.  2.  a random number for
                            simulations ***/
        char         *argv[];
{
        int i;
        FILE *fpout,*fopen();  /*** for output data file ***/

        if(argc !=3 ){ /*** argument need for running ***/
```

```
                printf("input a file name and a random number \n");
                exit();
        }
/**** initialization ***********/
        i = atoi(argv[2]);
        srand((unsigned)(i)); /*** random number initiation
                                for noise generation. ***/
         init(argv[1]);         /*** read in the information from the
                        input file by the filename "argv[1]".
                        This file contains the system parameters. */
        sprintf(datafile,"datafile");  /* file name of fppattern */
        fppattern = fopen(datafile,"w"); /* for simulated data */
        fpout = fopen("extractout","w"); /* for information
                                extracted  from the simulated data
                                output "fppattern" file ***/

/**** simulation sub-package *******/
        initoutput(fppattern,i); /* initial documentation **/
        stepforward(nstep);     /* run simulation, record data */
        fclose(fppattern);      /*** done simulation running.**/
        extract(fpout,datafile,1); /* extract  information from
                the output datafile. fpout: outputfile pointer,
                datafile: name of the simulated datafile, 1:
                the flag to extract information from cell output */
        fclose(fpout); /** done **/
}
```

init.c:

```
#include<math.h>
#include<stdio.h>
#include        "dy_externs.h"
#define        next        for(;;) if(getc(fp)=='%') break
init(s)   /*** Read neural net information from the file with file
        name described by  string "s". This file has to write in
```

```
         the format such that it can be read by this routine ***/
char *s;
{
FILE        *fp,*fopen();
double x,y,sum;
double Controlodor[NMAX],controllevel;
int i,j;

        /** read in the net for the simulation**/
        fp =fopen(s,"r");
        if(fp == NULL) exit();
        next;           fscanf(fp,"%d",&ndim);
        next;           fscanf(fp,"%d",&nmitral);
                        fscanf(fp,"%d",&ngranule);
        next;           fscanf(fp,"%lf",&Sx);
        next;           fscanf(fp,"%lf",&Sx2);
        next;           fscanf(fp,"%lf",&Sy);
        next;           fscanf(fp,"%lf",&Sy2);
        next;           fscanf(fp,"%lf",&threshold);
        next;           fscanf(fp,"%lf",&exhalespeed);
        next;           fscanf(fp,"%lf",&noiselevel);
        next;           fscanf(fp,"%lf",&noisewidth);
        next;           for(i = 0;i<ndim;i++) fscanf(fp,"%lf",&alpha[i]);
        next;           for(i = 0;i<ndim;i++) fscanf(fp,"%lf",&init_in[i]);
        next;           for(i = 0;i<ndim;i++) fscanf(fp,"%lf",&resty[i]);
        next;           for(i = 0;i<ndim;i++) fscanf(fp,"%lf",&inity[i]);
        next;           fscanf(fp,"%lf",&initt);
        next;           fscanf(fp,"%lf",&t_exhale);
        next;           fscanf(fp,"%lf",&finalt);
        next;           fscanf(fp,"%d",&nstep);
        next;
                        for(i = 0;i<nmitral;i++)
                           fscanf(fp,"%lf",&P_odor[i]);
        next;           for(i = 0;i<ndim;i++)
                           for(j=0;j<ndim;j++)
                              fscanf(fp,"%lf",&connection[i][j]);
        next;
```

```
                fscanf(fp,"%d",&yescontrol);

        if(yescontrol == 1){
                /* read  in more information and calculate the
                central control signal Icontrol,see incextra.c */
                next;   fscanf(fp,"%lf",&Icdecay);
                next; for(i=0;i<nmitral;i++)
                        fscanf(fp,"%lf",&Controlodor[i]);
                next; fscanf(fp,"%lf",&controllevel);
                /*** if controllevel >0, olfactory adaptation is
                used, otherwise, olfactory enhancement is used.
                     the value of "controllevel" indicates the strength
                of the adaptation or enhancement  applied. e.g.,
                for self-adaptation, controllevel=1, when  full
                adaptation is desired, controllevel = 0.5 when half
                adaptation is desired. For enhancement,
                "controllevel" is equivalent to the "gamma" value
                in Equation (7.16)***/

                 /*** Calculate the Icontrol value ***/
                incextra(fp,Controlodor,controllevel);
        }
        fclose(fp);
        if(ndim>NMAX) {
                printf("too big a dimension for y\n");
                exit();
        }
}
```

incextra.c:

```
#include<math.h>
#include<stdio.h>
#include        "dy_externs.h"
incextra(fp,Controlodor, controllevel)
```

```
double *Controlodor,controllevel;
                /*** From an input file pointed by  fp, read inverse
                of matrix H_o needed to calculate central control.
                This routine is then to calculate the central
                control signal needed for adaptation or enhancement
                to a particular odor whose P_odor value is described
                by "Controlodor," "controllevel" describes the level
                to which adaptation or enhancement applied.***/

FILE        *fp;
#define next        for(;;) if(getc(fp) == '%') break
{
double x,g1,g2,gp,sum;
int i,j;
double celloutput();   /*** cell gain function g defined in
                Section (3.2) ***/
/*** Calculating Icontrol value ***/
        next;
        for(j=nmitral;j<ndim;j++)
        {
                /* Calculate the "G'_y(Y_o)" in Equation (7.13) ***/
                g1 = celloutput(inity[j]
                        +0.001*threshold,Sy2,Sy,threshold);
                g2 = celloutput(inity[j]
                        -0.001*threshold,Sy2,Sy,threshold);
                gp = (g1-g2)/0.002/threshold;
                        /* calculate the derivative by difference**/
                /*** "gp" is "g'_y", the component of "G'_y" ***/
                /**Calculate "Icontrol[j]", the component of the
                 control signal, Equation (7.15) and/or (7.16) */
                sum = 0.0;
                for(i=0;i<nmitral;i++) {
                        fscanf(fp,"%lf",&x); /*** read in the
                                elements of inverse of H_o **/
                        sum += x*Controlodor[i];
                }
                Icontrol[j] = sum/gp;
```

```
                /*** add the control type and level ***/
                Icontrol[j] *= (12.2*controllevel);
                        /*** 12.2 is the factor used for default,
                        proportional to beta in Equation (7.15)*/
        }
}
```

netforthesis:

```
/*** This is the net file which provides the network
characteristics and is read by "init" and "incextra" subroutines.
comments should not be put inside the datas**/
%20         /*** "ndim", the total number of neurons**/
%10  10         /** "nmitral" and "ngranule"**/
        /** for mitral cells**/
%1.43         /*** "Sx", "S_x" in Equation (3.3) **/
%0.143         /*** "Sx2",  "S'_x" in Equation (3.3) **/
        /** for granule cells**/
%2.86         /*** "Sy", "S_y" in Equation (3.3) **/
%0.286         /*** "Sy2", "S'_y" in Equation (3.3) **/
%1.0         /*** "threshold", "th" in Equation (3.3) **/
%0.03    /*** "exhalespeed" =1/tau_exhale in Equation (3.1)  **/
%0.00143         /** "noiselevel" in the input**/
%7         /**  "noisewidth",the duration in milliseconds of
        each noise pulse*/

        /*  decay constants "alpha" of the (20) neurons**/
%0.15         0.15         0.15         0.15         0.15
 0.15         0.15         0.15         0.15         0.15
 0.15         0.15         0.15         0.15         0.15
 0.15         0.15         0.15         0.15         0.15
        /*** initial external inputs "init_in" to neurons**/
        /*** The upper two rows are "I_background" in Equation
        (3.3), also see Section 3.3;  the lower two rows are
        "I_c" in Equation (3.3). ***/
```

```
%0.243      0.243       0.243       0.243       0.243
 0.243      0.243       0.243       0.243       0.243
 0.1         0.1         0.1         0.1         0.1
 0.1         0.1         0.1         0.1         0.1

        /**  Listed below is "resty",
        the equilibrium point with the background input above**/
%0.691868  0.633856  0.741968  0.698668  0.723730
0.646060  0.635226  0.796132  0.623564  0.714763
0.691868  0.633856  0.741968  0.698668  0.723730
0.646060  0.635226  0.796132  0.623564  0.714763
        /** Below are the "inity", the initial cell internal
        state values. Usually  "inity" is close to "resty"**/
%0.682865  0.657688  0.724149  0.719735  0.698454
0.718061  0.614442  0.796200  0.541007  0.734889
0.710565  0.729583  0.689668  0.704451  0.699861
0.740185  0.722373  0.737577  0.713682  0.717238

%25         /* "t_inhale", initial time of the sniff cycle in msec **/
%205         /* "t_exhale", initial exhalation time
                of the sniff cycle in msec **/
%395         /*** "finalt", end of the sniff cycle in msec **/

%1024          /*** "nstep", number of steps or time intervals used in
        the simulation of differential Equation (3.3) ***/
        /* Below is "P_odor": the odor input vector, the
        paticular example used here is "P_odor_1" in Eq. (6.2) */
%0.00429   0.00429   0.00429   0.00429   0.00429
 0.00429   0.00429   0.00429   0.00429   0.00429

        /** Below is "connection" matrix, see dy_externs.h **/
%0.0   0.0   0.0    0.0    0.0    0.0    0.0    0.0    0.0    0.0
-0.3  -0.9  -0.0    0.0    0.0    0.0    0.0    0.0    0.0   -0.7
 0.0   0.0   0.0    0.0    0.0    0.0    0.0    0.0    0.0    0.0
-0.9  -0.4  -1.0    0.0    0.0    0.0    0.0    0.0    0.0    0.0
 0.0   0.0   0.0    0.0    0.0    0.0    0.0    0.0    0.0    0.0
-0.0  -0.8  -0.3   -0.8    0.0    0.0    0.0    0.0    0.0    0.0
```

```
 0.0   0.0   0.0   0.0   0.0   0.0   0.0   0.0   0.0   0.0
 0.0  -0.0  -0.7  -0.5  -0.9   0.0   0.0   0.0   0.0   0.0
 0.0   0.0   0.0   0.0   0.0   0.0   0.0   0.0   0.0   0.0
 0.0   0.0   0.0  -0.8  -0.3  -0.8   0.0   0.0   0.0   0.0
 0.0   0.0   0.0   0.0   0.0   0.0   0.0   0.0   0.0   0.0
 0.0   0.0   0.0   0.0  -0.7  -0.3  -0.9   0.0   0.0   0.0
 0.0   0.0   0.0   0.0   0.0   0.0   0.0   0.0   0.0   0.0
 0.0   0.0   0.0   0.0   0.0  -0.7  -0.4  -0.9   0.0   0.0
 0.0   0.0   0.0   0.0   0.0   0.0   0.0   0.0   0.0   0.0
 0.0   0.0   0.0   0.0   0.0   0.0  -0.5  -0.5  -0.7   0.0
 0.0   0.0   0.0   0.0   0.0   0.0   0.0   0.0   0.0   0.0
 0.0   0.0   0.0   0.0   0.0   0.0   0.0  -0.9  -0.3  -0.9
 0.0   0.0   0.0   0.0   0.0   0.0   0.0   0.0   0.0   0.0
-0.9   0.0   0.0   0.0   0.0   0.0   0.0   0.0  -0.8  -0.3
 0.3   0.7   0.0   0.0   0.0   0.0   0.0   0.0   0.5   0.3
 0.0   0.0   0.0   0.0   0.0   0.0   0.0   0.0   0.0   0.0
 0.3   0.2   0.5   0.0   0.0   0.0   0.0   0.0   0.0   0.7
 0.0   0.0   0.0   0.0   0.0   0.0   0.0   0.0   0.0   0.0
 0.0   0.1   0.3   0.5   0.0   0.0   0.0   0.0   0.0   0.0
 0.0   0.0   0.0   0.0   0.0   0.0   0.0   0.0   0.0   0.0
 0.0   0.5   0.2   0.2   0.5   0.0   0.0   0.0   0.0   0.0
 0.0   0.0   0.0   0.0   0.0   0.0   0.0   0.0   0.0   0.0
 0.5   0.0   0.0   0.5   0.1   0.9   0.0   0.0   0.0   0.0
 0.0   0.0   0.0   0.0   0.0   0.0   0.0   0.0   0.0   0.0
 0.0   0.0   0.0   0.0   0.3   0.3   0.5   0.4   0.0   0.0
 0.0   0.0   0.0   0.0   0.0   0.0   0.0   0.0   0.0   0.0
 0.0   0.0   0.0   0.6   0.0   0.2   0.3   0.5   0.0   0.0
 0.0   0.0   0.0   0.0   0.0   0.0   0.0   0.0   0.0   0.0
 0.0   0.0   0.0   0.0   0.0   0.0   0.5   0.3   0.5   0.0
 0.0   0.0   0.0   0.0   0.0   0.0   0.0   0.0   0.0   0.0
 0.0   0.0   0.0   0.0   0.0   0.2   0.0   0.2   0.3   0.7
 0.0   0.0   0.0   0.0   0.0   0.0   0.0   0.0   0.0   0.0
 0.7   0.0   0.0   0.0   0.0   0.0   0.0   0.2   0.3   0.5
 0.0   0.0   0.0   0.0   0.0   0.0   0.0   0.0   0.0   0.0

%1          /*** "yescontrol". If no central control is desired
```

```
        (yescontrol = 0), the rest of this file is ignored.
        the rest of this file is read by  subroutine "incextra"
        to set up the desired central control signal. ***/
%0.03        /* Icdecay, **/
        /** Below is the "Controlodor", the P_odor value of the
        odor for which the central control is desired. The
        particular example used here is P_odor,1, i.e.,
        "Controlodor" = "P_odor" (see above)
        in this particular simulation. With the particular
         "controllevel" (see below) in this example, we simulate
        the olfactory self-adaptation. If cross-adaptation or
        cross-enhancement is desired, "Controlodor" not = "P_odor".
        **/
%0.00429   0.00429   0.00429        0.00429   0.00429
 0.00429   0.00429   0.00429        0.00429   0.00429

%0.5         /*** "controllevel", In this example, controllevel= 0.5
        implies that half-adaptation is desired. If full
        adaptation is desired, controllevel = 1.0.
        If olfactory  enhancement is desired, controllevel < 0,
        and "-controllevel" should take the value of "gamma" in
        Equation (7.16) ***/

        /*** Below is the elements of the inverse of H_o,
        listed in the order of from left to right, then from
        top to bottom in a matrix.
        used to calculate "Icontrol" as in Equation (7.3), (7.15)
         , (7.16) and (7.13). ***/

%-0.936234  -0.222037  1.164281  -0.181781  -1.050668
0.684005  0.907618  -1.957304  0.179773  1.645226
1.223855  -0.426973  0.086650  0.572826  -0.444666
-0.545919  0.742155  0.388930  -0.958227  0.019022
0.353068  1.370623  -1.082513  -0.065527  1.123468
 -0.397237  -1.113719  1.606002  0.221495  -1.488312
-1.356255  -0.087011  1.569292  -0.548253  0.023366
0.694883  -0.324511  -0.991181  0.875167  0.539096
```

```
0.478866  -1.017701  -0.029874  1.466662  -0.886789
-0.077084  1.046509  -0.698457  -0.658478  0.858079
1.176680  0.468648  -1.558090  -0.001745  1.559180
-0.665976  -0.067930  1.253102  -0.628237  -0.860875
-0.764678  0.635329  0.542599  -1.140155  0.169998
1.393057  -0.791308  0.125543  0.721562  -0.380436
-0.575339  -0.646873  0.970692  0.508093  -1.288250
-0.101155  1.515638  -1.030432  0.167935  0.838652
0.957155  0.008246  -1.080922  0.451473  0.798752
-0.922787  -0.517379  2.074920  -0.635355  -0.327297
0.256287  0.644124  -0.610385  -0.658584  1.022000
0.408751  -1.343179  0.338792  1.154961  -0.729553
```

initoutput.c:

```
#include<math.h>
#include<stdio.h>
#include        "dy_externs.h"
initoutput(fp,seed)
        /***  initialize the output file , and a little others***/
FILE *fp;         /** the pointer for output file ***/
int seed;         /*** the random number seed ***/
{
double x,y,sum;
int i,j,k,m,a,b,c;

/**  initialize the output file **/
        fprintf(fp,"number of cells p and m #%d  %d  %d  ",
                ndim,nmitral,ngranule);
        fprintf(fp,"time interval is #%f  %f\n",initt,finalt);
        fprintf(fp,"Sx2,Sx,Sy2,Sy,threshold are  ");
        fprintf(fp,"#%f  %f  %f  %f  %f\n",Sx2,Sx,Sy2,Sy,threshold);
        fprintf(fp,"first cycle input is  ");
        for(j=0;j<nmitral;j++)        fprintf(fp,"%f  ",P_odor[j]);
        fprintf(fp,"\n");
```

```
        fprintf(fp,"background mitral cell state value is #");
        for(j=0;j<nmitral;j++)        fprintf(fp,"%f  ",resty[j]);
        fprintf(fp,"\n");
        if (yescontrol == 1) {
                fprintf(fp," extra ic exists, it is \n");
                for(j=nmitral;j<ndim;j++)
                        fprintf(fp,"%f  ",Icontrol[j]);
                fprintf(fp,"\n");
        }
        else                    fprintf(fp," no  extra ic  \n");
        fprintf(fp,"the random number seed is %d\n",seed);
        /** set the initial "lastnoise" **/
        for(j=0;j<ndim;j++)  lastnoise[j] = initt - noisewidth;
}
```

stepforward.c:

```
#include        <math.h>
#include        <stdio.h>
#include        "dy_externs.h"
stepforward(numbersteps)
        /* carry out the simulation with (numbersteps-1)  steps.*/
int numbersteps;
/*** the "nstep" value ***/
{
void derivative();
double        stepsize;
int i,j;
        /*** Document the output file ***/
        fprintf(fppattern,"total number of time points is %d\n",
                numbersteps);
        fprintf(fppattern,"#%f  ",initt);
        for(j=0;j<ndim;j++){
                fprintf(fppattern,"%f  ",inity[j]);
        }
```

```
        fprintf(fppattern,"\n");
        stepsize = (finalt-initt)/(numbersteps-1.);
        simulate(inity,ndim,initt, finalt, stepsize, derivative);
                /** simulate the differential equation given the
                initial values, record the data. ***/
        fprintf(fppattern,"%f\n", stepsize);
}

simulate(y, n, t,t2, step,  derivs)
double *y, t,t2, step;
int n;
void (*derivs)();
{
        /*        This routine takes the initial values and run a
                differential equation to give the final values.
                Record the simulated data as it goes along.
                Inputs are:
                y:  a pointer to the array of initial values
                        for the variables in the differential
                        equation to be simulated;
                n: the dimension of the array;
                t:  the initial time, (its value advances during
                        simulation);
                t2:  the desired final time;
                step: stepsize used (fixed) in simulation;
                derivs: a pointer to the function that calculates
                    derivatives dy/dt in the differential equation.
                Output is the final state vector in the array y. */

        double calcdel();

        double y1[NMAX], dydt[NMAX],tol,left;
        int i, ender;

        (*derivs)(t, y, dydt);
        ender = 0;
        tol = 1.0e-30;
```

```
        do{
                rk4(y, dydt, n, t, step, derivs, y1);
                /*** advance one step, y -> y1 **/
                t = t + step;
                for (i = 0;  i <= n - 1;  i++)
                        y[i] = y1[i];
                record(y,t);  /*** record the data in fppattern,
                                setup the noise ***/
                (*derivs)(t, y, dydt);
                left = t2 - t;
                if (left <= step)
                        step = left;
                if (left < tol)
                        ender = 1;
        }
        while (ender == 0);
}

rk4(y, dydt, n, t, s, derivs, yout)
double *y, t, *dydt, s, *yout;
int n;
void (*derivs)();
{
/* Given the n variables in the array "y" and their derivatives
"dydt" at time "t", use the fourth-order Runge-Kutta method to
advance the solution vector over an interval "s" and return
the incremented variables in "yout."  derivs is a pointer
to a function that computes the derivatives of "y."*/

        double ts, ss, s6;
        int i;
        double dym[NMAX], dyt[NMAX], yt[NMAX];

        ss = s * .5;
        s6 = s / 6.0;
        ts = t + ss;
        for (i = 0;  i <= n - 1;  i++)
```

```
                yt[i] = y[i] + ss * dydt[i];
        (*derivs)(ts, yt, dyt);
        for (i = 0;  i <= n - 1;  i++)
                yt[i] = y[i] + ss * dyt[i];
        (*derivs)(ts, yt, dym);
        for (i = 0;  i <= n - 1;  i++) {
                yt[i] = y[i] + s * dym[i];
                dym[i] = dyt[i] + dym[i];
        }
        (*derivs)(t + s, yt, dyt);
        for (i = 0;  i <= n - 1;  i++)
                yout[i] = y[i] + s6 * (dydt[i] + dyt[i] +
                                2.0 * dym[i]);
}

record(y,t)         /** write out data, set up the noise*/
double        t,y[NMAX];
{
        int i,j,k,m,a,b;

        /** write output file**/
        fprintf(fppattern,"%f  ",t);
        for(j=0;j<ndim;j++) fprintf(fppattern,"%f  ",y[j]);
        fprintf(fppattern, "\n");

        /** setup the noise **/
        for(j=0;j<ndim;j++){
                if((t-lastnoise[j])/noisewidth >
                        (0.8 + rand()/2.15e+9)) {
                        lastnoise[j] = t;
                        noise[j] = noiselevel*
                                (rand()-1.07e+9)/1.07e+9;
                }
        }
}
```

derivative.c:

```
#include<math.h>
#include<stdio.h>
#include "dy_externs.h"
derivative(t,y,dydt)
double t,y[NMAX],dydt[NMAX];
{
double        celloutput();        /*** the function g_x(x) or g_y(y) in
            thesis sect. (3.2) for mitral cells and granule cells*/
int i,j,k;
double g[NMAX]; /*** cell outputs ***/
        /** put in the nonlinearity of neurons**/
        for(i=0;i<nmitral;i++){
                g[i] = celloutput(y[i],Sx2,Sx,threshold);
        }
        for(i=nmitral;i<ndim;i++){
                g[i] = celloutput(y[i],Sy2,Sy,threshold);
        }

        /** set up velocity  dydt in y[i]'s, see Equation (3.3) **/
        for(i=0;i<ndim;i++){
                /** inputs from noise**/
                dydt[i]= noise[i]*(t - lastnoise[i]);
                /** inputs from other neurons**/
                for(j=0;j<ndim;j++)
                        dydt[i] += connection[i][j]*g[j];
                /** decay terms**/
                dydt[i] -= alpha[i]*y[i];
        }
        /**external input**/
        /*** Inputs to the excitatory cells: the receptor inputs
                to mitral cells***/
        for(i=0;i<nmitral;i++){
                if(t<t_exhale) /*** inhalation ***/
                        dydt[i] += (init_in[i]+P_odor[i]*(t-initt));
```

```
                else   /*** exhalation ***/
                        dydt[i] += (init_in[i]+
                        P_odor[i]*(t_exhale-initt)*
                        exp(-exhalespeed*(t-t_exhale)));
        }
        /*** Inputs to the inhibitory cells:
                the central inputs to granule cells ***/
        for(i=nmitral;i<ndim;i++) dydt[i] += init_in[i];

        if(yescontrol == 1){ /** Add extra central control **/
                for(i=nmitral;i<ndim;i++)
                        if(t<t_exhale) /*** inhalation ***/
                           dydt[i] += Icontrol[i]*
                                (t-initt)/(t_exhale-initt);
                        else           /*** exhalation ***/
                           dydt[i] += Icontrol[i]*
                                exp(-(t-t_exhale)*Icdecay);
        }
}
```

celloutput.c:

```
#include<math.h>
#include<stdio.h>
double          celloutput(x,S2,S,th)        /*** cell output function
     g_x(x) or g_y(y) of neurons defined in thesis sect. (3.2)*/
double         x,S2,S,th;
{
        double g;
        if(x<th) {
                g = S2*tanh((x-th)/S2)+S2;
                return(g);
        }
        if(x>=th) {
                g = S*tanh((x-th)/S)+S2;
```

```
                return(g);
        }
}
```

extract.c:

```
#define         MAX_CELL        50   /* maximum  number of cells */
#define         MAX_TIME        2000 /*** maximum time interval **/
#define         MAX_TIME_SHIFT                35
#define         MIN_TIME_SHIFT                5
/*** all the "TIME"'s above are in the units of millisecond ***/
#include<math.h>
#include<stdio.h>
#define MIN(a,b)  ((a<b)? a:b)
#define MAX(a,b)  ((a>b)? a:b)

int        ndim,nmitral,ngranule;
double u,v,x,initt,finalt;
double mainperiod,period[MAX_CELL],amplitude[MAX_CELL],
                phase[MAX_CELL],mean[MAX_CELL];
        /** mainperiod is the period of the oscillation pattern,
        period[] contains the periods for each mitral cell.
        amplitude[] and phase[] describe the O_osci.
        mean[] describes O_mean. **/
double rmsamplitude,rmsmean,frequency;
        /*** rmsamplitude is the root-mean-square of amplitude[] **/
        /*** rmsmean is the root-mean-square of mean[] **/
int i,j,k,m,l,n,a,b,c,time;
double Sx2, Sx, threshold;
double y[MAX_CELL][MAX_TIME],ymean[MAX_CELL][MAX_TIME],
                yfft[MAX_CELL][MAX_TIME];
        /*** the signals are in y, ymean is S_l in Section 6.2 of
        thesis. y in the later part of this routine becomes the
        S_h in Section 6.2 of thesis.
        yfft is the fourier transform of the original signal y  **/
```

```
double filtermask[MAX_TIME]; /*** the band-pass filter ***/
double backy[MAX_CELL];  /*** the resty in simulation program ***/

extract(fpout,string,signalflag) /** extract information from the
                simulated data files, see thesis Chapter 6.2.
                Do fft to help to get the extractions, compile with
                realft.o fft.o, Output to file pointed by fpout,
                input file name is in string[], signalflag signals
                to extract from the output or the cell internal
                states.  **/
FILE *fpout;          /* pointer to the file for extracted information */
char string[20]; /* contains the datafile name from which to
                        extract information ***/
int signalflag;         /*** flag to set the signal as the g(u) (output)
                        or u (cell internal state)**/
{
FILE        *fp,*fopen();

        if(fpout == NULL){
                printf("can't write to file\n"); exit();
        }
        fp = fopen(string,"r");
        if(fp == NULL) {
                printf("can't open %s\n",string); exit();
        }
        fprintf(fpout,"#%s\n",string);
        fflush(fpout);

        /***
        By default,  y[][] (S_h in Section 6.2) is obtained by
        high-passing the original signal (above 20 Hz), and the
        ymean[][] (S_l in Section 6.2) is got by low-passing the
        signal ( below the 20hz). The phase of O_osci (phase[])
         is got by further filtering out the higher frequency part
        of y[][]. ****/

        readfile(fp,signalflag);   /* read the input data file **/
```

```
        buildfilter(20.0, 3000.0); /* set up the band-pass filter */
        getsignal();       /* get y[][] and ymean[][] ***/
        catchperiod();     /* calculate the oscillation period(s) **/
        catchamplitude();   /*** calculate the amplitude[] **/
        catchmean();           /*** calculate the mean[]   ***/
        catchphase();           /*** calculate the phase[], the phases
                are all normalized from 0 to 1  **/
        /* write the extracted information in the output file */
        fprintf(fpout,"Mainperiod: #%f  ",mainperiod);
        frequency = 1000./mainperiod;   /** in unit of Hz **/
        fprintf(fpout,"frequency: #%f\n",frequency);
        fprintf(fpout,"Periods for each : \n#");
        for(j=0;j<nmitral;j++)
                fprintf(fpout,"%f  ",period[j]);
        fprintf(fpout,"\n rmsAmplitude  :  #%f", rmsamplitude);
        fprintf(fpout,"\n Amplitudes for each: \n#");
        for(j=0;j<nmitral;j++)
                fprintf(fpout,"%f  ",amplitude[j]);
        fprintf(fpout,"\n Phases for each: \n#");
        for(j=0;j<nmitral;j++)
                fprintf(fpout,"%f  ",phase[j]);
        fprintf(fpout,"\n rmsMeans : #%f",rmsmean);
        fprintf(fpout,"\n Means for each: \n#");
        for(j=0;j<nmitral;j++)
                fprintf(fpout,"%f  ",mean[j]);
        fprintf(fpout,"\n\n");
        fflush(fpout);
}

readfile(fp,signalflag)
        /*** read the input simulated data file pointed by fp***/
#define        next        for(;;) if(getc(fp)=='#') break
FILE *fp;
int signalflag;
{
double gx();  /*** neuron output function gx(x) ***/
```

```
        next;       fscanf(fp,"%d",&ndim);
        if(ndim>MAX_CELL) {
                printf("too big a dimension for y\n");
                exit();
        }
                fscanf(fp,"%d",&nmitral);
                fscanf(fp,"%d",&ngranule);
        next;       fscanf(fp,"%lf",&initt);
                fscanf(fp,"%lf",&finalt);
        next;       fscanf(fp,"%lf",&Sx2);
                fscanf(fp,"%lf",&Sx);
                fscanf(fp,"%lf",&x);
                fscanf(fp,"%lf",&x);
                fscanf(fp,"%lf",&threshold);
        next;       for(j=0;j<nmitral;j++) fscanf(fp,"%lf",&backy[j]);
        if(signalflag == 1)
                for(j=0;j<nmitral;j++)
                        backy[j] = gx(backy[j], Sx2, Sx, threshold);
        next; fscanf(fp,"%lf",&x);
        time = 0;
        for(;;) {
                for(j=0;j<ndim;j++){
                        fscanf(fp,"%lf",&u);
                        if(j<nmitral) {
                           if(signalflag == 1)  /* get the outputs*/
                                y[j][time] = gx(u,Sx2,Sx,threshold);
                           else y[j][time] = u; /* get the internal
                                                   states ***/
                        }
                }
                if(x>=finalt){   time++; break;}
                time ++;
                fscanf(fp,"%lf",&x);
        }
        fclose(fp);
}
```

```
buildfilter(highpass,lowpass)
        /*** Build a filter band from "highpass" to "lowpass," with
         some smoothing to avoid sharp edges, filter result stored
        in "filtermask."  ***/
double highpass,lowpass;  /*** in units of hz***/
{
double smooth;
        a = (int)(0.001*highpass*(finalt-initt)); /*** high pass***/
        b = (int)(0.001*lowpass*(finalt - initt)); /*** low pass***/
        b = MIN(b, time/2);
        smooth = 5.0;   /*** default ***/
        /** high pass **/
        if(a>0){
             for(i=0;i<a;i++){
                 u = smooth*(a-i);
                 filtermask[2*i] = (double)(1.- (1.+u)/(2.+u));
                 /**  treat filtermask[1] separately, because it is
                 the highest real frequency slot ,see realft()**/
                if(i!=0)
                    filtermask[2*i+1] = (double)(1.- (1.+u)/(2.+u));
             } filtermask[1] = 1.0;
                for(i=a;i<time/2;i++) {
                        u = smooth*(i-a);
                        filtermask[2*i] = (double)((1.+u)/(2.+u));
                        filtermask[2*i+1] = (double)((1.+u)/(2.+u));
                }
        } else for(i=0;i<time;i++) filtermask[i] = 1.;

        /** low pass **/
        if(b<time/2){
            for(i=b;i<time/2;i++) {
                u = smooth*(i-b);
                filtermask[2*i] *= (double)(1.- (1.+u)/(2.+u));
                filtermask[2*i+1] *= (double)(1.- (1.+u)/(2.+u));
            }
            u = smooth*(time/2-b);
```

```
            filtermask[1] = (double)(1.- (1.+u)/(2.+u));
            for(i=0;i<b;i++) {
                u = smooth*(b-i);
                filtermask[2*i] *= (double) ((1.+u)/(2.+u));
                if(i!=0)
                    filtermask[2*i+1] *= (double) ((1.+u)/(2.+u));
            }
        }
}

getsignal()
         /*** With the signal y[][], do FFT on it, filter the signal
         into high-and low-frequency part with the filter
        "filtermask". Inverse FFT. High-frequency part in array
        y[][], low-frequency part in ymean[][]. yfft[][] stores the
                FFT result of the original signal y[][].  ***/
{

        /*** do FFT **/
        for(j=0;j<nmitral;j++)
                realft(&y[j][0],time/2,1);
        for(j=0;j<nmitral;j++)
                for(i=0;i<time;i++)
                        yfft[j][i] = y[j][i];
        /*** filter the signal , and do the inverse fft **/
        for(j=0;j<nmitral;j++) {
                /** filter signal , for mean part: low pass **/
                for(i=0;i<time;i++)
                        ymean[j][i] = y[j][i]*(1.-filtermask[i]);
                /* filter signal , for high frequency: high pass */
                for(i=0;i<time;i++)
                        y[j][i] *= filtermask[i];
                /** do inverse FFT **/
                realft(&ymean[j][0], time/2, -1);
                realft(&y[j][0], time/2, -1);
        }
```

```
}

double gx(x, S2,S,threshold)        /*output function g(x) of neurons */
double        x,S2,S,threshold;
{
        double g;
        if(x<threshold/**&& x >0**/) {
                g = S2*tanh((x-threshold)/S2)+S2;
                return(g);
        }
        if(x>=threshold) {
                g = S*tanh((x-threshold)/S)+S2;
                return(g);
        }
}

catchperiod() /*** calculate the period by auto-corelation
                from the oscillating signal y[][].
                mainperiod is the period of the vector y; while
                period[] is the period of individual components of
                vector y.  The period calculated are within the
                range MIN_TIME_SHIFT and MAX_TIME_SHIFT in units
                of milliseconds. ***/
{
int  shift,k,i,j,minshift,maxshift;
double sum1,sum2,x,similar,maxsimilar,ylen[MAX_TIME];

        minshift  = time*MIN_TIME_SHIFT/(finalt-initt)+1;
        maxshift  = time*MAX_TIME_SHIFT/(finalt-initt)+1;
        for(k=0;k<time;k++) {
                sum1 = 0.;
                for(j=0;j<nmitral;j++) {
                        sum1 += y[j][k]*y[j][k];
                }
                ylen[k] = sqrt(sum1);
        }
        maxsimilar = -1.;
```

```
        for(shift =minshift;shift<=maxshift;shift++) {
                sum1=0; sum2 = 0.;
                for(k=0;k<time-shift;k++) {
                        for(j=0;j<nmitral;j++)
                                sum1 +=y[j][k]*y[j][k+shift];
                        sum2 += ylen[k]*ylen[k+shift];
                }
                similar = sum1/sum2;
                if(similar > maxsimilar) {
                        maxsimilar = similar;
                        mainperiod = (double)(shift)*
                                (finalt - initt)/(double)(time);
                }
        }
        for(j=0;j<nmitral;j++){
            maxsimilar = -1.;
            for(shift =minshift;shift<=maxshift;shift++) {
                sum1=0; sum2 = 0.;
                for(k=0;k<time-shift;k++) {
                        x =y[j][k]*y[j][k+shift];
                        sum1 += x;
                        sum2 += fabs(x);
                }
                similar = sum1/sum2;
                if(similar > maxsimilar) {
                        maxsimilar = similar;
                        period[j] = (double)(shift)*
                                (finalt - initt)/(double)(time);
                }
            }
           }
}


catchamplitude()
        /* Calculate the amplitudes for individual components of the
         oscillating vector signal y, "rmsamplitude" is the
```

```
         root-mean-square" amplitude from all the components. ***/
{
double sum1;

        for(j=0;j<nmitral;j++) {
                sum1 = 0.;
                for(k=0;k<time;k++)
                        sum1 += y[j][k]*y[j][k];
                amplitude[j] = sqrt(sum1/time);
        }
        rmsamplitude = 0.;
        for(j=0;j<nmitral;j++)
                rmsamplitude += amplitude[j]*amplitude[j];
        rmsamplitude = sqrt(rmsamplitude/(double)(nmitral));
}

catchphase() /*** Calculating the relative phases between the
        components of the vector y by cross-corelating them.
        The first component is finally set to phase zero as the
        reference point. Filter the signal first to eliminate the
        noise.***/
{
int zero,maxshift,shift,delay;
double  x,sum1,sum2,max,highpass,lowpass;
        max = 0.;
        for(j=0;j<nmitral;j++) {
                x = mainperiod-period[j];
                if(x<0.2*mainperiod) {
                        if(amplitude[j] > max) {
                                max = amplitude[j];
                                zero = j;
                        }
                }
        }
        maxshift =(int)(mainperiod*time/(finalt-initt));
/*** get the phase relative to zerophase **/
        /*** filter the signal first***/
```

```
        x = 1000.0/mainperiod;  /*** the frequency***/
        highpass = 20.0;        /*** high pass(Hz) : default***/
        lowpass = 1.3*x;        /*** low pass(Hz): default ***/
        buildfilter(highpass,lowpass);
        for(j=0;j<nmitral;j++) {
                for(i=0;i<time;i++)
                        y[j][i] = yfft[j][i]*filtermask[i];
                realft(&y[j][0],time/2,-1);
        }
/*** get phase by matching ***/
        for(j=0;j<nmitral;j++) {
                if(j== zero) phase[j] = 0.;
                else {
                        max = -1.;
                        for(shift = 0; shift<maxshift;shift++) {
                                sum1=0; sum2 = 0;
                                for(k=0;k<time-shift;k++) {
                                     x = y[j][k] * y[zero][k+shift];
                                     sum1 += x;
                                     sum2 += fabs(x);
                                }
                                x = sum1/sum2;
                                if(x>max) {
                                        max = x;
                                        delay = shift;
                                }
                        }
                        phase[j] = (double)(delay)/(double)(time)*
                                (finalt-initt)/mainperiod;
                }
        }

/*** make them all relative to the 0-th cell, all phase values are
normalized to the range from 0 to 1, i.e., phase = 1 means one
cycle of the oscillation period. ***/
        for(j=1;j<nmitral;j++) {
                phase[j] = phase[j] - phase[0];
```

```
                if(phase[j]< 0.) phase[j] = 1. + phase[j];
        }
        phase[0] = 0.;
}

catchmean()  /*** Calculate the mean values of the signal from the
        low frequency part "ymean" of the signal. mean[] stores the
         individual mean of the component for vector signal "ymean,"
     rmsmean is the root-mean-square average from the components. */
{
double sum1;

        for(j=0;j<nmitral;j++) {
                sum1 = 0.;
                for(k=0;k<time;k++)
                        sum1 += ymean[j][k];
                mean[j] = sum1/time - backy[j];
        }
        rmsmean = 0.;
        for(j=0;j<nmitral;j++)
                rmsmean += mean[j]*mean[j];
        rmsmean = sqrt(rmsmean/(double)(nmitral));
}
```

realft.c:

```
/** This is copied and modified from p.417 of the book
"Numerical recipe." To do FFT, compile with four1,(fft.o) **/

#include <math.h>
#include <stdio.h>

void realft(data,n,isign)

double data[];
```

```
int n,isign;

/* Calculates the Fourier transform of a set of 2n real-valued data
 points. Replaces these data (which are stored in array data[0...2n-1]
 by the positive frequency half of its complex Fourier Transform.
The real-valued first and last components of the complex transform
are returned as elements data[0] and data[1], respectively.
n must be a power of 2. This routine also calculates the inverse
transform of a complex data array if it is the transform of real
data.  **/
{
        int i,i1,i2,i3,i4,n2p3;
        double c1=0.5,c2,h1r,h1i,h2r,h2i;
        double wr,wi,wpr,wpi,wtemp,theta; /** double precision for
                        the trigonometric recurrences**/
        void four1();
        /** check if n if a power of 2**/
        i = 2;
        for(i1=0;i1< 50;i1++) {
                if(n == i) break;
                i*=2;
        }
        if(i1 == 50){
                fprintf(stderr, "wrong number of data for fft, or
                        number too large\n");
                exit();
        }
        theta = 3.141592653589793 /(double)n;
                /** initialize the recurrence**/
        if(isign == 1) {
                c2 = -0.5;
                four1(data,n,1);
                        /** The forward transform is here**/
        }else{
                c2 = 0.5;   /** otherwise setup for the inverse
                                transform*/
                theta = -theta;
```

```
        }
        wtemp = sin(0.5*theta);
        wpr = -2.0*wtemp*wtemp;
        wpi = sin(theta);
        wr = 1.0+wpr;
        wi = wpi;
        n2p3 = 2*n + 3;
        for(i=2;i<=n/2;i++){ /** case i=1 done separately below **/
                i4 = 1+(i3=n2p3-(i2=1+(i1=i+i-1)));
                /** the two separate transforms are separated out
                        of data**/
                h1r =  c1*(data[i1-1]+data[i3-1]);
                h1i =  c1*(data[i2-1]-data[i4-1]);
                h2r = -c2*(data[i2-1]+data[i4-1]);
                h2i =  c2*(data[i1-1]-data[i3-1]);
                /** here they are recombined to form the true
                        transform of the original real data **/
                data[i1-1] =  h1r + wr*h2r - wi*h2i;
                data[i2-1] =  h1i + wr*h2i + wi*h2r;
                data[i3-1] =  h1r - wr*h2r + wi*h2i;
                data[i4-1] = -h1i + wr*h2i + wi*h2r;
                /** the recurrence**/
                wr = (wtemp=wr)*wpr-wi*wpi + wr;
                wi = wi*wpr+wtemp*wpi+wi;
        }

        if(isign == 1 ) { /** squeeze the first and last data
                together to get them all within the original array*/
                data[0] = (h1r=data[0])+data[1];
                data[1] = h1r-data[1];
        } else {
                data[0] = c1*(( h1r=data[0])+data[1]);
                data[1] = c1*( h1r - data[1]);
                four1(data, n,-1); /**This is the inverse
                        transform for the case isign = -1 **/
        }
}
```

fft.c:

```
/* This is copied and modified from the book "Numerical Recipe,"*/

#include        <math.h>
#include        <stdio.h>

#define SWAP(a,b)  tempr = (a); (a)=(b); (b) = tempr

void four1(data, nn, isign)

double data[];
int nn, isign;

/** replaces data by its discrete Fourier transform, if isign is
input as 1; or replaces data by  its inverse discrete Fourier
transform, if isign is input as -1. data is a complex array of
length nn, input as a real array data[0...2*nn-1]. nn MUST be an
integer power of 2 **/
{
        int n,mmax,m,j,istep,i,nncopy;
        double wtemp,wr,wpr,wpi,wi,theta;
           /* Double precision for the trigonometric recurrences**/
        double tempr,tempi;
        /** check to see if nn is a power of 2**/
        m = 2;
        for(n=0;n<50;n++) {
                if(nn == m) break;
                m *= 2;
        }
        if(n== 50){
                fprintf(stderr,"wrong number of data for fft, or
                        number too large\n");
                exit();
```

```
}
nncopy = nn;

n=nn << 1;
j=1;
for (i=1;i<n;i+=2){/** this is the bit-reversal section
                        of the routine**/
        if(j>i){ /** exchange the two complex numbers**/
                SWAP(data[j-1], data[i-1]);
                SWAP(data[j], data[i]);
        }
        m=n >> 1;
        while (m >=2 && j> m) {
                j -= m;
                m >>= 1;
        }
        j += m;
}
mmax = 2;         /** here begins the Danielson-Lanczos
                section of the routine**/
while(n> mmax ){  /** outer loop executed log2(nn) times**/
        istep = 2*mmax;
        theta = 6.28318530717959/(isign*mmax);
         /** initialize for the trigonometric recurrence**/
        wtemp = sin(0.5*theta);
        wpr = -2.0*wtemp*wtemp;
        wpi = sin(theta);
        wr = 1.0;
        wi = 0.0;
        for(m=1;m<mmax;m+=2){
                /** here are the two nested inner loops*/
                for(i=m;i<=n;i+=istep){
                        j = i+mmax; /* This is the
                            Danielson- Lanczos formula;**/
                        tempr = wr*data[j-1]- wi*data[j];
                        tempi = wr*data[j] + wi*data[j-1];
                        data[j-1] = data[i-1] - tempr;
```

```
                        data[j] = data[i] - tempi;
                        data[i-1] += tempr;
                        data[i] += tempi;
                } /** trigonometric recurrence **/
                wr = (wtemp=wr)*wpr - wi*wpi + wr;
                wi = wi*wpr + wtemp*wpi + wi;
        }
        mmax = istep;
    }
    if(isign == -1){  /** make the inverse transform exact **/
        for(i=0;i<2*nncopy;i++)
                data[i] /= (double)(nncopy);
    }
}
```